MODELING THE INFLUENCE OF SURFACTANT ARCHITECTURE ON THE CRITICAL MICELLE CONCENTRATION OF DOUBLE-HEADED AND GEMINI SURFACTANTS

by

Douglas R. Jackson

Submitted in partial fulfillment of the requirements
for the degree of Master of Science

at

Dalhousie University
Halifax, Nova Scotia
August 2009

DALHOUSIE UNIVERSITY

DEPARTMENT OF CHEMISTRY

The undersigned hereby certify that they have read and recommend to the Faculty of Graduate Studies for acceptance a thesis entitled "MODELING THE INFLUENCE OF SURFACTANT ARCHITECTURE ON THE CRITICAL MICELLE CONCENTRATION OF DOUBLE-HEADED AND GEMINI SURFACTANTS" by Douglas R. Jackson in partial fulfillment of the requirements for the degree of Master of Science.

Dated: August 27, 2009

Supervisor: _____

Readers: _____

_____

_____

Departmental Representative: _____

DALHOUSIE UNIVERSITY

DATE: August 27, 2009

AUTHOR: Douglas R. Jackson

TITLE: MODELING THE INFLUENCE OF SURFACTANT ARCHITECTURE ON THE CRITICAL MICELLE CONCENTRATION OF DOUBLE-HEADED AND GEMINI SURFACTANTS

DEPARTMENT OR SCHOOL: Department of Chemistry

DEGREE: MSc CONVOCATION: October YEAR: 2010

Permission is herewith granted to Dalhousie University to circulate and to have copied for non-commercial purposes, at its discretion, the above title upon the request of individuals or institutions.

_____

Signature of Author

Dedicated to my mother, Shirley Buist Jackson (1950-2004).

TABLE OF CONTENTS

LIST OF TABLES

LIST OF FIGURES

ABSTRACT

Monte Carlo simulations have been used in the past to investigate a variety of surfactant systems; however, there is little published literature for double-headed and gemini surfactants with asymmetric tails. We perform Larson-type Monte Carlo simulations of double-headed and gemini surfactant systems with asymmetric tails in two- and three-dimensions. The model predicts that the addition of a second head group to form a double-headed surfactant results in an increase in the critical micelle concentration (CMC) compared to a single-headed surfactant, in agreement with experiment. It also indicates that the placement of the second head group has an impact on the final CMC value. We study a series of gemini surfactants with asymmetric tails and find no change in the value of the CMC as the ratio of the lengths of the two tails increases. This is contrary to the only experimental study that found there was a slight decrease in the CMC as the ratio of the lengths of the two tails increases. We examine this difference in terms of the relatively small effect surfactant asymmetry has on value of the CMC and the fact that the model is capable of qualitatively reproducing the known dependence of the CMC on other architectural properties. This initial probe into systems of double-headed and gemini surfactants with asymmetric tails confirms many of the previously published findings and provides avenues for possible future research using Monte Carlo simulations.

LIST OF ABBREVIATIONS AND SYMBOLS USED

ΔE	Change in energy
ΔG	Change in Gibbs energy
ΔH	Change in enthalpy
ΔS	Change in entropy
$\varepsilon_{a,b}$	Nearest neighbour a-b interaction energy
ε_b	Conformation interaction energy
ε_{HH}	Nearest neighbour head-head interaction energy
ε_{HS}	Nearest neighbour head-solvent interaction energy
ε_{HW}	Nearest neighbour head-water interaction energy
ε_{SH}	Nearest neighbour spacer-head interaction energy
ε_{SS}	Nearest neighbour spacer-spacer interaction energy
ε_{ST}	Nearest neighbour spacer-tail interaction energy
ε_{SW}	Nearest neighbour spacer-water interaction energy
ε_{TH}	Nearest neighbour tail-head interaction energy
ε_{TS}	Nearest neighbour tail-solvent interaction energy
ε_{TT}	Nearest neighbour tail-tail interaction energy
ε_{TW}	Nearest neighbour tail-water interaction energy
ε_{WW}	Nearest neighbour water-water interaction energy
γ	Surface tension
γ_{CMC}	Surface tension at the critical micelle concentration
π	Osmotic pressure

σ	Interfacial tension
A	Value of any thermodynamic property at equilibrium
A_c	Value of any thermodynamic property in a particular state c
C12(-)	A conventional anionic single-tailed surfactant with a tail length of 12 carbon atoms
C12(-)-C12(+)	A zwitterionic gemini surfactant with a tail length of 12 carbon atoms and a spacer length of 2 carbon atoms
C_{20}	The surfactant concentration that reduces the surface tension of water by 20 mN m^{-1}
$C_{12}C_SC_{12}Br_2$	Gemini surfactants of the form $\left[{}_{12}H_{25}(CH_3)_2N-(CH_2)_SN(CH_3)_2C_{12}H_{25}\right]Br_2$ where s represents 4, 6, 8, 10 or 12 carbon atoms in the spacer
$C_mC_6C_nBr_2$	Asymmetric gemini surfactants of the form $\left[{}_mH_{2m+1}(CH_3)_2N(CH_2)_6N(CH_3)_2C_nH_{2n+1}\right]Br_2$ with a constant n + m = 24 and m = 12, 13, 14, 16, 18
CAC	Critical aggregation concentration
CMC	Critical micelle concentration
CMC_a	Tanford[23] definition of the critical micelle concentration
CMC_b	Israelachvilli[22] definition of the critical micelle concentration
CMC_{f_H}	Critical micelle concentration as a result of the factor in the Hamiltonian to vary the all interaction energies involving head groups
$CMC_{f_{HH}}$	Critical micelle concentration as a result of the factor in the Hamiltonian to vary the head-head interaction energy
$CMC_{f_{HT}}$	Critical micelle concentration as a result of the factor in the Hamiltonian to vary the head-tail interaction energy
$CMC_{f_{HW}}$	Critical micelle concentration as a result of the factor in the Hamiltonian to vary the head-water interaction energy

$CMC_{f_{TW}}$	Critical micelle concentration as a result of the factor in the Hamiltonian to vary the tail-water interaction energy
DNA	Deoxyribonucleic acid
DTAB	Dodecyltrimethylammonium bromide
f_H	Factor in the Hamiltonian to vary the all interaction energies involving head groups
f_{HH}	Factor in the Hamiltonian to vary the head-head interaction energy
f_{HT}	Factor in the Hamiltonian to vary the head-tail interaction energy
f_{HW}	Factor in the Hamiltonian to vary the head-water interaction energy
f_{TW}	Factor in the Hamiltonian to vary the tail-water interaction energy
H	Head group
H	Hamiltonian for the system
H_c	Value of the Hamiltonian for state c
H_xT_y	Surfactant with x hydrophilic head units and y hydrophobic tail units
H_1T_{12}	Surfactant with 1 hydrophilic head units and 12 hydrophobic tail units
H_2T_2	Surfactant with 2 hydrophilic head units and 2 hydrophobic tail units
H_7T_{12}	Surfactant with 7 hydrophilic head units and 12 hydrophobic tail units
H-T3	Conventional single-tailed surfactant with tail length of 3
H-T6	Conventional single-tailed surfactant with tail length of 6
H-T31	Conventional single-tailed surfactant with tail length of 31
H2-T30	A double-headed surfactant with head groups located at site 1 and 2 on the chain and a tail length of 30

H-S6-H-T24	A double-headed surfactant with head groups located at site 1 and 7 on the chain, a spacer length of 6, and a tail length of 24
I_{sc}	Light scattering
k_B	Boltzmann constant
l_s	Total length of a surfactant chain
L_x	The length of the x side of the lattice
L_y	The length of the y side of the lattice
L_z	The length of the z side of the lattice
MC	Monte Carlo
MD	Molecular dynamics
$n_{a,b}$	The number of a,b nearest neighbour interactions in the system
n_{HH}	The number of head-head nearest neighbour interactions
n_{HT}	The number of head-tail nearest neighbour interactions
n_{HW}	The number of head-water nearest neighbour interactions
n_{TT}	The number of tail-tail nearest neighbour interactions
n_{TS}	The number of tail-solvent nearest neighbour interactions
n_{TW}	The number of tail-water nearest neighbour interactions
N	Neutral group
N	Total number of points in the standard deviation
N_1	Number of free monomers in the system
N_g	Average micelle size distribution
NMR	Nuclear magnetic resonance
N(n)	Average number of clusters of size n in the system
N_s	Number of surfactants in the system

P	Boltzmann probability
PBS-PEP	poly{1,4-phenylene-[9,9-bis(4-phenoxy-butylsulfonate)]fluorine-2,7-diyl}copolymer
P_c	Probability that the state c occurs in equilibrium
P(n)	Cluster-size distribution
Py-3-12	N^1-dodecyl,N^1,N^1,N^3,N^3-tetramethyl-N^3-(6-(pyren-6-yl)-hexyl) propane-1,3-diammonium dibromide
Py-6-12	N^1-dodecyl,N^1,N^1,N^6,N^6-tetramethyl-N^6-(6-(pyren-6-yl)-hexyl)hexane-1,6-diammonium dibromide
R_1	Alkyl chain group 1
$\frac{1}{R}$	Molar conductivity
S	Spacer group
s_n	Standard deviation
SST	Single surfactant transport move
T	Tail group
T	Temperature
T_x	Oil molecule of length x
T6-H-S2-H-T6	A gemini surfactant with a tail length 6 and a spacer length of 2
T6-H-S6-H-T6	A gemini surfactant with a tail length 6 and a spacer length of 6
T7-H-S2-H-T5	An asymmetric gemini surfactant with tail lengths of 7 and 5 and a spacer length of 2
T8-H-S2-H-T4	An asymmetric gemini surfactant with tail lengths of 8 and 4 and a spacer length of 2
T9-H-S2-H-T3	An asymmetric gemini surfactant with tail lengths of 9 and 3 and a spacer length of 2

T10-H-S2-H-T2	An asymmetric gemini surfactant with tail lengths of 10 and 2 and a spacer length of 2
T11-H-S2-H-T1	An asymmetric gemini surfactant with tail lengths of 11 and 1 and a spacer length of 2
T11-H2-S6-H2-T11	A double-headed gemini surfactant with a tail length of 11 and a spacer length of 6
T12-H-S6-H-T12	A gemini surfactant with a tail length 12 and a spacer length of 6
T13-H-S6-H-T11	An asymmetric gemini surfactant with tail lengths of 13 and 11 and a spacer length of 6
T14-H-S6-H-T10	An asymmetric gemini surfactant with tail lengths of 14 and 10 and a spacer length of 6
T16-H-S6-H-T8	An asymmetric gemini surfactant with tail lengths of 16 and 8 and a spacer length of 6
T17-H2-S6-H2-T5	An double-headed asymmetric gemini surfactant with tail lengths of 17 and 5 and a spacer length of 6
T18-H-S6-H-T6	An asymmetric gemini surfactant with tail lengths of 18 and 6 and a spacer length of 6
T23-H-S6-H-T1	An asymmetric gemini surfactant with tail lengths of 23 and 1 and a spacer length of 6
T_m-H-S6-H-T_n	A series of asymmetric gemini surfactants where the tails n + m = 24 and m = 12, 13, 14, 16, 18
$T_mN_pH_qS_nH_qN_pT_m$	A gemini surfactant where p=q=1, m=5, 15, or 25 and $2 \le n \le 20$
W	Water
X	Total surfactant concentration
X_1	Free monomer concentration
x_i	Value of the point being considered
$\bar{x}$	Mean average of all the points
Z	Partition coefficient

ACKNOWLEDGEMENTS

I would like to express my sincere thanks to my supervisor, Dr. Gerry Marangoni for allowing me to carry out this research. In particular I would like to thank him for his patience, guidance and support in completing this thesis, as I was not the "typical" graduate student.

Dr. Peter Poole, I could not have completed this research without your collaboration. Your support in completing the computer modeling, assistance in debugging my code, and help in pulling together this thesis was invaluable. I have truly enjoyed working with you!

I would also like to thank AIF, CFI, NSERC, StFX University and Dalhousie University for providing me with stipends, equipment and facilities, all of which permitted me to carry out my research.

A very special thank you to my beautiful wife Melanie and son Keagan for putting up with the long nights and summers of extra work. I could not have done it without your love, support and encouragement. As well, thank you to my extended family; it has been a long road and I have appreciated your constant interest and support.

Thank you also to the following people:

- Dr. Shah Razul, Greg Lukeman, Chance Creelman and Amir Mohareb for their assistance with the coding of various programs.
- Jennifer MacNeil for helping to run the initial asymmetric gemini surfactant runs in two-dimensions.
- The members of the "think tank." You definitely made it an experience I will never forget. Thanks for your support and laughs!

CHAPTER 1 – INTRODUCTION

1.1 – Introduction

Surfactants are an integral part of modern life and have a wide variety of uses in agrochemicals, electroplating, metalworking fluids and lubricants, mineral processing, oil field chemicals, pulp and paper and textile processing.[1,2] As a result, surfactant technology continues to be on the forefront of scientific research. As new types of surfactants are synthesized, there is an increasing demand to understand the origins of surfactant activity in terms of its molecular structure to enable the creation of surfactants tailored to a specific purpose. Academic and industrial interests aim to understand such properties as the critical micelle concentration (CMC) and surface activity in terms of the specific architecture of the surfactant. The impact of chain length, shape (single-chain, double-chain, or gemini), and head group type on the CMC and surface activity are of particular interest.[2,3]

Ideally, computer models[4,5,6] would predict the CMC and surface activity data obtained from experimentally determined values of surfactants and forecast the behaviour of those yet to be synthesized. As a result, when particular surfactant behaviour is desired a modeling program could predict the required surfactant structure and reduce research time and costs. Even if the model does not predict an exact structure, it could indicate a starting point for synthetic research. For example, pharmaceutical scientists have shown interest in the results from previous computer models of surfactant systems which indicated the formation of specific micellar structures.[7] They envision the potential use of surfactants either as drug vehicles/carriers or more recently as targeting

systems where the surfactant delivers the drug to a specific part of the body and deposits it.[8]

1.2 – Surfactant Structure and Classification

The word surfactant is a hybrid of the words **surf**ace **act**ive **a**ge**nt**.[9] Surfactants are commonly used to lower the surface or interfacial tension between two immiscible liquids or a solid and a liquid, by adsorbing to the interface between the two liquids or the liquid and the solid. The chemical composition and structure of surfactant molecules makes the lowering of the surface tension possible.[9] The composition and organization of the surfactant will be studied in this work.

Surfactants typically have two main parts, referred to as the head group and the tail group. Surfactants are called amphiphilic molecules since the head group of the surfactant is hydrophilic and the tail group is hydrophobic. Surfactants are divided into a number of distinct classes based on the charge on the head group after it dissolves in an aqueous environment: anionic, cationic, non-ionic, and zwitterionic.[9]

- Anionic Surfactants – dissociate into an amphiphilic anion and a cation (e.g. sodium stearate).
- Cationic Surfactants – dissociate into an amphililic cation and an anion, typically a halogen (e.g. Dodecylamine hydrochloride).
- Non-Ionic Surfactants – do not dissociate in aqueous solutions because the hydrophilic head group cannot dissociate, for example head groups could be alcohols, ethers, esters, or amides (e.g. Polyethylene oxides).

- Zwitterionic Surfactants – surfactant molecules that contain both anions and cations as head groups (e.g. Dodecyl betaine).

Many surfactants tails consist of a single hydrocarbon[10] chain whereas others (e.g. phospholipids) are made of two hydrocarbon tails,[11] both of which are connected to the same head group. Still others have two head groups connected to a single hydrocarbon tail.[12] Another structural division of surfactants, gemini surfactants, consists of two single-chain surfactants whose head groups are connected by a spacer chain (Figure 1). This class of amphiphiles is sometimes referred to as "dimeric surfactants" or "bis-surfactants."[13] Both the class and structure of the surfactant molecule have been shown to significantly influence its chemical and physical properties.[3,9]

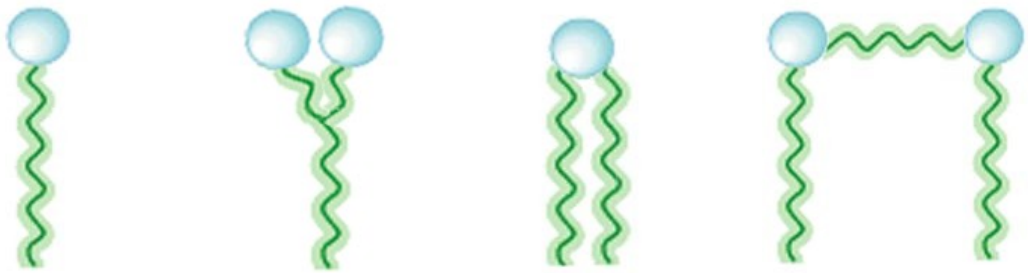

Single-Tail Double-Head Double-Tail Gemini

Figure 1 – The main structural divisions for surfactant molecules.

1.3 – Critical Micelle Concentration

The CMC marks a dramatic change in several physical properties of a surfactant system including osmotic pressure, light scattering, molar conductivity and interfacial (surface) tension (Figure 2).[9] These changes are a result of aggregation (micellization) of surfactants in solution. Below the CMC, surfactant molecules are loosely integrated into

the water structure, primarily as isolated surfactant molecules. Above the CMC, the surfactant-water structure is changed in such a way that the surfactant molecules begin to aggregate (Figure 3).[9] In aqueous environments, surfactants with polar head groups can join together to form spherical[14] or cylindrical[15] micelles, vesicles[16] or planar mono- or bi-layers.[14] The hydrophobic tails make up the center of the micelle and are protected by the hydrophilic head groups, which remain in contact with the water molecules.

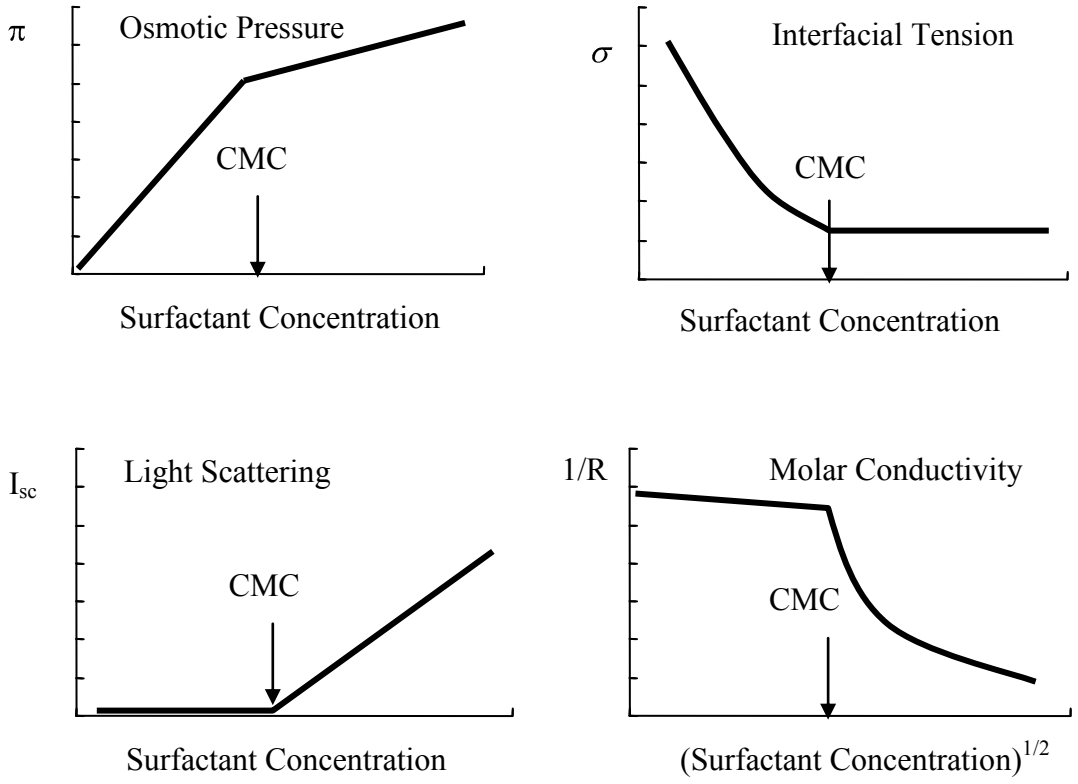

Figure 2 – Plots showing the dramatic effect the CMC has on physical properties of a solution.[9]

In an aqueous solvent, there are two main driving forces for micellization – the formation of favorable tail-tail interactions limiting the number of tail-water interactions and the increase in the amount of hydrogen bonding between solvent molecules. In non-polar solvents, reverse micelles form with the heads towards the interior of the micelle to

minimize the interaction with the solvent. The tails form the outer layer to maximize the interaction with the solvent because of their stronger affinity for the non-polar solvent.[9]

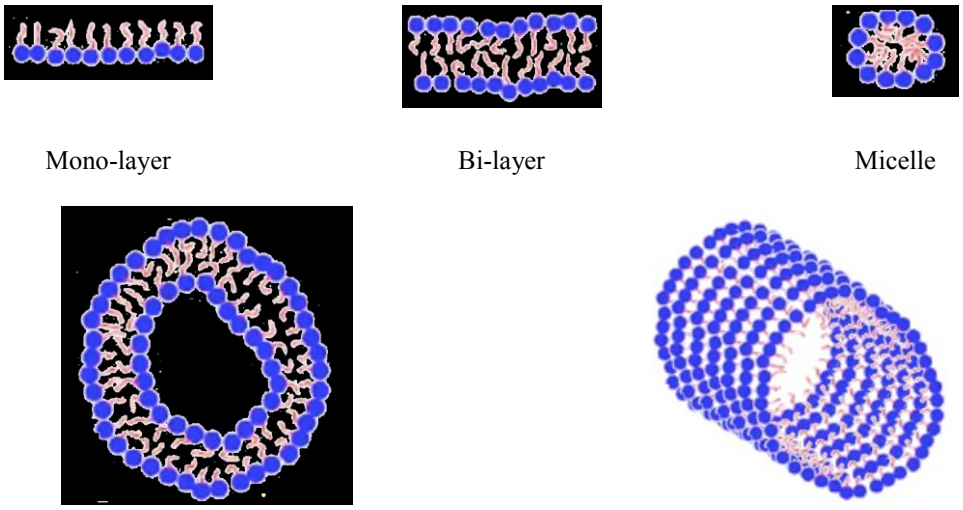

Figure 3 – Typical structures formed by surfactant aggregates.

The most practical uses of surfactants come from their ability to lower the surface and interfacial tension.[1] As the concentration of surfactant in solution is increased, the surface tension decreases. The presence of micelles, occurring at bulk surfactant concentrations above the CMC, greatly lowers the surface tension because surfactant monomers migrate to the interface.[9] The affinity of the surfactant monomers towards both the polar and non-polar phases means that the thermodynamic stability of the system is enhanced when the surfactant monomers are adsorbed at the polar/non-polar interface (e.g. water/air or water/oil). At concentrations above the CMC, equilibrium between micelles and monomers in solution is established and thus the surface tension remains constant. The micelles in the bulk solution act as a reservoir for monomers as they are consumed at the interface (Figure 4).[9]

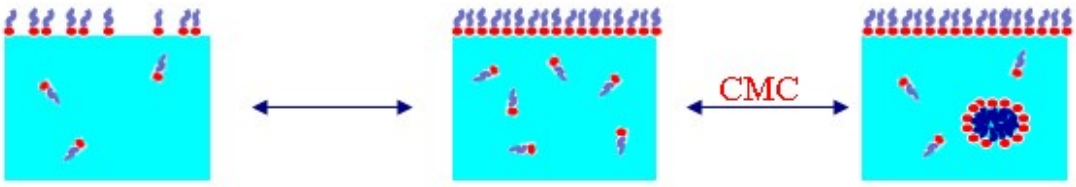

Figure 4 – Schematic showing the equilibrium established in the bulk of a surfactant/water solution. Moving left to right through the images, the surfactant concentration increases, showing migration of the monomers to the air/water interface until the CMC is reached and micelles are formed in the bulk solution.

Experimentally, CMCs are determined using a variety of methods including surface tension,[17] electrical conductivity,[18] ultraviolet absorption spectroscopy[18] and, fluorescence spectroscopy.[17,18] However, the obtained CMC varies slightly with the physical property studied and the procedure used to determine the point of discontinuity.[9] The plots in Figure 2 show the point of discontinuity as an "elbow" in the curve of the examined property versus concentration. The CMC determined from computer models has been defined in many ways, [19,20,21,22,23] however two methods developed by Israelachvili[22] and Tanford,[23] are used most commonly.[24,25,26,27] Israelachvili[22] defines the CMC as the point where the number of surfactant molecules found as free monomer is equal to the number found in micelles, where Israelachvili defines the persistence of micelles as at least one aggregate of 10 or more surfactant molecules in each snapshot (CMC_b in Figure 5). To determine the CMC using the Israelachvili[22] method one must examine the average cluster size distribution for each concentration. The cluster distribution is the number of monomers, dimers, trimers, and aggregates of four, five, and six, etc, present in the system at equilibrium. From this, one can find the concentration where the number of surfactant molecules found as free monomers is equal to the number found in micelles.[22]

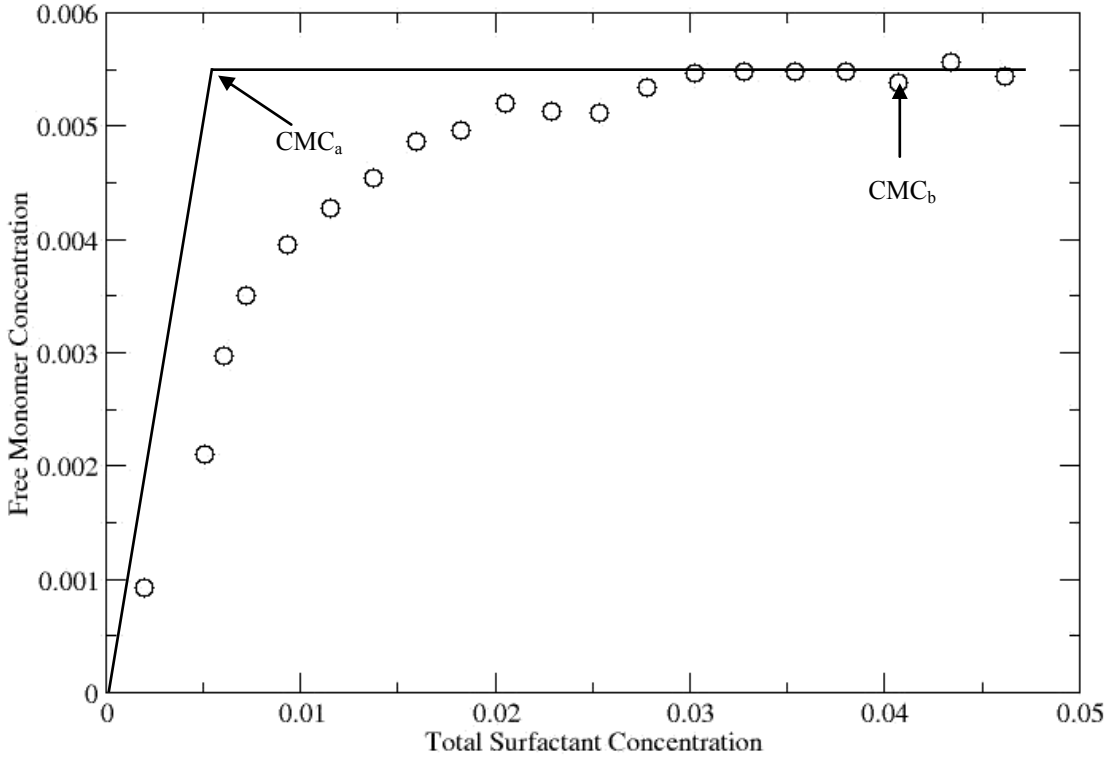

Figure 5 – The difference in the absolute value of the CMC according to the Tanford[23] definition (CMC_a) and the Israelachvili[22] definition (CMC_b – the total surfactant concentration with the first aggregate of 10 surfactants) for the code used in this thesis modeling a single-tailed surfactant with a tail length of 3 at a temperature = 1.0 on a 100 × 100 two-dimensional lattice.

For this thesis we adopt the Tanford[23] definition of the CMC. Tanford's method uses a plot of free monomer concentration versus total surfactant concentration and defines the concentration where a line passing through the origin with a slope of 1 intercepts a horizontal line formed by the average free monomer concentration after the onset of micellization as the CMC (CMC_a in Figure 5).[23]

From Figure 5, it is evident that the Tanford[23] definition (CMC_a) of the CMC will always be less than that defined by Israelachvilli[22] (CMC_b). We have chosen the Tanford definition because it does not rely on a secondary definition of what constitutes a micelle. Previous models have defined micelles as aggregates of 2 or more surfactants and as large as 10 or more surfactant molecules, sparking much debate.[4,22] Instead we define free monomers as surfactant molecules that have no surfactant molecules as nearest neighbours (i.e. surfactant molecules which do not have head-head, tail-tail or head-tail contacts). Regardless, both the Israelachvilli and Tanford definitions show the same trends, although with different CMC values.

Both definitions use the free monomer concentration to determine the CMC. It should be noted that the free monomer concentration is not constant above the CMC. In fact, as seen with most of the results of this thesis, the free monomer concentration decreases slightly as the total surfactant concentration is increased. This result is consistent with both previous experimental and simulation findings.[25,28,29] This decrease is caused by the small, but finite, volume of the solution that is occupied by micelles. Although the slight downward drift affects the average free monomer concentration and therefore the CMC, the impact on our analysis seems negligible. The error introduced by our definition of the CMC also applies to most other published CMC measurements and does not appear to affect certain systems more or less than others.[25,28,29]

Several factors can affect the CMC including increasing the size of the hydrophobic portion of the surfactant molecule, increasing the temperature of the solution, or the addition of electrolytes (for ionic surfactants) or organic molecules. As the hydrophobic tail portion of a surfactant is increased, surfactant molecules favour

micelle formation. In aqueous solutions, the addition of two CH_2 groups approximately quarters the value of the CMC (Table 1). This trend is even more pronounced for non-ionic surfactants.[9]

Table 1 – CMC values for a series of sodium alkyl sulphates in water in 40°C.[9]

	Number of Carbon Atoms					
	8	10	12	14	16	18
CMC ($\times 10^{-3}$ M)	140	33	8.6	2.2	0.58	0.23

The CMC generally increases with the temperature of the bulk surfactant solution (Table 2).[30,31] Thermal agitation of the solution opposes the formation of micelles. For example, Akhter and Alawi examined the temperature effect on surfactants using conductance and surface tension methods. They found that the CMC values increased with increasing temperature.[31]

Table 2 – CMC values of sodium laurate at different temperatures.[31]

Surfactant	CMC ($\times 10^{-4}$ M)			
	22°C	27°C	32°C	35°C
Sodium laurate	7.5	7.9	8.3	8.6

The addition of electrolytes to a solution of ionic surfactants lowers the CMC. The electrolyte reduces the repulsion between the charged groups at the surface of the micelle by the screening action of the added ions.[9]

The addition of organic molecules can affect the CMC in a variety of ways. Akhter and Alawi examined the effect of the presence of alcohols at different

concentrations on the CMC of anionic surfactants.[31] They found that the CMC increased with the addition of methanol and ethanol and decreased with the addition of higher alcohols. They explained that the increase in CMC with the addition of methanol and ethanol was because these formamide – alcohol mixtures acted as better solvents; however, the decrease in CMC on addition of n-propanol, n-butanol and n-pentanol may result from the penetration of alcohol molecules into the micelles. They also explained that the CMC increased when the concentration of the alcohol in formamide was increased because the increased alcohol concentration improves the solubility of the non-polar part of the anionic surfactant in non-aqueous solutions.[31]

Significant research time and resources have been spent trying to synthesize new surfactants with lower CMC values.[2,8,32] The practical uses of surfactants drive this endeavour. The use of surfactants in drug delivery requires an accurate measure of the surfactant's CMC.[8] For example, precipitation of the transported drug may occur when the surfactant system undergoes a large dilution after introduction into the body. Precipitation may occur if the surfactant is diluted below its CMC and may have very serious consequences. Therefore, ideally the CMC of the surfactant used should be as low as possible in order to avoid such problems.[8] In addition, surfactants are the emulsifiers, solubilizers, wetting and cleaning agents, foam producers and conditioning aids that are found in everyday products from make-up to skin care. For example, surfactants are the main constituents of shower gels, bath foams, and shampoos. The use of surfactants with a lower CMC has been shown to reduce the potential for skin irritation and decrease the cost of the formulation.[1,2]

1.4 – Micelles

The formation of micelles, like other processes, can be explained by considering the Gibbs energy of the system. The reduction in Gibbs energy of a surfactant solution drives the system to reach equilibrium between free surfactant monomers and surfactants in micelles.[2,9]

The structure of surfactants dictates the favorable arrangements that will decrease the enthalpy (ΔH) and/or increase the entropy (ΔS) to result in an overall reduction in the Gibbs free energy (ΔG) of the system; see Equation [1]. In water, hydrophobic forces cause the tail or hydrophobic spacers to congregate to reduce the number of water contacts. This shielding of the hydrophobic sections of a surfactant molecule results in lower system enthalpy and higher system entropy.[2,9]

$$\Delta = \lambda - \Delta \qquad [1]$$

The system enthalpy is impacted by micellar shape, concentration, and surfactant morphology. Structural curvature usually costs the system energy; therefore, the formation of micellar structures that minimize curvature, such as spheres, minimizes this cost. In comparison, micelles in the shape of rods, cones, and disks would have higher structural curvature and therefore cost the system more energy. When the concentration of the surfactant in solution is sufficiently increased, surfactants tend to align in bi-layers, which have no structural curvature and are lower in energy.[9,33,34]

Surfactant morphology also affects the shape of the micelles formed. Tail length, head configuration and spacers all influence the packing arrangement. For example,

when using Monte Carlo[4] and molecular dynamics[35] modeling, gemini surfactants with short hydrophobic spacers have been found to give thread-like micelles, while long hydrophobic spacers tend to form rod-like micelles. As well, gemini surfactants with hydrophilic spacers produce spherical micelles.

Entropy plays a prominent role in micelle formation. The entropy or tendency towards system disorder should increase to result in a decrease in the free energy of the system. According to the second law of thermodynamics, the entropy of the universe is always increasing or remains constant. Thus the entropy of the system can decrease, as long as it is balanced by an equivalent or greater increase in the entropy of the surroundings.[2,9]

Consider a solution of surfactants. If we think of the surfactants as the system, then the water acts as the surroundings. Thus the formation of micelles constitutes a decrease in the entropy of the system as the surfactants become more ordered and separate from the water. As micelles are formed, the number of free surfactant monomers in solution decreases, reducing the number of water/surfactant contacts. This results in an increased number of water/water contacts, which constitutes a higher water entropy. The formation of micelles is therefore entropically driven by the increase of water entropy of a surfactant solution.[2,9]

1.5 – Double-Headed (Dicephalic) Surfactants

The need for surfactant technology in a wide range of applications has lead to the development of several novel surfactant systems with unique properties. Since the mid 1980s a number of groups have focused on preparing surfactants with two or more head

groups contained on a single tail.[12,36,37] A variety of double-headed surfactants have been produced, many with very elaborate head groups (Figure 6 for example).[38,39,40]

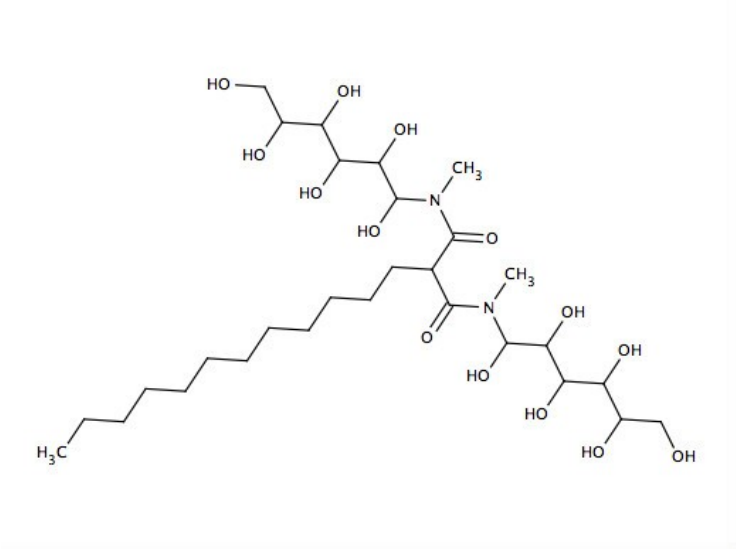

Figure 6 – Structural formula of dodecyl-malono-bis-N-methylglucamide.[40]

Haldar et al.[41] synthesized and characterized a series of multi-head pyridinium surfactants using small-angle neutron scattering (Figure 7). They found the nature of the surfactant aggregates was dependant on the number of head groups. Aggregates of single-headed surfactants tended to contain more surfactant molecules and form in layers while the double- and triple-headed preferred to form spherical micelles with fewer molecules.[41]

Jobe et al.[36] and MacInnis et al.[37] synthesized and studied the micellar properties of a series of double-headed surfactants disodium 4-alkyl-3-sulfonatosuccinates. In particular, they investigated surfactants with an alkyl chain (R1) of length 7 – 10 carbon atoms (Figure 8).

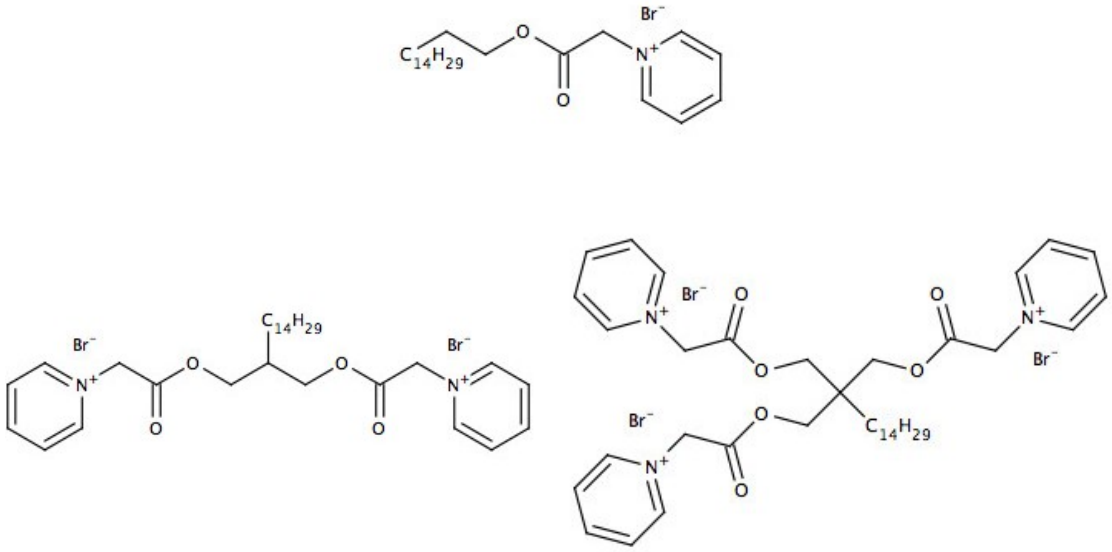

Figure 7 – Structural formula of multi-headed pyridinium surfactants.[41]

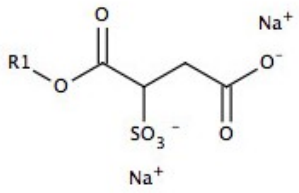

Figure 8 – The structural formula of the disodium 4-alkyl-3-sulfosuccinate surfactants where R1 represents the carbon chain of length 7 - 10.[36,37]

In a related series where the charged head groups are on adjacent carbons, Comeau et al.[12] synthesized disodium 1,2-alkanedisulfates with an alkyl chain length between 10 and 16 carbon atoms (Figure 9). All three groups found that the addition of the second head group greatly affected the CMC values and average micelle size distribution (N_g). N_g gives the average concentration of micelles of size N at a specific total surfactant concentration. The N_g is an important characteristic of a surfactant solution above the CMC and it is a measure of the size and dispersity of the micelles.

The N_g has typically been found using light-scattering,[42] sedimentation rates in an ultra-centrifuge,[43] NMR self-diffusion coefficients,[44] small-angle neutron scattering,[45] freezing point and vapour pressure methods.[46]

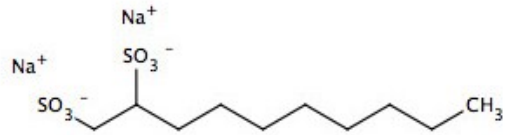

Figure 9 – The structural formula of disodium 1,2-decanedisulfate.[12]

Comeau et al.[12] found that the second head group made the molecules more water soluble and made it more difficult for them to cluster and form micelles. This resulted in higher CMC values and lower average micelle sizes than that of a conventional single-tailed surfactant. Comeau et al.[12] found that the CMC values for a double-headed surfactant were significantly higher (approximately 5 times) than the corresponding single-headed surfactant of equal chain length. A series of disodium 1,2-alkanedisulfates were synthesized by the addition of chlorosulfonic acid to the corresponding 1,2-alkanediol. The CMC values, obtained from conductance and counter-ion emf measurements for this double-headed series, were compared to the values for the corresponding single-tailed sodium alkanesulfates (Table 3).

In a recent article, Roszak et al.[47] again confirmed the previous findings with CMC trends for double-headed surfactants. They completed a detailed CMC study using conductivity and ^{1}H NMR measurements (Table 4) for a series of surfactants composed of a linear alkoxy chain and two trimethylammonium bromide head groups connected to a benzene ring (Figure 10).

Table 3 – The CMC values for disodium 1,2-alkanedisulfates and sodium alkanesulfates as a function of carbon chain length.[12]

Carbon Chain Length	Alkanedisulfates	Alkanesulfates
	CMC ($\times 10^{-3}$ M)	CMC ($\times 10^{-3}$ M)
10	162.2	32.5
12	38.5	8.36
14	11.6	2.20
16	3.76	0.57

Table 4 – The CMC values obtained by Roszak et al. from conductivity (1/R) and ^{1}H NMR (NMR) measurements on a series of double-headed surfactants and compared to the single-headed surfactants of the same length (mono) at 25°C.[47]

R1 Group	CMC ($\times 10^{-3}$ M) (1/R)	CMC ($\times 10^{-3}$ M) (NMR)
$C_{10}H_{21}$	43.4	45.2
$C_{12}H_{25}$	16.4	14.6
$C_{14}H_{29}$	5.54	4.73
$C_{16}H_{33}$	2.02	1.57
$C_{18}H_{37}$	(a)	(a)
Mono-$C_{10}H_{21}$	2.14	2.08
Mono-$C_{14}H_{29}$	0.140	(b)

(a) Below the Krafft Temperature.
(b) Too low for NMR measurement.

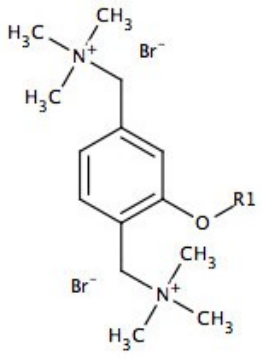

Figure 10 – Structural formula for the series of double-headed surfactants synthesized by Roszak et al. (R1 = $C_{10}H_{21}$, $C_{12}H_{25}$, $C_{14}H_{29}$, $C_{16}H_{33}$ or $C_{18}H_{37}$).[47]

A sub-group of the double-headed surfactants is called the bolaform surfactants.[48,49,50] The head groups in bolaform surfactants are at both ends of the nonpolar chain. Several examples of bolaform surfactants have been synthesized. Franceschi et al.[51] synthesized and characterized a series of urocanic bolaform surfactants using surface tension and conductance measurements, spectrophotometry, as well as light scattering and electron microscopy (Figure 11).

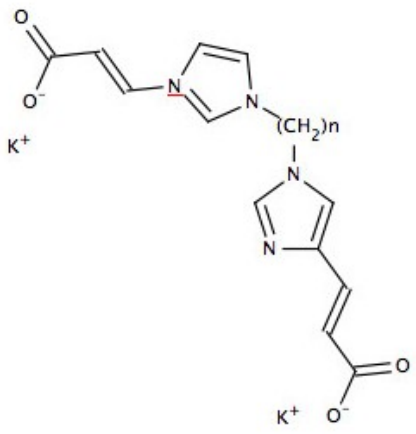

Figure 11 – Structure of a urocanic bolaform surfactant, where n = 8, 12 or 16.[51]

Other examples of bolaform surfactants have been formed with gluconamide head groups and an alkyl chain or cyclohexane as the nonpolar spacer.[39] In all cases it has been found that the head groups on the extremes of the surfactant molecule significantly restrict the molecule's configuration either as a monomer or in micelles. Plots of the surface tension versus the log of the surfactant concentration have indicated that the cross-sectional area of bolaform surfactants is almost twice that of a conventional single-tailed surfactant of the same chain length. This indicates that bolaform surfactants adopt a looped configuration at the air-water interface. This is supported by the fact that CMC values for bolaform surfactants tend to be the same as conventional single-tailed surfactants of half the alkyl chain length.[52,53,54,55]

1.6 – Gemini (Dimeric) Surfactants

Gemini surfactants are a relatively new class of surfactants composed of two single-tailed surfactant molecules attached together by a spacer.[13,56,57,58] The single-tailed surfactant molecules can be fastened together by the spacer at both head groups or on the tails. The spacer can either be hydrophilic or hydrophobic in nature however, hydrophobic is more common. The term gemini surfactants was assigned to bis–surfactants with a rigid spacer (i.e. benzene, stilbene) by Menger and Littau.[13] The name was then extended to include other bis-, dimeric or double-tailed surfactants with two identical heads and tails connected by a spacer.

Research interest into gemini surfactants is driven by their distinct properties (discussed below) and practical applications. Gemini surfactants are associated with thousands of patents with uses ranging from biodegradable cleaners to certain cationic

gemini surfactants with low toxicity that have been shown to have superior ability to introduce genes into cells.[59]

Gemini surfactants have several favorable properties over conventional single-tailed surfactants. Of primary importance are the remarkably low CMC values of gemini surfactants compared to conventional single-tailed surfactants of equivalent chain length. Increasing the tail length of a single-tailed cationic surfactant by four carbon atoms lowers the CMC by 16-fold (Table 5). However, increasing the tail length of a corresponding gemini series lowers the CMC by two orders of magnitude (Table 5).[56]

Table 5 – The CMC values for conventional single-tailed surfactants (1 and 2) and their corresponding gemini surfactants (3 and 4).[56]

	Surfactant	CMC ($\times 10^{-3}$ M)
1	$C_{12}H_{25}N^{+}(CH_3)_3Br^{-}$	16
2	$C_{16}H_{33}N^{+}(CH_3)_3Br^{-}$	1
3	$C_{12}H_{25}N^{+}(CH_3)_2-(CH_2)_{16}-N^{+}(CH_3)_2C_{12}H_{25}2Br^{-}$	0.12
4	$C_{16}H_{33}N^{+}(CH_3)_2-(CH_2)_2-N^{+}(CH_3)_2C_{16}H_{33}2Br^{-}$	0.003

The CMC of gemini surfactants is also sensitive to the length of the spacer. A long hydrocarbon spacer of 16 methylene groups reduces the CMC by almost ten-fold when compared to a spacer of three to eight methylene groups. Increasing the number of carbon atoms in the spacer increases the overall hydrophobicity of the gemini monomer, reducing its solubility and enhancing its tendency to self-assemble (Table 6).[57]

Table 6 – The CMC values for a series of gemini surfactants of the form $\left[{}^{1}{}_{12}H_{25}(\ {}^{2}H_3)_2N-(\ {}^{3}H_2)_sN(\ {}^{4}H_3)_2C_{12}H_{25}\right]Br_2$ (designated $C_{12}C_sC_{12}Br_2$), where s represents the number of carbon atoms in the spacer.[57]

Surfactant	CMC ($\times 10^{-3}$ M)
$C_{12}C_4C_{12}Br_2$	1.01
$C_{12}C_6C_{12}Br_2$	0.83
$C_{12}C_8C_{12}Br_2$	0.68
$C_{12}C_{10}C_{12}Br_2$	0.28
$C_{12}C_{12}C_{12}Br_2$	0.21

Solubilization is an important property required in ternary (i.e. three component systems, in this case a mixture of oil, water and surfactant) oil recovery and detergency, as both are involved with the phenomenon of homogenization. Engberts et al.[58] have shown that cationic gemini surfactants are better solublizers than single-tailed surfactants, because of their very low CMC values.

Surface activity, the strong adsorption of surfactants at surfaces or interfaces in the form of a monolayer, has wide industrial applications. The surface tension (γ) of water (72 mN m^{-1} at 25°C) is normally reduced to a value of 30-40 mN m^{-1} at the CMC of the surfactant.[9] Another means of reporting surface activity is in terms of the C_{20} values. This value corresponds to the surfactant concentration that reduces the surface tension by 20 mN m^{-1}. The C_{20} value is a comparative measure of a surfactant's ability to adsorb at the air-water interface.[9] Interest in gemini surfactants has been fuelled by the fact that they are more surface active by three orders of magnitude than single-tailed surfactants (Table 7). For example, Sun et al.[60] investigated the surface activity of a homologous

series of gemini surfactants with identical hydrophobic tails but different ionic head groups (Figure 12).

Table 7 – CMC, C_{20} and γ_{CMC} obtained for the zwitterionic gemini [C12(-)-C12(+)] surfactant in Figure 12 as well as the corresponding single-tailed [C12(-)]surfactant.[60]

Surfactant	CMC ($\times 10^{-3}$ M)	C_{20} ($\times 10^{-3}$ M)	γ_{CMC} ($\times 10^{-3}$ N/m)
C12(-)	17.4	1.48	34.6
C12(-)-C12(+)	0.0743	0.0013	26.2

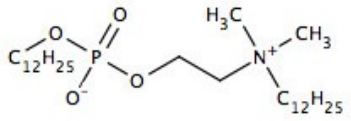

Figure 12 – Zwitterionic Gemini surfactant C12(-)-C12(+).[60]

Gemini surfactants are equivalent to two conventional single-tailed surfactants linked by a spacer on or close to the head groups. It has been found that the packing of the hydrophobic groups in gemini surfactants at the air–water interface, when the spacer is small and hydrophilic, is closer than that found in comparable conventional surfactants. The tighter packing of the hydrophilic groups of gemini surfactant results in a more cohesive and stable interfacial film. This may be the reason for more lowering of surface tension at the CMC by gemini surfactants.[59]

Gemini surfactants have also shown promise in the formation of vesicles[16] and gels,[61,62] which have several practical uses. One of the most intensely investigated aspects of vesicles relates to their ability to encapsulate drugs within their bi-layer shells.

Many gels consist of long fibers or crystals that cross-link non-convalently or simply entangle with one another creating a three-dimensional network that imparts rigidity to the system. Gels are useful colloidal systems with wide applications in photography, drug delivery, cosmetics, sensors, and food processing. [59,63]

1.7 – Asymmetric Gemini Surfactants

In recent years the definition of gemini surfactants has broadened to include species with different polar head groups and asymmetric tail groups. Very few examples of asymmetric surfactants exist. Menger and Peresypkin[63] synthesized 10 asymmetric gemini surfactants with the general structure $ROPO_2^-OCH_2CH_2N^+(CH_3)_2R'$, where tail R contained between 14 and 22 carbon atoms and R' contained between 6 and 9 carbon atoms (Figure 13).[63] Using dynamic light scattering, transmission electron microscopy and cryo-high resolution electron microscopy, they investigated the self-assembly of the asymmetric gemini surfactants into vesicles. Menger and Peresypkin found that the molecules formed strings of vesicles that rigidified the aqueous systems (i.e. formed gels).[63]

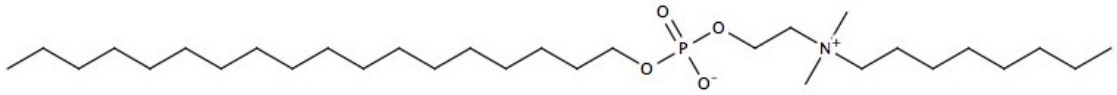

Figure 13 – The gemini surfactants $ROPO_2^-OCH_2CH_2N^+(CH_3)_2R'$, where tail R contains 18 carbon atoms and R' contains 8 carbon atoms.[63]

With the ultimate goal of better understanding the potential of gemini surfactants to act as synthetic vectors for delivery of genes into cells to induce protein expression, Wang et al.[64] synthesized two new pyrene-based asymmetric gemini surfactants as fluorescence probes: N^1-dodecyl,N^1,N^1,N^3,N^3-tetramethyl-N^3-(6-(pyren-6-yl)-hexyl) propane-1,3-diammonium dibromide (Py-3-12) (Figure 14) and N^1-dodecyl,N^1,N^1,N^6,N^6-tetramethyl-N^6-(6-(pyren-6-yl)-hexyl)hexane-1,6-diammonium dibromide (Py-6-12). Aqueous solutions of Py-3-12 and Py-6-12 were studied using surface tension, specific conductance, dynamic light scattering, isothermal titration calorimetry, and fluorescence techniques to examine the physicochemical properties and morphologies of the self-assembled aggregates. As well, they investigated the interaction between the asymmetric gemini surfactants and DNA (salmon sperm) using UV-vis and fluorescence spectroscopy.[64]

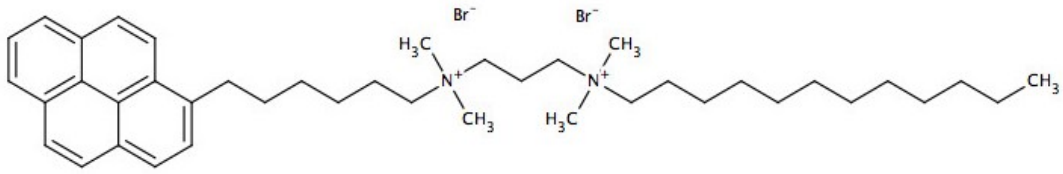

Figure 14 – Structure of Py-3-12.[64]

Using surface tension measurements, Wang et al.[64] determined that the CMCs of Py-3-12 (0.22 ± 0.02 mM) and Py-6-12 (0.30 ± 0.06 mM) are less than their symmetrical counterpoints 12-3-12 (0.91 mM) and 12-6-12 (1.12 mM). They attribute this to the presence of the more hydrophobic pyrene group.

Wang et al.[65] used microcalorimetric measurement, electrical conductivity measurement, steady-state fluorescence measurement, and time-resolved fluorescence

quenching to measure the CMCs and enthalpies of micellizaton of a series of asymmetric gemini surfactants, $\left[C_mH_{2m+1}(CH_3)_2N(CH_2)_6N(CH_3)_2C_nH_{2n+1} \right]Br_2$ designated $C_mC_6C_nBr_2$ with a constant n + m = 24 and m = 12, 13, 14, 16, 18, where m and n are the chain length of each tail. The study of this series of asymmetric gemini surfactants reported that the degree of asymmetry of the tails (m/n) had a measurable effect on micellization. They found that as the m/n ratio increased, the CMC decreased linearly by about 35%, the average micelle size at the CMC increased slightly, and the Gibbs free energy of micellization became more negative (Table 8).[65]

Table 8 – The CMC values for a series of asymmetric gemini surfactants with the general formula $\left[C_mH_{2m+1}(CH_3)_2N(CH_2)_6N(CH_3)_2C_nH_{2n+1} \right]Br_2$.[65]

		CMC ($\times 10^{-3}$ M)		
	m/n	Conductivity Measurement	Fluorescence Measurement	Microcalorimetric Measurement
$C_{12}C_6C_{12}Br_2$	1	1.01	1.09	0.89
$C_{13}C_6C_{11}Br_2$	1.18	0.98	1.04	0.86
$C_{14}C_6C_{10}Br_2$	1.4	0.95	0.99	0.82
$C_{16}C_6C_8Br_2$	2	0.83	0.88	0.73
$C_{18}C_6C_6Br_2$	3	0.65	0.71	0.58

It is interesting to note that in an earlier paper from the same group,[66] they used only microcalorimetry and concluded that there was a small decrease in CMC as the ratio m/n increased but that this decrease was not much larger than the error in measurement. This is not surprising given that observed changes due to asymmetry, while observable, are small compared to those caused by a change in, for example, tail or spacer length which can change the CMC by factors of 10-100.[56,57] Therefore by comparison to other

architectural properties, asymmetry does not have a strong influence. As we describe in more detail in the following chapters, this thesis attempts to test if this is a general feature of surfactant systems.

CHAPTER 2 – SIMULATION MODELS

2.1 – Monte Carlo Computer Simulations

Surfactant systems have been modeled in the past by Monte Carlo (MC) and molecular dynamics (MD) simulation methods. MD simulates the time evolution of the model molecular system according to classical equations of motion and provides the trajectory of the system in its phase space.[67,68] In MD, the evolution of the molecular system is modeled as a series of snapshots or configurations evaluated at close time intervals. Consecutive configurations are typically on the order of 1 femtosecond apart and a full-scale run would be 1 – 100 nanoseconds in length. One disadvantage of MD simulations is that current computational power limits system size to approximately 10^4 to 10^6 atoms. MD simulations are continuous in time and space.

An alternative approach is to use MC techniques.[69,70] Instead of trying to reproduce the dynamics of the system, MC generates states according to appropriate Boltzmann probabilities. A large number of system configurations are accumulated and the desired properties for each state are calculated. These data are then used to calculate thermodynamic averages of the system. MC methods are typically divided into two classes: on-lattice MC, which is discrete in both space and time; and off-lattice MC, which is discrete in time but continuous in space.

MC methods are based on the principles of equilibrium statistical mechanics, in which the fundamental premise is that all of the essential information about the system under consideration can be represented by a partition function.[71] The general form of the partition function for a classical system is:

$$Z = \sum_{all\ states} e^{-H/k_B T} \qquad [2]$$

where H is the Hamiltonian for the system, T is the temperature, and k_B is the Boltzmann constant. The sum is over all possible states of the system and therefore is dependent on the size of the system and the number of degrees of freedom for each particle.

In equilibrium, the value of any thermodynamic property A (e.g. the system energy or the average number of free monomers in a surfactant solution) can be expressed as,

$$A = \sum_{c=all\,states} A_c P_c \qquad [3]$$

where A_c is the value of the property A in a particular state c, and P_c is the probability that state c occurs in equilibrium. P_c is given by,

$$P_c = \frac{e^{-H_c/kT}}{Z} \qquad [4]$$

where H_c is the value of the Hamiltonian for state c.

In 1949 Metropolis and Ulam, introduced the use of Monte Carlo simulations using "modern computing machines."[72] Most of the MC simulations of surfactants have employed the Metropolis algorithm.[4,7,27] The Metropolis MC method starts with a randomly configured system. A new trial configuration of the system is then created by making a random change to some subset of the system. Following the randomly selected

move, the total energy of the trial configuration is calculated and the energy difference between the initial and trial configuration is found. If the trial configuration is lower in energy than the initial configuration, it is automatically accepted. However if it is higher in energy, then the trial configuration is accepted based on a Boltzmann probability,

$$P = \quad ^{-\Delta E/k_b T} \qquad [5]$$

In other words, uphill moves are accepted based on the Boltzmann probability (P) where ΔE is the change in energy from one system configuration to the next.

The Metropolis MC method works because it can be proven[72,73,74] that by selecting new states based on the Boltzmann probability P, then the set of system configurations generated by the MC method each occur with the correct probabilities P_c given in Equation [4]. As a result, the thermodynamic value of a property A is estimated from a MC simulation simply from,

$$A = \sum_{c=states sampled} A_c \qquad [6]$$

where A is the sum is over all the states of the system generated by the MC selection procedure. The accuracy of A obtained from a MC simulation increases as the number of sampled states increases.

It is important to note that the MC method correctly incorporates the influence of both energy and entropy on the value of thermodynamic properties obtained from the approach. The energy is included through the Hamiltonian required to compute the

Boltzmann factor. The entropy is accounted for in the exploration of states required to form the sum over configurations. For high entropy thermodynamic states, there will be a wider range of configurations to sample than for low entropy thermodynamic states. This difference is automatically accounted for when the selection of states is controlled according to the Boltzmann probability.[72,73,74]

Why use On-Lattice Monte Carlo?

One of the main goals of this thesis is to design a versatile code capable of simulating several possible surfactant environments, as well as many surfactant structures. This is important so that the code can be more readily used as a preliminary step to possible synthetic research avenues. The use of on-lattice MC allows for larger system sizes, both in terms of lattice sites and surfactant concentration compared to MD. It also allows for longer relaxation times, facilitating for example the study of lower temperatures. As well, on-lattice MC is a widely accepted method for modeling surfactant systems and obtaining CMC values,[75,76,77] thanks largely to the pioneering work of Larson.[5,78,79] Although on-lattice MC has been used to model several surfactant systems, there are still gaps in the literature for possible exploration.

2.2 – Larson-Type Models

Surfactants form micelles in water because of the "hydrophobic effect".[23] The configurational entropy of water is significantly lowered by contact with hydrophobic solutes because the number of ways the water molecules can hydrogen bond with neighbouring water molecules is reduced when in the presence of a solute molecule. This

effect can dominate all other contributions to the total free energy of the system. As a result, hydrophobic solutes in water are driven to aggregate in order to minimize the surface area of the solutes in contact with water, and hence minimize the total system free energy.

Larson completed the first simulation studies of surfactants on a lattice using an effective Hamiltonian to mimic the consequences of the hydrophobic effect, without having to model the solvent explicitly.[5,78,79] In Larson's approach, the surfactants are represented by linear chains of connected sites on a lattice. Sites of the lattice that are not occupied by surfactant chains are considered to be occupied by solvent molecules. The total energy of the system configuration is calculated using a specific Hamiltonian. The hydrophilic or hydrophobic nature of any component on the lattice is established by appropriate assignment of interaction energies. The energy of the system is defined as the sum of all the nearest-neighbour interactions in the system. Each lattice site interacts with its neighbours through specific dimensionless interaction energies, $\varepsilon_{a,b}$, where a and b represent, for example, either a head (H), tail (T), spacer (S) or water (W) lattice site. Energy and temperature are both expressed as dimensionless quantities, relative to a specific interaction energy. Therefore the total (dimensionless) energy of the system, can be found by the following Hamiltonian, where $n_{a,b}$ is the number of a,b interactions in the system; see Equation [7].

$$H = \sum_{a,b} {}_{b}\varepsilon_{a,b} \qquad [7]$$

In a Larson-type model, such as that used in this thesis, the pair-wise interaction energies between species are chosen so as to reproduce the consequences of the hydrophobic effect, without having to explicitly include the hydrogen bonding degrees of freedom of the solvent. Even though the bonding energy between water molecules (hydrogen bonding) is much stronger than that between hydrophobic tail molecules (due to dispersion forces), numerous simulation studies[5,78,79,80,81,82,83] have shown that the result of the hydrophobic effect (aggregation of the tails), can be qualitatively reproduced in a Larson-type model. This can be accomplished by, for example, setting both the tail-tail and water-water interactions to zero and assuming instead that the tail molecules have a strong repulsive interaction with the water. This achieves the goal of driving the tails to spatially segregate from the water molecules, while at the same time vastly reducing the computational demands of the model, since all tail-tail and water-water contacts are ignored. As shown in Section 3.5, the value of the tail-water interaction makes the dominant contribution to the behavior of the system, largely because tail-water contacts are the most numerous of all contacts in the system.

The solvent in a Larson-type model is thus called an "implicit solvent", in the sense that the solute-solvent interactions are chosen so that the influence of the solvent is represented in the behavior of the solute molecules, without having to model the solvent-solvent interactions explicitly.

Many studies have been completed using the Larson-type model, and a variety of interaction energies have been chosen to reproduce the consequences of the hydrophobic effect. Kim et al.[84] used a cubic lattice to examine the ternary system of oil, water and surfactants with the form H_xT_y, with x hydrophilic head units and y hydrophobic tail

units. Their study also involved oil molecules (T_x) of length x and single-site water molecules. They state that interactions between two head groups, a head group and a water monomer, and two water monomers are represented by ε_{HH}. Similarly, ε_{TT} represents interactions between two tail groups, a tail group and oil monomer, and two oil monomers. Interactions between head or water groups and tail or oil groups are defined by ε_{HT}. Kim et al.[84] set ε_{HH} and ε_{HT} interaction to zero and the ε_{TT} interactions to –2. This results in attractive interactions for neighbouring tail-tail, tail-oil and oil-oil groups.

In another study of surfactants in the form H_xT_y, Nelson et al.[85] examined the symmetric H_2T_2 surfactant on a 20×20×20 cubic lattice. Using the interaction energies ε_{HH}, ε_{TT}, ε_{WW} and $\varepsilon_{HW} = 0$ and ε_{HT} and $\varepsilon_{TW} = 1$, they found their model to be consistent with simple thermodynamic models showing micelles of spherical and cylindrical shape in equilibrium with each other.

Three papers have been published by the same research group using the interaction energies ε_{HH}, ε_{TT} and $\varepsilon_{HW} = -1$ and ε_{HT} and $\varepsilon_{TH} = 1$, as well as, $\varepsilon_b = 1$ a conformation energy that costs the system energy for every bend in a surfactant molecule. In their first two papers, de Moraes et al.[77,86] examined conventional single-tailed surfactants of length 3 on a two-dimensional 100×100 square lattice. In their third, Girardi et al.[75] modeled conventional single-tailed surfactants of length 4 on a cubic 40×40×40 lattice. They found that the value of the CMC increased with increasing temperature.

Kapila et al.[6] chose parameters equivalent to $\varepsilon_{TW} = +1$, $\varepsilon_{TH} = +1$, $\varepsilon_{HW} = -5.77$ and $\varepsilon_{HH} = +5.77$, with all others set to zero. They studied the surfactants H_1T_{12} and H_7T_{12} on a two-dimensional 192×192 square lattice. They examine the effect on surfactant

aggregation as a result of the number of head groups and the interactions between them (short-range versus long-range).

For all these papers, there are clear similarities even though there are varied interaction energies. First, the magnitudes of the interaction energies are all on the same order. Second in most cases the differences in the various interaction energies are the same; in other words the same interactions are favorable or unfavorable, relative to one another. Third, despite the differences in the energy parameters employed, in all cases there was formation of micelle-like aggregates.

2.3 – Monte Carlo Dynamics for Surfactant Systems

To implement the Metropolis MC procedure described in Section 2.1 for a particular system, one must decide how new system configurations will be generated from existing configurations. In the case of a Larson-type model of a surfactant system, this means deciding how the surfactant chains will move on the lattice. Many MC simulations of polymer and surfactant systems employ a configuration-changing move called reptation.[87] Reptation is based on a "slithering snake" algorithm where: (i) The terminal head or tail unit randomly moves to a nearest neighbour site. In Figure 15, the head unit labeled 1 is chosen to move to the lattice site with a solvent molecule "A". (ii) The second unit (attached to the terminal head or tail unit) moves forward to replace the original lattice position of the terminal head or tail unit. In Figure 15, the tail unit labeled 2 moves up to the position of the head group labeled 1. (iii) The third unit in the chain moves forward to replace the original lattice position of the second unit and the process repeats itself as it propagates along the length of the surfactant molecule (Figure 15).

(iv) The displaced solvent molecule takes the place of the old terminal head or tail unit site. In Figure 15, the solvent molecule labeled "A" moves to the old terminal tail unit site labeled 6. The end result is a one-lattice-site move by the whole surfactant in the randomly chosen direction. Through reptation, all statistically significant configurations of the system can be obtained.[88] However, reaching equilibrium using solely reptation takes a significant number of MC steps. As a result, several other moves have been employed in the literature to facilitate the formation and dissolution of micelles and also as aides in shortening equilibrium times. To ensure that the equilibrium state is not changed by the added move it must have a corresponding move which can undo the change to satisfy the"detailed balance" condition.[89] Some moves, e.g. reptation, can undo themselves.

Additional local moves include spontaneous chain buckling, the "pull" move, and kink movement (Figure 15). These moves are classified as local moves because they cause a change in less than five lattice sites adjacent to the randomly chosen surfactant molecule. An example of a global move is the single surfactant transport move (SST) (Figure 15). The spontaneous chain buckling move occurs when a portion of the tail or spacer is randomly picked up and allowed to buckle. The pull move is the reverse of spontaneous chain buckling; a portion of the tail or spacer is pulled to make the buckle straight. The kink move allows for the extension of a buckle or a rotation of an end of a chain. The SST move relocates the surfactant with the same orientation to any location on the lattice, provided it does not overlap any other surfactant at that location.

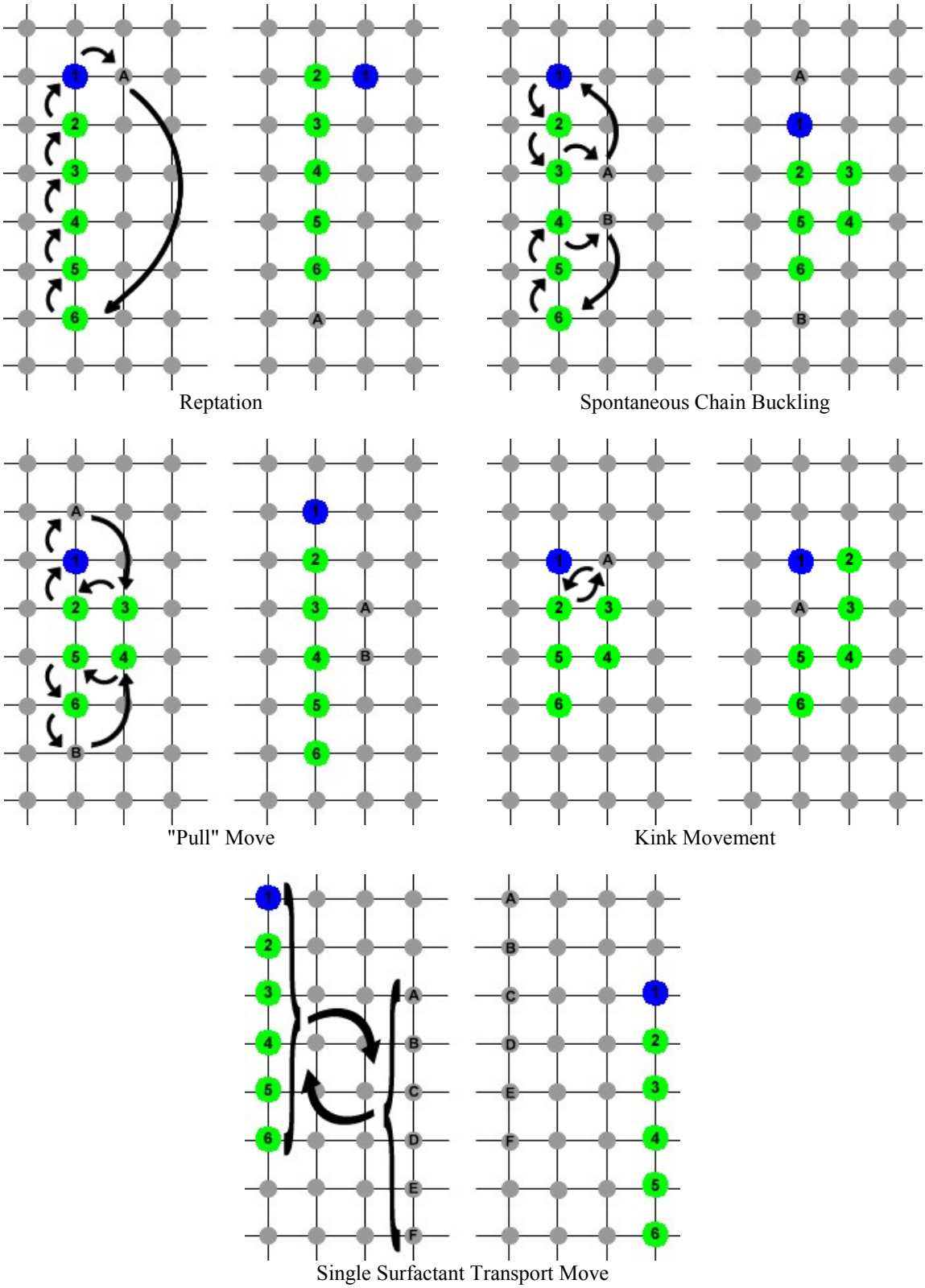

Figure 15 – A schematic of the system configuration changing moves employed by many MC models. Head(●) – Tail(●) – Water(●)

Once the configuration-changing moves have been decided, the other key dynamical issue in MC simulations is deciding how many MC steps to carry out in order to accurately estimate the values of thermodynamic properties. It is important that the system has reached equilibrium before measuring the desired property. Typically initial runs of the code are completed to monitor the system energy in order to determine the number of MC steps required for the system to reach equilibrium. Production runs of the code are typically broken into 3 phases: (i) a system relaxation phase that contains a sufficient number of MC steps for the system to reach equilibrium; (ii) an equilibrium running phase in which the equilibrium state of the system is monitored to ensure that equilibrium has truly been established; and (iii), a production phase over which the desired properties are determined as averages over time.

2.4 – Previous Computer Models of Gemini Surfactant Systems

To our knowledge, there are no previous simulation studies of the CMC of double-headed surfactant systems, as compared to single-headed case. There are also very few MC models of gemini surfactants and no studies of asymmetric gemini surfactants. Below we summarize what has been learned in previous simulation studies of gemini surfactants.

The interactions of anionic polyelectrolytes with anionic gemini surfactants has been investigated using MD simulations. The model of Xu et al.[90,91] accounts for long-ranged electrostatic and short-ranged hydrophobic interactions and shows how the surfactant/polyelectrolyte mixture evolves over time. They found that gemini surfactants interacted more strongly with the oppositely charged polyion chains than the

conventional single-tailed surfactant equivalent. They found that the critical aggregation concentration (CAC) of the gemini/polyelectrolyte was lower than the CMC of the free surfactant. The CAC is the surfactant concentration at which mixed aggregates of surfactants and polyelectrolytes form.

Burrows et al.[92] used MD modeling and fluorescence measurements to examine the electrostatic and hydrophobic effects in a mixture of a cationic gemini surfactant and a conjugated polyanion. They found that the initial aggregates of poly[1,4-phenylene-[9,9-bis(4-phenoxy-butylsulfonate)fluorene-2,7-diyl]copolymer (PBS-PEP) were broken up upon the addition of the gemini surfactants $C_sH_{2s}-\alpha,\omega$-bis$(C_{12}H_{25}N^+(CH_3)_2Br^-)$, where s = 2, 3, 5, 6, 10 or 12. This occurred as a result of the new interactions formed between PBS-PEP and the gemini surfactants. The interactions between PBS-PEP and the gemini surfactants with short spacers were mostly electrostatic between the tetraalkylammonium group of the surfactant and the sulfonate of the polymer. MD simulations suggest Coulombic and hydrophobic effects contribute to the disruption of the polymer aggregates and assist with the formation of polymer/surfactant aggregates.

MD simulations have been used to compare the rheological properties and surface activity at the air/water interface of dodecyltrimethylammonium bromide (DTAB) to the gemini surfactants ethyl-α,ω-bis(dodecyldimethylammonium bromide).[21,93] It was found that both the surface activity and the dilational modulus of the gemini surfactants is higher than the conventional surfactant DTAB.

Khurana et al.[94] investigated a similar series of gemini surfactants to that of Burrow et al.[92] at the air/water interface. They used MD to obtain the surface tension and

to investigate the migration of surfactant monomers from the air/water interface. By varying the initial surface area per surfactant for a series of gemini surfactants, $C_sH_{2s}-\alpha,\omega-bis\left(\ _{12}H_{25}N^{+}\left(\ ^{\prime}H_3\right)_2Cl^{-}\right)$, where s = 3, 4, 6, 12, 14 and 16, they found that certain surfactant lengths gave rise to stable monomer layers at the air/water interface. In most cases, they observed movement of some surfactant molecules from the air/water interface into the aqueous phase, resulting in a stable primary mono-layer of surfactants at the air/water interface and a small concentration of surfactant molecules below it.

There have been several MD models that have investigated the shape of the micelles[95] and bilayers[96] formed by gemini surfactants. Maiti et al.[4] found that gemini surfactants underwent a transition from spherical micelles to cylindrical micelles with increasing surfactant concentration. Further increasing the gemini concentration resulted in the cylindrical micelles transforming into extremely long "wormlike" or "threadlike" micelles. Oda et al.[97] used polarization modulation infrared linear dichroism and MD modeling to investigate exclusively the cylindrical micelles formed by the cationic gemini surfactant $C_2H_4-1,2-\left(\ ^{\prime}H_3\right)_2N^{+}-C_4H_8-C_8F_{17}\Big)_2$. They concluded that there was competition between the charge repulsion of head groups, which favours a surfactant orientation perpendicular to the cylinder axis (high curvature) and the steric repulsion of hydrophobic tails, which favours a surfactant orientation parallel with the cylinder axis (flat curvature).

As previously mentioned, there are very few examples of MC modeling of gemini surfactants. We are aware of only four publications coming from two research groups. Maiti and Chowdhury published the first MC model of gemini surfactants in early 1998.[98] Their results, like the ones presented in this thesis, were based on a Larson-type

simulation model. A follow-up paper was published in late 1998.[4] Their gemini surfactants involved tail (T), spacer (S), and head (H) lattice sites, as well as a neutral (N) site adjacent to each head group. The neutral site was meant to simulate the shielding effects of the charged head group. The structure of the gemini surfactants they studied can be represented by $T_mN_pH_qS_nH_qN_pT_m$, where p=q=1, m=5, 15, or 25 and $2 \leq n \leq 20$. They investigated how the main features of the aggregation of gemini surfactants changed when the spacer was modified.[98]

With respect to hydrophobic spacers, they found that the micelles were far from spherical – "threadlike" for short spacers and "rodlike" for long spacers. As well, they observed non-monotonic behaviour with the CMC as the hydrophobic spacer length was increased. Increased bending stiffness of the hydrophobic tails and spacers resulted in an increase in the CMC. They found that with hydrophilic spacers, the micelles were more or less spherical. They observed a monotonic decrease in the CMC as the length of the hydrophilic spacer was increased.[98] As well, increased bending stiffness of the hydrophilic spacer resulted in a decrease in the CMC. Maiti and Chowdhury concluded that with either hydrophobic or hydrophilic spacers, the aggregate shape was determined by the geometric shape and size of the molecules. As well, with either hydrophobic or hydrophilic spacers, the variation of the CMC with spacer length was strongly influenced by the ionic charge of the head group.[98]

Maiti and Chowdhury[80] also investigated the effect of the addition of lipids or gemini surfactants on the nature of micelles initially formed by conventional single-tailed surfactants. MC simulations showed that when the spacer of the gemini surfactant was hydrophilic and sufficiently long, cross-linking of the micelles formed by the

conventional single-tailed surfactants occurred at a low mole percent of gemini surfactants. When the spacer was hydrophobic, it needed to be completely rigid to facilitate cross-linking. When lipids were added to the solution of conventional single-tailed surfactants, no cross-linking occurred. The mixtures in water formed only isolated micelles containing a mixture of conventional surfactants and lipids.[80]

MC simulations were used by Layn et al.[81] to examine the dependence of temperature, surfactant solubility, surfactant rigidity, and oil chain length on the phase behaviour of ternary mixtures of gemini surfactant, oil, and water. Single site oil molecules exhibited two-phase equilibrium. However, when the oil molecules were lengthened beyond a single lattice site, a three-phase equilibrium first resulted, followed by a return to a two-phase system as a result of increased surfactant solubility in the aqueous phase.

Modifications to the gemini surfactants also resulted in varied phase behaviour. The more hydrophilic surfactants first eliminated the miscibility gap with water followed by the loss of immiscibility with oil at higher temperatures. The transition from a three- to a two-phase equilibrium was promoted by imposing rigidity within the surfactant which decreased the number of contacts available for solvation.

A temperature series of the ternary mixtures studied by Layn et al.[81] yielded expected results. At low temperatures, a three-phase equilibrium is established with the exception of highly soluble surfactants, which yielded only a two-phase equilibrium. In the three-phase equilibrium system, the three-phase region is surrounded on two sides by two-phase envelopes and the surfactant was immiscible with both water and oil over a large composition range. A third two-phase region was established along the water-oil

axis of the phase diagram with an increase in temperature. A further increase in temperature totally eliminated the three-phase region resulting in a stable two-phase region.

2.5 – Direction of this Thesis

Despite the studies summarized in the previous section, there remain several gaps in the literature. One omission of interest to us is the fact that there are no published models of the CMC of double-headed surfactants, or any simulations studies of asymmetric gemini surfactants. Obtaining a better understanding of these two relatively new classes of surfactants will be a primary goal of this thesis, since experimental work on these systems is underway concurrently at StFX University.

In examining these new classes of surfactants we want to explore many choices of parameters (tail length, asymmetry, concentration, temperature, etc.), something synthetic chemists would like to do as a preliminary step. MD is simply too time consuming computationally to allow for this. As a result, MC is the better option for our purposes.

There are two main goals for this thesis. The first is to develop a highly versatile MC code that will allow for the testing of several surfactant systems both in two- and three-dimensions. A versatile code capable of simulating several possible surfactant environments could more readily be used as a precursor to possible synthetic research avenues.

The second is to be the first to model double-headed and asymmetric gemini surfactants to investigate the CMC trends reported by Comeau et al.,[12] Wang et al.,[65] and Bai et al.[66] Comeau et al.[12] found that the addition of the second head group moiety in

double-headed surfactants resulted in a significant increase in the CMC value. However, there is little published literature to provide insight into how the second head group affects the CMC values. The placement and nature of the head group added also has an obvious effect on CMC values. We will use MC simulations to model two double-headed surfactant systems and compare them to a conventional single-tailed surfactant of the same length.

The work of Wang et al.[65] and Bai et al.[66] found that there was a decrease in the CMC values with an increasing ratio of the two tail lengths in asymmetric gemini surfactants. We will examine in both two- and three-dimensions the same series of five asymmetric gemini surfactants used by both Wang et al.[65] and Bai et al.[66] We will also expand this series to include the extremes in surfactant architecture and double-headed asymmetric surfactants.

CHAPTER 3 – DEVELOPING AND TESTING OUR MODEL

3.1 – Materials and Methods

One of the primary goals of this work, from a training perspective, was for me to develop the required simulation code from scratch. At the beginning of the project, I lacked programming experience at this level and I wanted to develop my expertise in scientific computation. Writing the code from scratch guaranteed that I would understand all the required algorithms and their relationship to the scientific problem examined here.

The code for this thesis was written in the Fortran90 programming language, using the "emacs" editing program on a Mac PowerBook G4. Initial code development and testing was carried out on the PowerBook, while computationally demanding tests, and final production runs, were carried out on the Atlantic Computational Excellence Network (ACEnet) high-performance computing clusters.

ACEnet is a partnership between ten Atlantic Canadian universities. Six of the partnering universities have clusters for a total of 3250 computer processors, hundreds of terabytes of storage capacity, and hundreds of gigabytes of available memory. The work for this thesis was completed on the StFX university cluster of 1000 computer processors. In addition to the hardware, ACEnet provides computational assistance through five computational research assistants, a software specialist and 3 Unix systems administrators. Dr. Shah Razul, one of the computational research consultants, gave guidance on this project.

Development and testing of the code was broken into stages. Step one was establishing the list of parameters and coding statements needed to initialize surfactants on a lattice without allowing them to overlap. Next the coding statements for calculating the total system energy were developed and checked manually using a number of system sizes and conditions.

The next step was to develop the coding for the movement of surfactants on the lattice. This involved the development of code statements that chose a surfactant at random, made random changes to the surfactant's location, ensured no overlaps occurred, calculated the new system energy, determined the size and location of the clusters and monomers, and rejected or accepted that move based on the Boltzmann probability. The development and testing of this phase of the coding process was the most time consuming.

Following the development and testing of the code, production runs were carried out using a series of independent data runs on the ACEnet facilities at StFX University. Production runs had to be run on a cluster because of the resources necessary to obtain a single data point. When running, the code easily functioned within the 2 gigabytes of available working memory and the yielded data consumes from approximately 100 megabytes to several gigabytes of storage space depending on the lattice size, surfactant concentration, sampling rate, etc.

The code written for this thesis is not a "parallel" code because there is no communication between runs. Instead, the code must be run with one surfactant architecture, at one temperature, at one concentration, on one processor. However, with the use of queuing software, hundreds of runs can be conducted at the same time. This

method is called “parameter space exploration” and is an example of “embarrassingly parallel computation.”

Three Unix shell scripts were also written to control several features of the code. The first script modified parameters in the code to prepare a series of runs and stored the necessary files in separate folders. Each folder represented one point on the CMC curve. This scripted allowed hundreds of runs to be prepared simultaneously to examine a temperature or architecture series.

The second script went into each of the newly created folders, compiled the code and submitted the executable file to the queuing system. The queuing system provided me with a single access point to the cluster of computers. The resource management software used by the queue accepted jobs submitted by all users and used policies to schedule jobs to be run on appropriate processors on the cluster. This allowed me to submit hundreds of jobs to the cluster without being concerned about where the jobs ran on the cluster or blocking other users.

The final script went into each of the separate folders in a series following completion of the run, pulled out the relevant data and combined it to produce, for example, the final free monomer concentration versus total surfactant concentration curve used to obtain the CMC.

At any given time, between 50 and 100 separate jobs for this thesis would be running on the cluster. For each of the 26 surfactant architectures examined in this thesis, between 60 and 100 separate runs were needed to complete the CMC curves presented. Initial exploratory runs were often first examined and then three production runs for each total surfactant concentration were carried out and averaged to produce 20 unique total

surfactant concentrations points on the CMC curves. A typical 100 × 100 square lattice run at temperature = 2.0, would take approximately 1 day to finish, while a 100 × 100 × 100 cubic lattice would take up to a month. Not all runs in a series took the same length of time to complete. Run times increased with increased surfactant concentration, increased lattice size, increased surfactant length or decreased temperature.

In addition to the working code, a second code was created with the help of Chance Creelman and Amir Mohareb in the C programming language on a Mac Powerbook G4. This code generates snapshots of the surfactant system based on an output file from the working code. This code is essential for monitoring the progress of a run or creating snapshots of the system in equilibrium.

3.2 – Our Larson-Type Model

To complete the first goal of this thesis we develop an on-lattice Larson-type MC code capable of modeling a wide variety of surfactant systems. It is a versatile code capable of simulating several possible surfactant environments so that the code can be more readily used as a precursor to possible synthetic research avenues. Our MC code is designed to model either a two-dimensional ($L_x \times L_y$) or three-dimensional lattice ($L_x \times L_y \times L_z$) with periodic boundary conditions in all directions. Interfacial studies can also be handled by the code. Although they will not be considered here, interfaces can be established at the top and bottom of the z-axis through the introduction of air molecules, with periodic boundary conditions in the x and y directions. As well, the code easily handles either single-tailed, double-headed, or gemini surfactant species. Ternary

systems of oil, water and surfactant species can also be modeled when needed. In any case, the lattice is completely occupied by either surfactant or solvent species.

As described in the previous chapter, the hydrophilic or hydrophobic nature of any component on the lattice is established by appropriate assignment of interaction energies. Our Larson-type model uses Equation [7] to define the energy of the system. As in all Larson-type models, the energy of our system is defined as the sum of all the nearest-neighbour interactions in the system. We use a square lattice in two-dimensions and a simple cubic lattice in three-dimensions. Each lattice site interacts with its neighbours through specific dimensionless interaction energies, $\varepsilon_{a,b}$, where a and b represent either a head (H), tail (T), spacer (S) or water (W) lattice site. Energy and temperature are both expressed as dimensionless quantities, relative to the head-tail interaction energy, which is set to unity. In our code, spacer units are treated the same as tail units, therefore their interaction energies follow suit (i.e. $\varepsilon_{TW} = \varepsilon_{SW}$, $\varepsilon_{TH} = \varepsilon_{SH}$ and $\varepsilon_{TT} = \varepsilon_{SS}$).

Our choice of nearest-neighbour interaction energies is similar to that of Kapila et al.[6] who chose parameters equivalent to $\varepsilon_{TW} = +1.0$, $\varepsilon_{TH} = +1.0$, $\varepsilon_{HW} = -5.77$ and $\varepsilon_{HH} = +5.77$, with all others set to zero. We use a somewhat simplified version of their parameter choices: $\varepsilon_{TW} = +1.0$, $\varepsilon_{TH} = +1.0$, $\varepsilon_{HW} = -1.0$ and $\varepsilon_{HH} = +2.0$, with all others set to zero. For a complete list, see Table 9.

We base our parameters on those of Kapila et al.[6] because their work, like ours, examines chain lengths longer than have been typically examined in two-dimensional lattice simulations.[82,83] Kapila et al.[6] studied chains of up to 19 units in total length, while we study chains of length 16 and 32. Kapila et al.[6] also examine influences due to

different surfactant architecture (in their case, H_1T_{12} and H_7T_{12}), as is the general focus here.

Table 9 – A list of the nearest-neighbour interaction energies.

Interaction Energies									
ε_{HH}	ε_{HW}	ε_{TW}	ε_{TH}	ε_{TT}	ε_{WW}	ε_{SH}	ε_{SW}	ε_{ST}	ε_{SS}
+2.0	–1.0	+1.0	+1.0	0.0	0.0	+1.0	+1.0	0.0	0.0

As discussed in the previous chapter, many studies have been done since Larson using a wide range of parameter choices. In all cases, the effect of the parameter choices is to mimic the hydrophobic effects using an effective repulsion between tail and water units (as we have done here), or equivalently, an effective attraction between tail units, with water-water interactions set to zero.[4,35,99] To further support the driving force for micelles to form, we (like Kapila et al.[6]) have set the head-tail interaction to be repulsive and the head-water interaction to be attractive. Finally, as also done by Kapila et al.,[6] we have set the head-head interaction to be repulsive to include the effect of Coulombic repulsion of ionic heads. As we show in Section 3.5, this turns out to have only a minor influence on the system behavior.

The most important system properties that we evaluate in our simulations are: the total surfactant concentration, X; the free monomer concentration, X_1; and the cluster-size distribution, $P(n)$. The total surfactant concentration is defined as

$$X = \frac{N_s}{L_x L_y L_z - N_s l_s} \qquad [8]$$

where N_s is the number of surfactants in the system, l_s is the total length of a surfactant chain, and L_x, L_y and L_z are the lengths of the lattice along the x, y and z-axis respectively. When modeling in two-dimensions, the L_z term is not included in the calculation.

To determine the free monomer concentration in the system we use a slight modification of Equation [8]. We define free monomers as surfactant molecules that have no surfactant molecules as nearest neighbours. Therefore,

$$X_1 = \frac{N_1}{L_x L_y L_z - N_s l_s} \qquad [9]$$

where N_1 is the number of free monomers in the system. It is important to note that both the total surfactant and free monomer concentrations are dimensionless quantities as they are a ratio of the number of surfactant molecules and the number of lattice sites.

The cluster-size distribution $P(n)$ is the probability that a randomly chosen surfactant molecule is part of a cluster containing n surfactants, and is defined by:

$$P(\ ) = \frac{nN(\ )}{N_s} \qquad [10]$$

where $N(n)$ is the average number of clusters of size n. The emergence of a shoulder or a peak in $P(n)$ at non-zero n is an indication of the appearance of micelle-like aggregates.

3.3 – Our Monte Carlo Dynamics

Our MC simulation procedure starts with surfactant molecules randomly distributed throughout the lattice. The initial orientation of each molecule is a straight line segment aligned along the *y*-axis (Figure 16(a)) and the energy of this configuration is calculated. A surfactant molecule is then chosen at random to complete a reptation move, generating a new configuration. The total energy of this new configuration is calculated and if the move results in a decrease in the total energy of the system ($\Delta E < 0$) the move is always accepted, unless it overlaps another surfactant molecule. If $\Delta E > 0$, the move is accepted with a Boltzmann probability, according to the Metropolis algorithm. For the first 30,000 accepted trial moves the surfactants only undergo reptation. This number of steps is sufficient to allow a surfactant molecule to relax its initial straight shape and adopt a random configuration (Figure 16(b)).

The 30,000 steps allocated to the initial reptation-only phase can be understood in the following way. Reptation can be described as a random walk, in which the chain moves randomly back and forth along the path it explores over time. The path-length displacement of one end of the chain along this path increases as the square of the number of successful moves. The chains studied here are of the order of twenty units long, so a single chain will move a complete path length in a time on the order of 400 MC steps. A typical simulation near the concentration of the CMC contains on the order of 50 chains. This suggests that on the order of 20,000 MC steps are required to ensure that all the chains in the system are initially relaxed in shape. Our choice of 30,000 MC steps is consistent with this estimate.

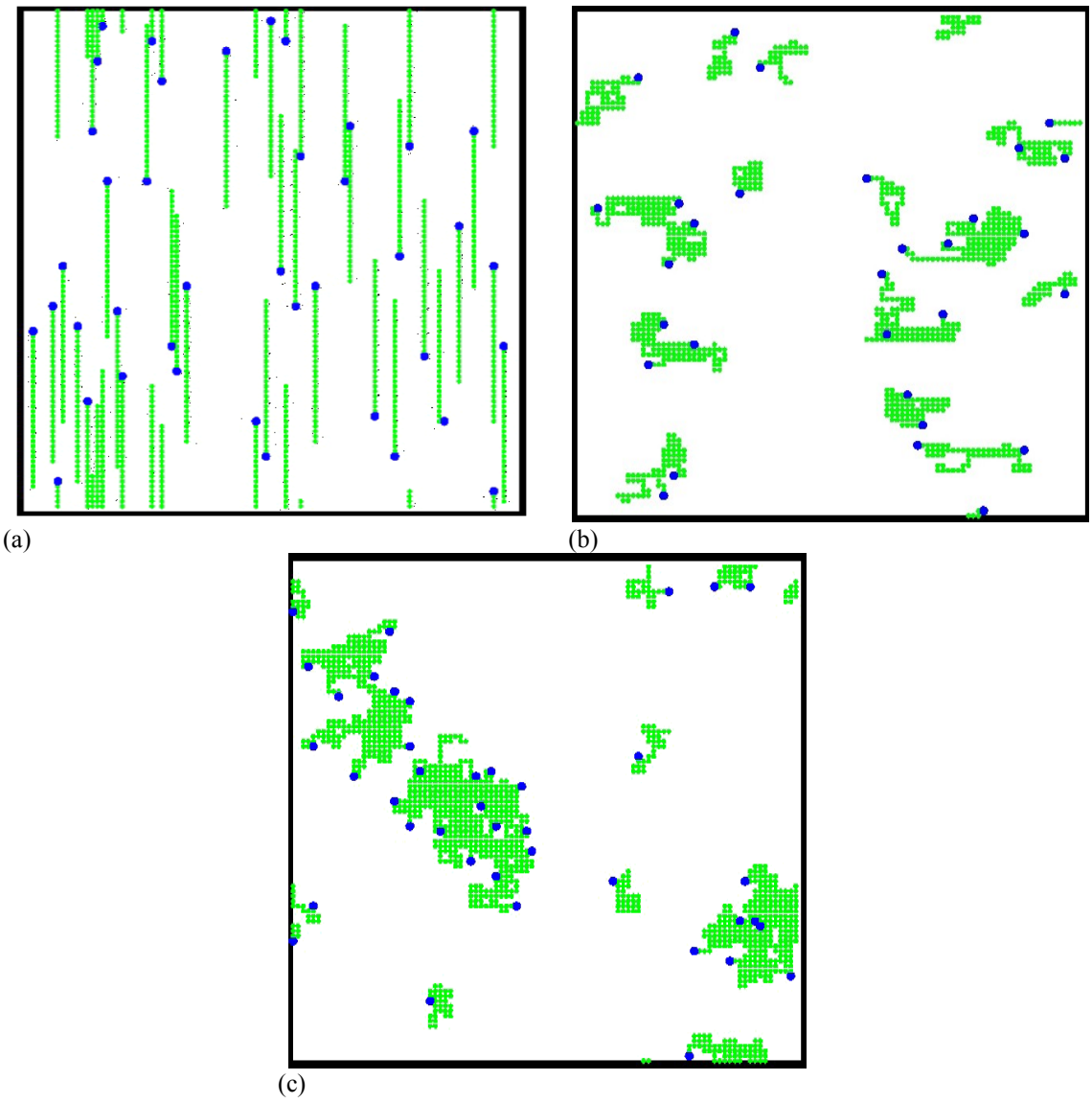

Figure 16 – Snapshots of 30 conventional single-tailed surfactant with a tail length of 31 at a temperature = 2.0 on a 100 × 100 two-dimensional lattice at (a) initialization, (b) 30,000 time-steps and (c) equilibrium. Head(●) – Tail(●)

After 30,000 accepted moves, the SST and reptation moves are assigned an equal probability of occurring. The run is equilibrated for as many MC steps as are required to accumulate 500,000 accepted moves. After this equilibrium period, a production run is carried out for as many MC steps as are required to accumulate another 500,000 accepted moves. All averages reported in this thesis are accumulated over this production phase (Figure 16(c)).

Our choice of 500,000 successful moves to first equilibrate the system, and then to evaluate the desired observables, is also consistent with a random-walk analysis of the motion of the chains. As shown in Figure 17, the acceptance rate for reptation moves is typically larger than that for SST moves for concentrations near to and above the CMC. Therefore, the majority of the successful moves in this regime will be reptation steps. If the characteristic time to relax the chain's shape and position in a typical system is taken as 20,000 MC steps, as estimated above, then 500,000 (mostly reptation) moves corresponds to on the order of 25 complete system rearrangements. This is consistent with our observation that, in all cases, we confirm that the number of MC steps used for the equilibration and production phases was sufficient to relax both the energy and free monomer concentrations to their steady-state values.

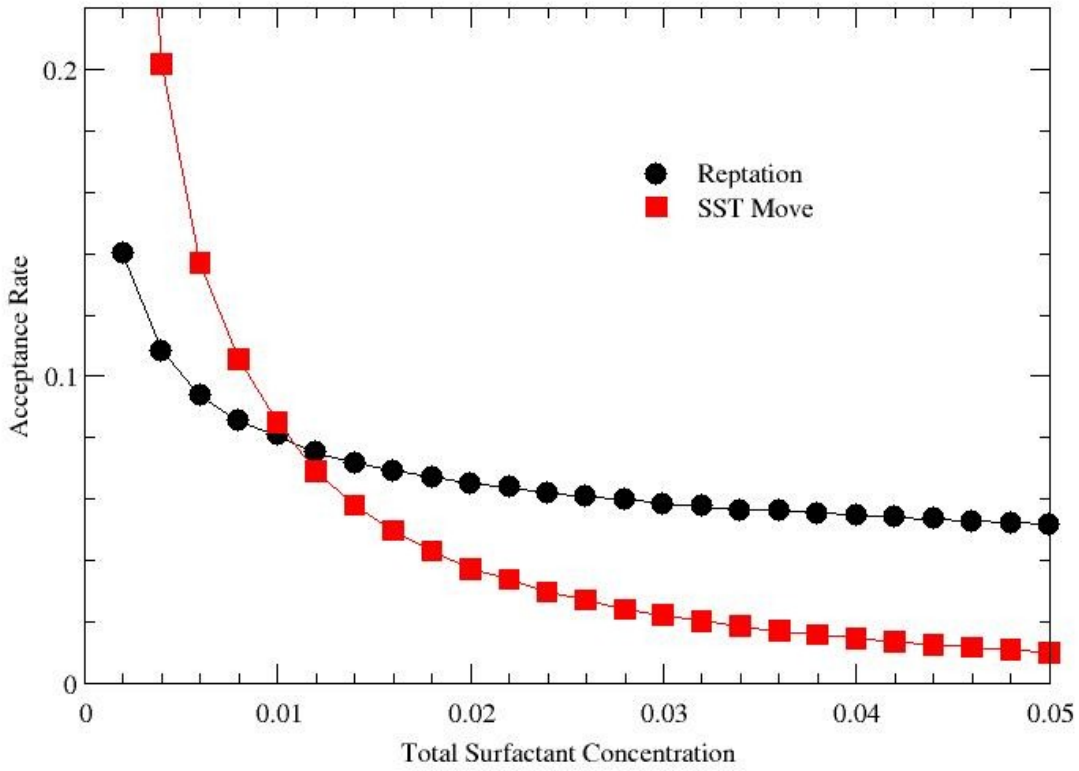

Figure 17 – The acceptance rates for the reptation and single surfactant transport moves for a conventional single-tailed surfactant with a tail length of 6 at a temperature = 1.0 and a total surfactant concentration of 0.01 on a 200 × 200 two-dimensional lattice.

For each temperature, concentration, and architecture of surfactants the energy of the system is monitored throughout the run. Figure 18 shows the approach of the system to equilibrium. As well, this figure shows the extent to which the addition of the SST move significantly decreases the number of MC time steps required for the system to reach equilibrium.

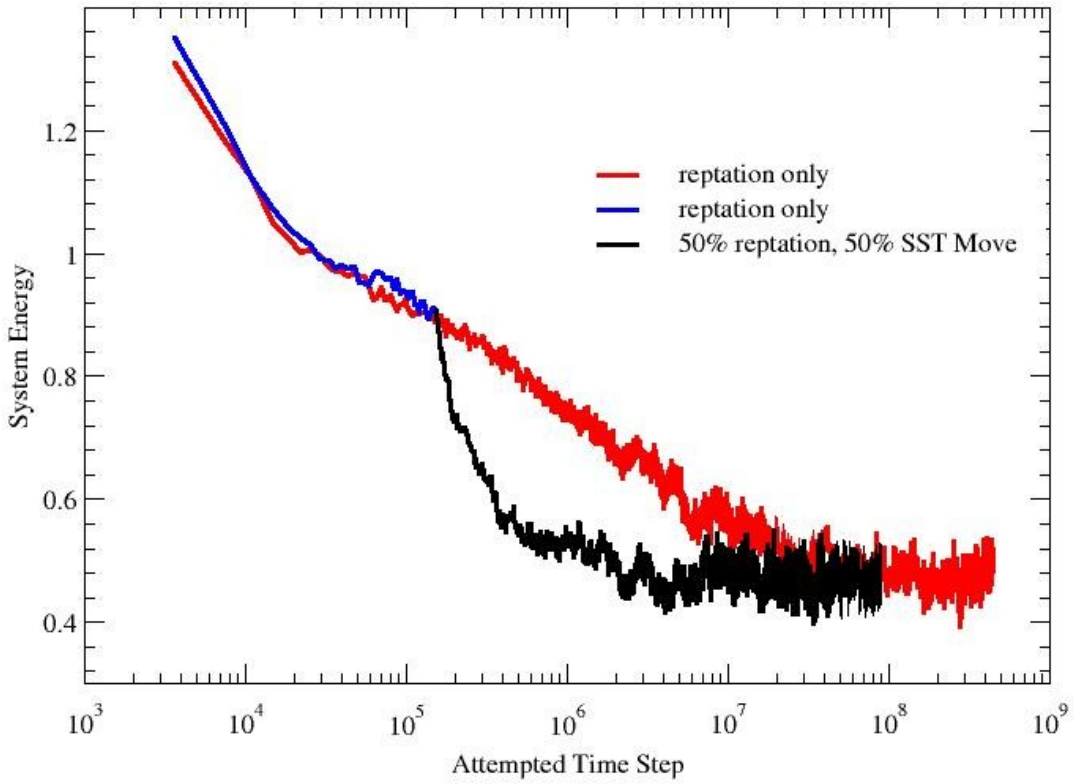

Figure 18 – The number of MC time steps needed for system to reach equilibrium with reptation only in comparison to an equal probability of reptation and the single surfactant transport move. For a conventional single-tailed surfactant with a tail length of 6 at a temperature = 1.0 on a 200 × 200 two-dimensional lattice.

In our code, reptation and the SST move have been set to have an equal probability of occurring. If we look at the acceptance rates for these two moves as a function of total surfactant concentration (Figure 17), we find that at low surfactant concentrations the SST move is more likely than reptation. At high surfactant concentrations the reverse is true. Thus our choice of an equal probability of reptation and the SST move is a compromise to ensure that we have enough reptation moves at low surfactant concentration to ensure the relaxation of the chain conformations, while a

sufficient number of aggregate-rearranging SST moves occur at high surfactant concentration. Although we may be attempting more SST moves than may be required at low surfactant concentration, thus wasting time, the optimal ratio of reptation to SST moves would have to be tailored for each temperature and surfactant concentration.

An examination of the system energy or free monomer concentration versus time step shows when the system has reached equilibrium and ensures equilibrium throughout the production phase of our runs (Figure 19 and Figure 20). At equilibrium, snapshots of the surfactant system are plotted to give a picture of the surfactant distribution in space (Figure 16(c)).

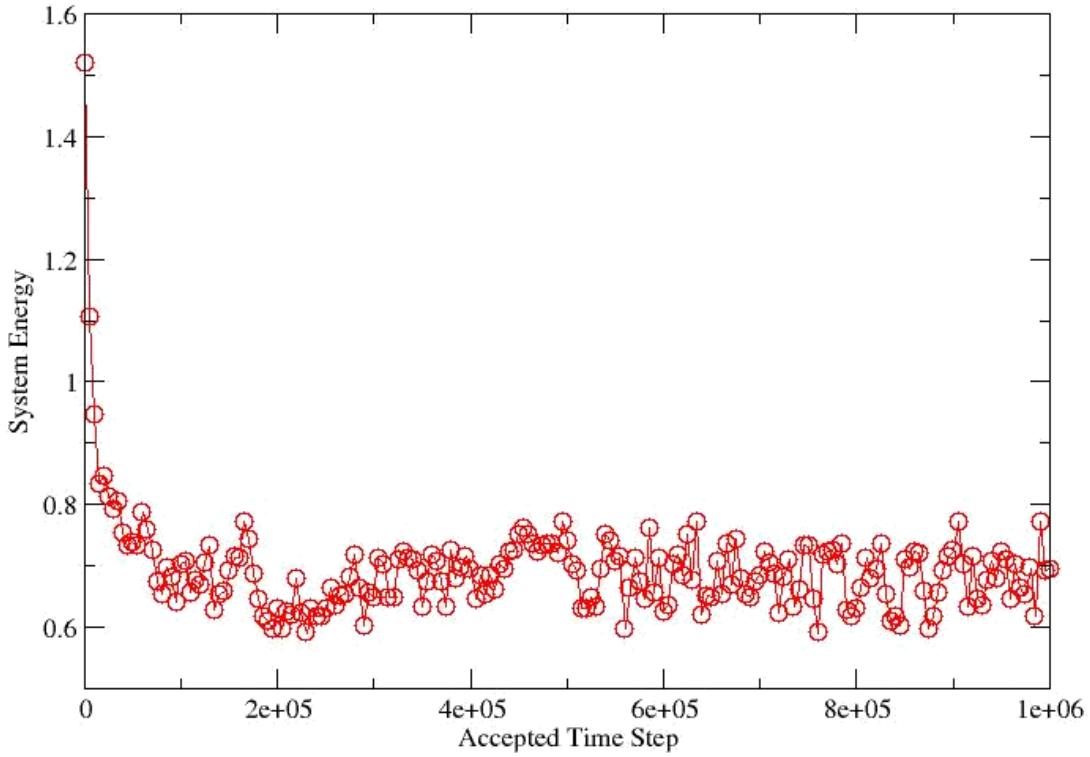

Figure 19 – A plot of the system energy versus time-step for a conventional single-tailed surfactant with a tail length of 31 at a temperature = 2.0 on a 100 × 100 two-dimensional lattice.

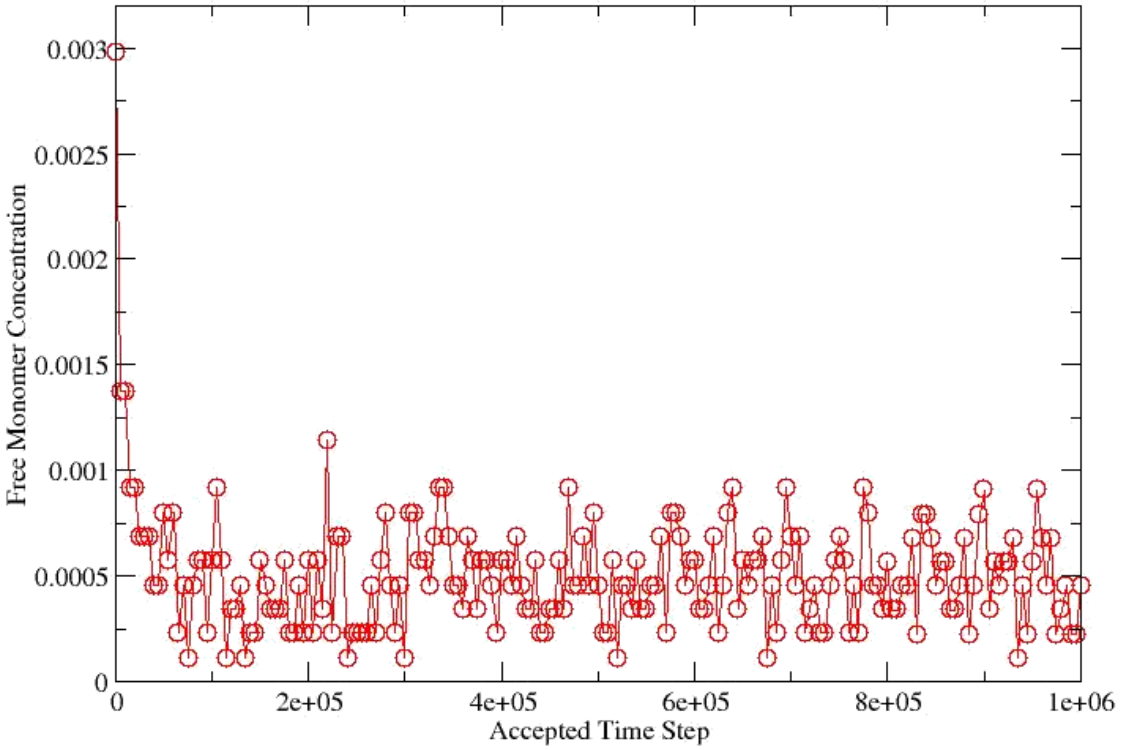

Figure 20 – A plot of the free monomer concentration versus time-step for a conventional single-tailed surfactant with a tail length of 31 at a temperature = 2.0 on a 100 × 100 two-dimensional lattice.

3.4 – Evaluating the CMC and the Uncertainty in the CMC

The free monomer concentration versus the total surfactant concentration is plotted to obtain the CMC from the plateau values. Since the plateau values are used to determine the CMC, we often do not calculate the CMC explicitly; instead we qualitatively examine the trends in the CMC values by comparing the plateau values of the free monomer concentration in different cases. For example, if the plateau value increases, the CMC must also increase.

The two-dimensional results presented below come from a 100 × 100 lattice at a temperature of 2.0. Three separate trials are averaged to produce the final curve presented (Figure 21). Using the average curve we define the concentration where a line passing through the origin with a slope of 1 intercepts a horizontal line formed by the average free monomer concentration after the onset of micellization as the CMC. In other words, we define the CMC as the average of the plateau values.

From the average curve we calculate the standard deviation (s_n) of the CMC value using 5 points from the plateau region. The same 5 points were used for all curves; they were the points with the total surfactant concentration between 0.00237 and 0.00332 (highlighted in yellow in Figure 21).

The following is the equation for standard deviation

$$s_n = \sqrt{\frac{1}{N}\sum_{i=1}^{N} x_i - \bar{x}^2} \qquad [11]$$

where N is the total number of points, x_i is the value of the point being considered and $\bar{x}$ is the mean average of all the points. Based on Figure 21 we find the value of the CMC to be $6.3 \times 10^{-4} \pm 3.2 \times 10^{-5}$.

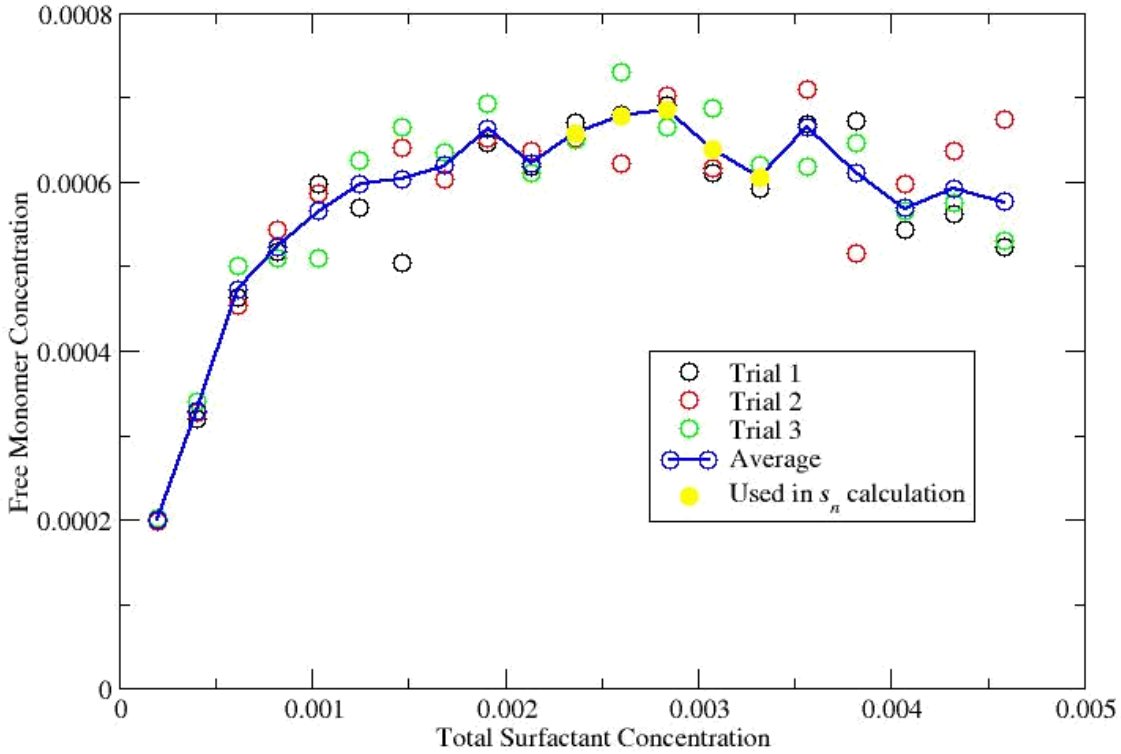

Figure 21 – A plot of the free monomer concentration versus the total surfactant concentration for three separate trials and their average for a symmetric gemini surfactant with a tail of length 12 and a spacer length of 6 at a temperature = 2.0 on a 100 × 100 two-dimensional lattice.

3.5 – Sensitivity of the CMC to the Interaction Parameters

In order to explore the sensitivity of our model to the choice of interactions, we examine the effect of varying the interaction parameters on a 200 × 200 square lattice for the case of the conventional single-headed, single-tailed surfactant molecule H-T6 at

temperature = 1.0. A special thank you to Dr. Peter Poole, StFX University for his collaboration in finalizing the analysis described in this section.

In order to vary the interaction energies, we modify our Larson-type Hamiltonian (Equation [7]) to:

$$H = f_{TW}\varepsilon_{TW}n_{TW} + f_H f_{HT}\varepsilon_{HT}n_{HT} + f_H f_{HW}\varepsilon_{HW}n_{HW} + f_H f_{HH}\varepsilon_{HH}n_{HH} \qquad [12]$$

where several factors f have been added to vary the magnitude of a particular interaction energy from the value presented in this work. When all the factors f are set equal to one, the Hamiltonian reduces to Equation [7]. By tuning a particular factor f to values greater than or less than one, while holding all others equal to one, we can explore how the corresponding term of the Hamiltonian contributes to the system behavior. Tuning f_{TW} tests for effects associated with changing the tail-water interaction energy; tuning f_{HT} tests for effects associated with changing the head-tail interaction energy; and so on for all four terms in the Hamiltonian. The additional factor f_H allows us to tune the magnitudes of all of the interactions involving head groups simultaneously, while leaving the tail-water contributions unchanged. Monitoring the free monomer concentration, we examine the changes to the system that result from these changes to the Hamiltonian.

To examine the impact of our choice of the head-head interaction, we vary f_{HH} from 0 to 2.0 in steps of 0.5. From the plot of the free monomer concentration versus total surfactant concentration (Figure 22), we see little change in the value of the CMC. This is perhaps not surprising since head-head contacts are likely to be the least numerous type of contact, relative to the other types of contacts occurring in the system.

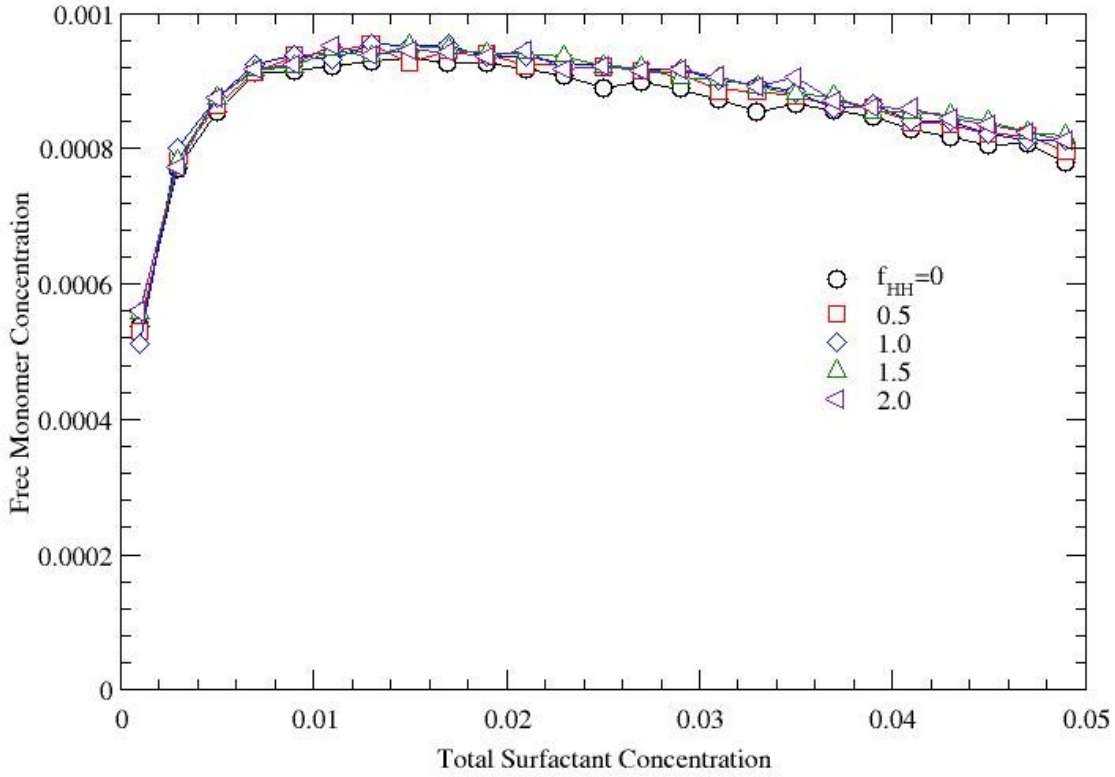

Figure 22 – Sensitivity of the free monomer concentration on the head to head interaction energy.

Next, we examine the tail-water interaction energy by multiplying our value of the interaction energy ($\varepsilon_{TW} = 1.0$) by the factor f_{TW}, varying from 0.8 to 1.2 in steps of 0.1 (Figure 23). Tail-water contacts are by far the most numerous contacts between unlike species in the system, and consequently dominate the value of the total interaction energy. As a result, the effect of varying the tail-water interaction is much like varying the temperature. The unfavorable tail-water interaction drives tail groups to aggregate so that they avoid contact with water. At fixed temperature, if the magnitude of the tail to water interaction decreases, then the drive to aggregate is suppressed, and more

surfactants will occur as monomers, exactly as would occur if the temperature is increased. As a result, the CMC increases as the magnitude of the tail to water interaction decreases.

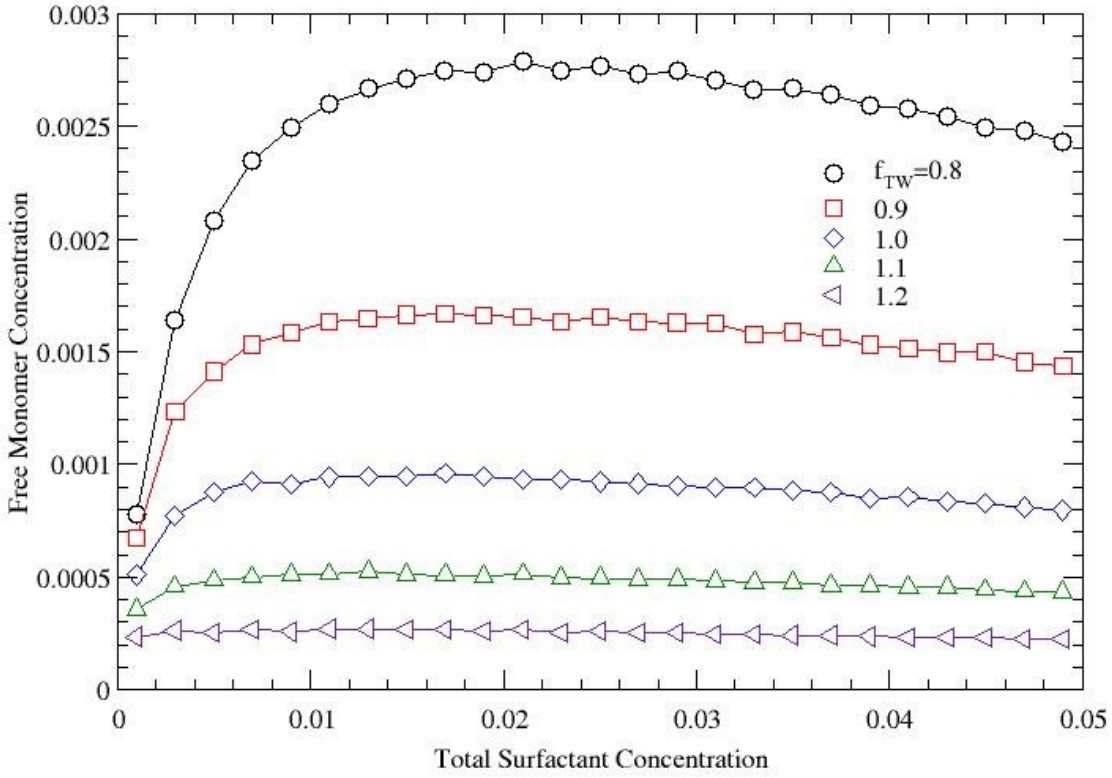

Figure 23 – Sensitivity of the free monomer concentration on the tail to water interaction energy.

We next examine the impact of all interactions involving head groups by changing the factor f_H from 0 to 1.0 in steps of 0.2 (Figure 24). Complete removal of all head interactions in the system ($f_H = 0$) results in segregation of all the surfactants into a single aggregate (i.e. bulk phase separation), since in this case only the unfavorable tail-water interactions remain. As a result, the free monomer concentration drops to very low values. As f_H increases, the influence of the head interactions in stabilizing finite-sized

aggregates emerges (with head groups located at the micelle-water interface). As finite-sized aggregates appear, the free monomer concentration rises because the existence of smaller aggregates means that aggregates of size one (i.e. monomers) will also be more prevalent. Hence the CMC found from Figure 24 rises as f_H increases. Hence, the head interactions play a crucial role in aggregate formation and in allowing surfactants to exist as monomers in the water.

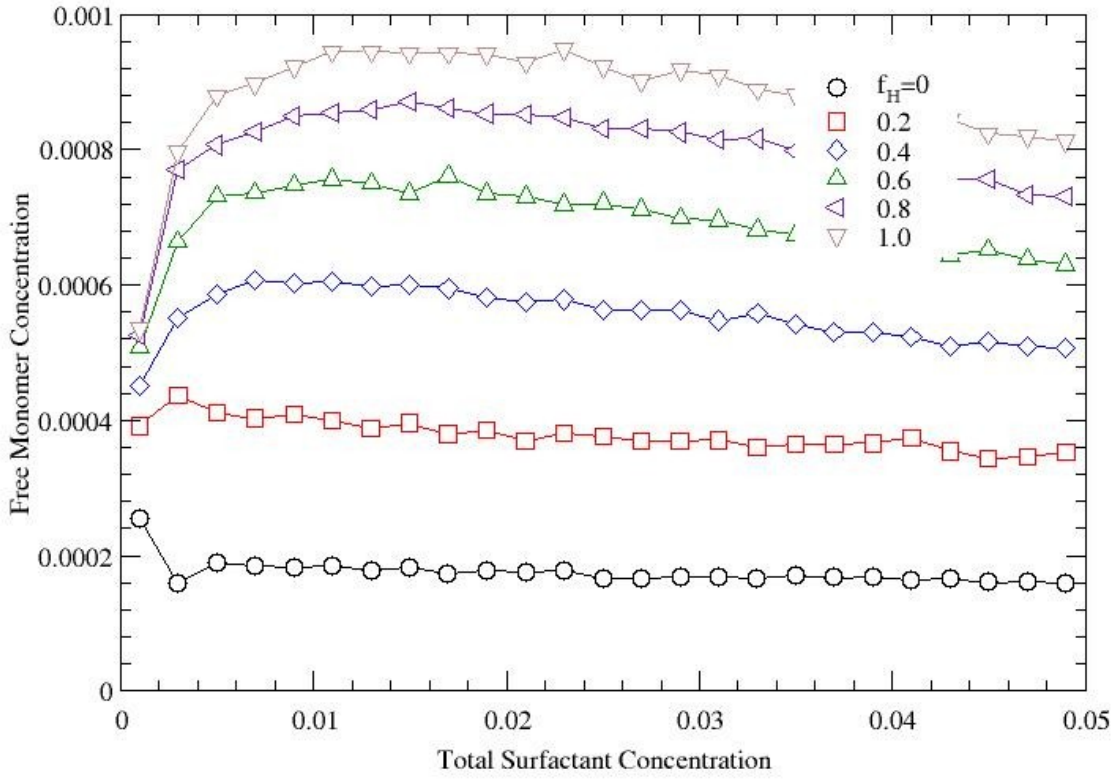

Figure 24 – Sensitivity of the free monomer concentration on all the head interactions in the system.

The same effect, though in weaker form, is observed when we vary solely the head-tail interaction, by varying the factor f_{HT} from 0 to 2.0 in steps of 0.5. We find that the CMC increases from approximately 0.0007 to 0.0011 as f_{HT} increases from 0 to 2

(Figure 25). The repulsive head-tail interaction serves to promote surfactants that are part of a micelle to orient in such a way that the heads avoid the tail-filled interior and are on the outer surface in contact with the water. This effect tends to stabilize finite-sized aggregates and thus maintains monomer surfactants in solution. As a consequence, increasing the magnitude of the (unfavorable) head-tail interaction increases the CMC, although the change is less than that produced by changing f_H, and much less than the impact of changing the tail-water interaction.

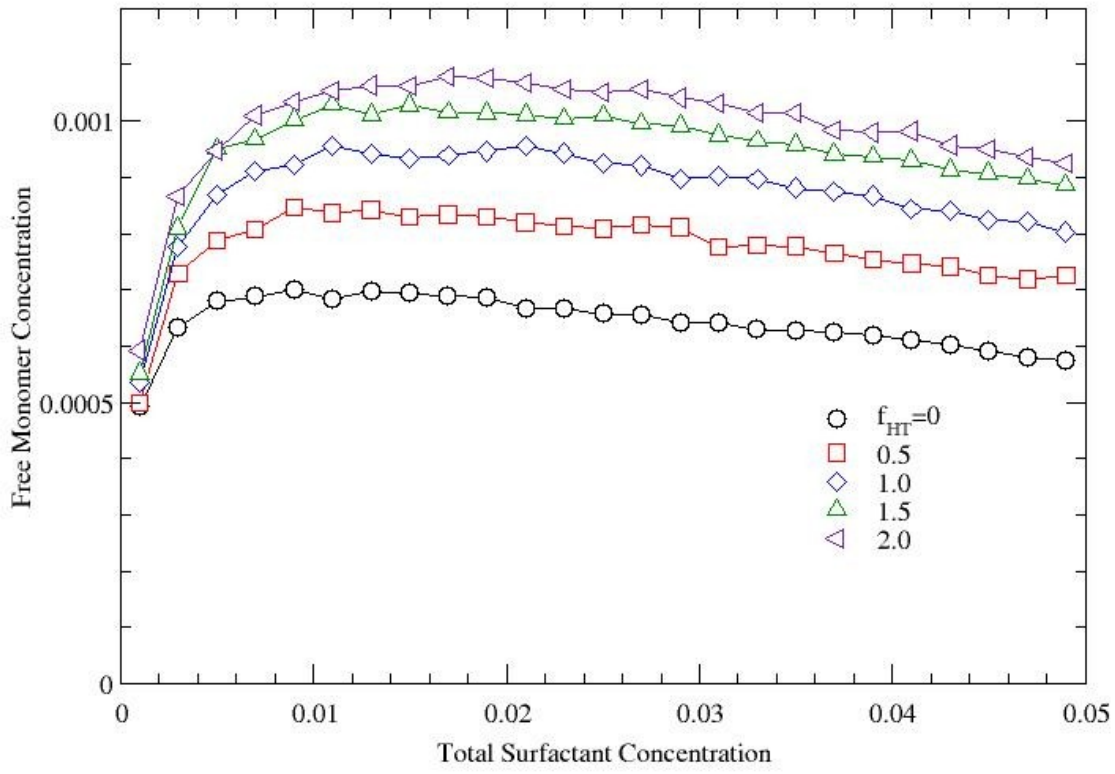

Figure 25 – Sensitivity of the free monomer concentration on the head to tail interaction energy.

For exactly the same reasons, we see a similar behavior when we examine the impact of our choice of the head-water interaction energy ($\varepsilon_{HW} = -1.0$) by varying f_{HW} from 0 to 2.0 in steps of 0.5 (Figure 26). The (favorable) head-water interaction also serves to drive head groups to the surface of micelles so that they are in contact with water. Hence, increasing the magnitude of the head-water interaction also promotes finite-sized aggregates, and maintains the remaining monomers in solution, thus increasing the CMC.

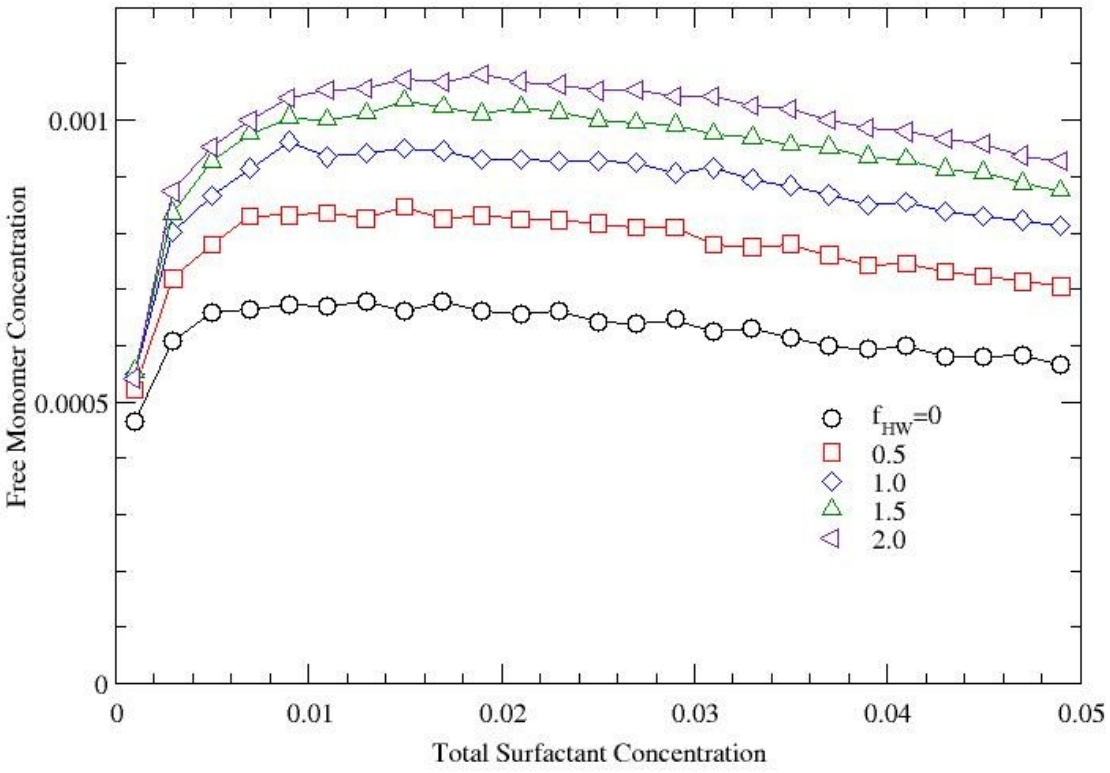

Figure 26 – Sensitivity of the free monomer concentration on the head to water interaction energy.

Figure 27 summarizes the impact of each of the interaction energies on the value of the CMC. As described above, the tail-water interaction has the greatest effect, while the role played by the various head interactions is also shown. It is important to remember that our choice of interaction energies is similar to those previously published,[6] yields aggregates for all the systems studied and can be used to reproduce trends for surfactant systems, as reported in section 3.5.

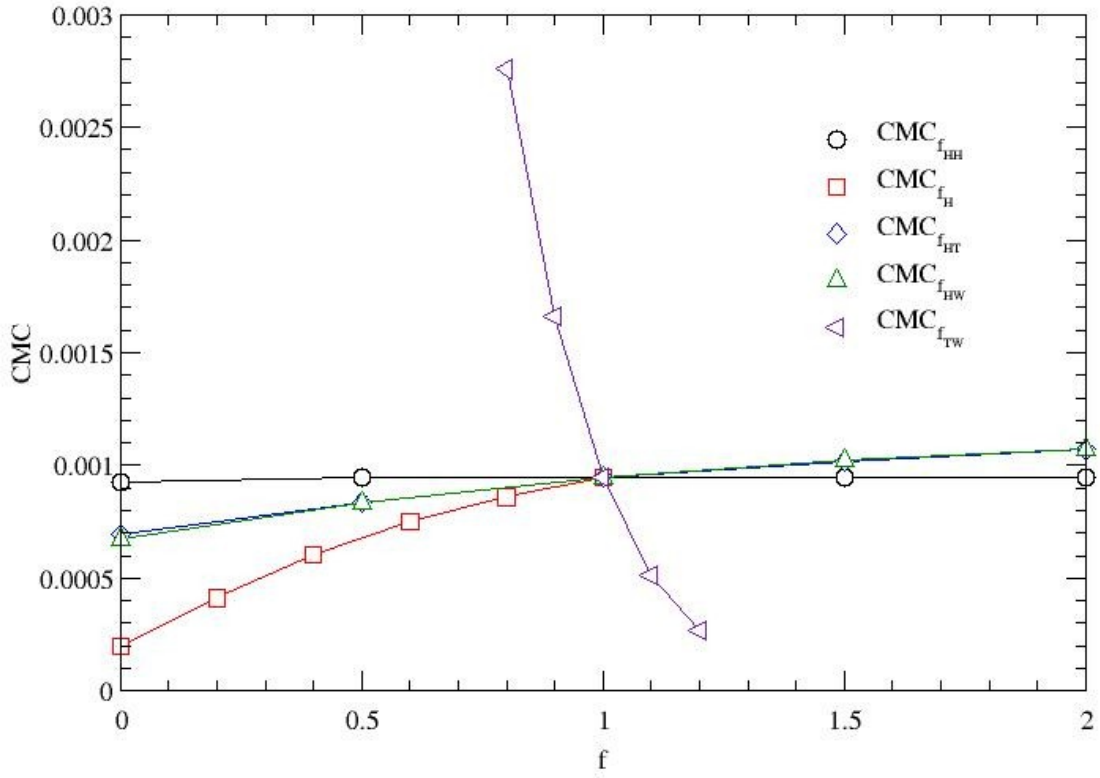

Figure 27 – A summary of the impact of the interaction energies on the value of the CMC.

3.6 – Verification of the Code using Conventional Single-Tailed Surfactants

Upon completion of the code, the first priority was to verify its functionality in two-dimensions. After a comprehensive literature search, we decided to verify the code by reproducing the results of Bhattacharya and Mahanti.[82] One of the primary goals of this research was to investigate trends in the CMC, which is obtained from a plot of free monomer concentration versus total surfactant concentration. The work by Bhattacharya and Mahanti was one of the only papers which clearly presented such a plot (solid lines in Figure 28) and favorable system conditions.[82]

Using a square lattice of size 128 × 128, Bhattacharya and Mahanti[82] varied the concentration of single-tailed surfactants with a chain length of 3 (1 head and 2 tail units). They investigated the effect of temperature on the free monomer concentration with total surfactant concentrations of 0.0018 to 0.056 (i.e. 30 – 780 surfactants on a lattice of this size).

When calculating the total energy of their system they used the following Hamiltonian, where n_{TS}, n_{HS} and n_{HH} are the total number of tail-solvent (TS), head-solvent (HS) and head-head (HH) interactions of strength ε_{TS}, ε_{HS} and, ε_{HH} respectively, and $\sum_i$ represents the conformation energy which may include bending energies; see Equation [13].

$$H = \varepsilon_{TS} n_{TS} + \varepsilon_{HS} n_{HS} + \varepsilon_{HH} n_{HH} + \sum_i \qquad [13]$$

There are three methodological issues to note when comparing the work of Bhattacharya and Mahanti[82] to that described here:

(i) Their algorithm used reptation moves, kink moves and end rotations, but did not employ a SST move. The code presented in this thesis uses reptation and a SST move. Since both their work and ours use the reptation move, which is commonly accepted as sufficient to bring the system to equilibrium,[88] these differences will not affect where equilibrium lies, but only how fast equilibrium is reached. This is confirmed in our simulation results described below.

(ii) While the Hamiltonian given in their paper (Equation [13]) included the conformation energy term, Bhattacharya and Mahanti's[82] results were generated for the case when this term is set to zero. This is equivalent to our model, in which the conformation energy term is absent. This means that all molecules in their simulations had the same degrees of freedom of motion as the code presented in this thesis.

(iii) Bhattacharya and Mahanti[82] define a cluster of surfactant chains to be a group of chains in which the tails share nearest-neighbor contacts; that is, head-head and head-tail contacts are ignored for the purpose of defining clusters. In our work, all chain-chain contacts are considered for defining clusters, regardless of whether they involve head or tail units.

We show the comparison of our data with that of Bhattacharya and Mahanti[82] in Figure 28, for the case where our definitions of a cluster differ as described above. As a result of this difference in what defines a cluster, there is a distinctive trend in the comparison of the data. At low temperatures where the surfactants are in a lower energy state and not as prone to forming energetically unfavorable head-head or head-tail

contacts, both codes show good agreement. However, as the temperature and thus the system energy increases, and the likelihood of unfavorable head-head or head-tail contacts increases, the results show greater discrepancy.

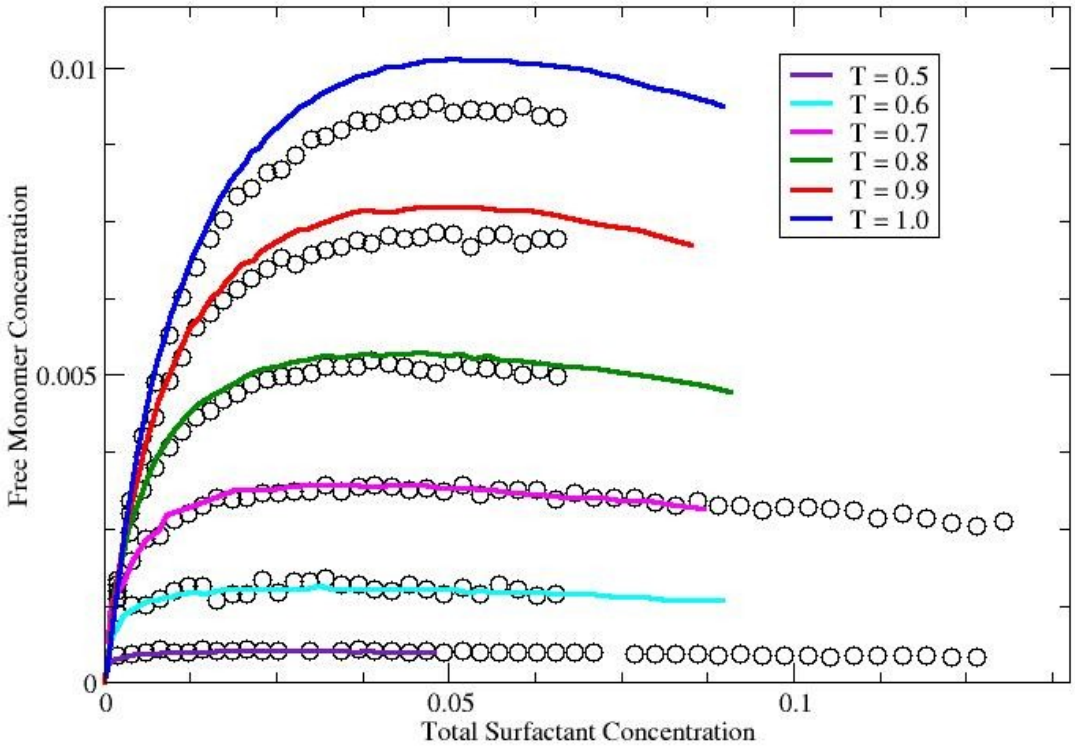

Figure 28 – A comparison of a plot of the free monomer concentration versus the total surfactant concentration obtained using Bhattacharya and Mahanti's[82] cluster definition (Solid Lines) and our cluster definition (Open Circles). Data is for a conventional single-tailed surfactant with a tail length of 2 for a series of temperatures on a 128 × 128 two-dimensional lattice.

If we modify our code to match the cluster definition of Bhattacharya and Mahanti, we find that our results come into excellent agreement with theirs (Figure 29). This confirms that our general algorithm, including our criteria for equilibrating the system, is able to reproduce the results of Bhattacharya and Mahanti.

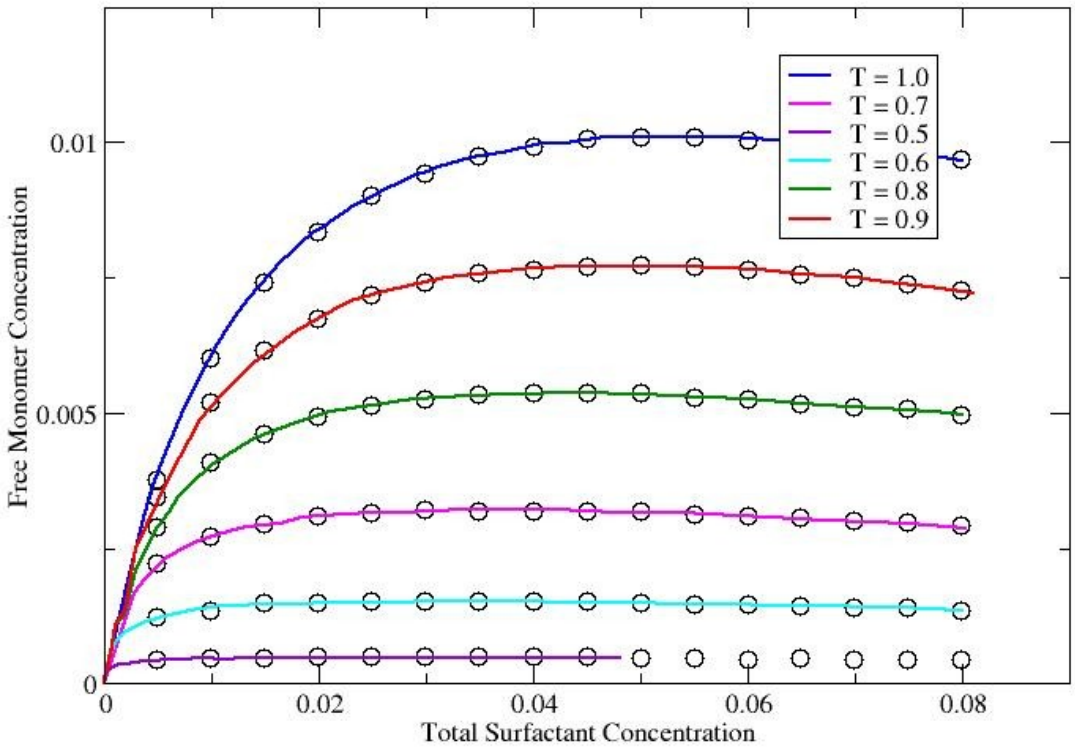

Figure 29 – A comparison of a plot of the free monomer concentration versus the total surfactant concentration obtained using Bhattacharya and Mahanti's[82] cluster definition (Solid Lines) in our code (Open Circles). Data is for a conventional single-tailed surfactant with a tail length of 2 for a series of temperatures on a 128 × 128 two-dimensional lattice.

Following the verification against the work of Bhattacharya and Mahanti,[82] we also wanted to ensure that our code was properly calculating the cluster-size distribution *P(n)*. The work of Care[83] used the Metropolis Monte Carlo technique on a 128 × 128 square lattice. The simulations contained 512, length=3 conventional single-tailed surfactants (1 head and two head units). Care defined his cluster as we did, assuming a cluster to be a set of surfactants which are connected by at least one nearest-neighbour

site. Our results are in excellent agreement with those of Care (Figure 30), again confirming the validity of our code.

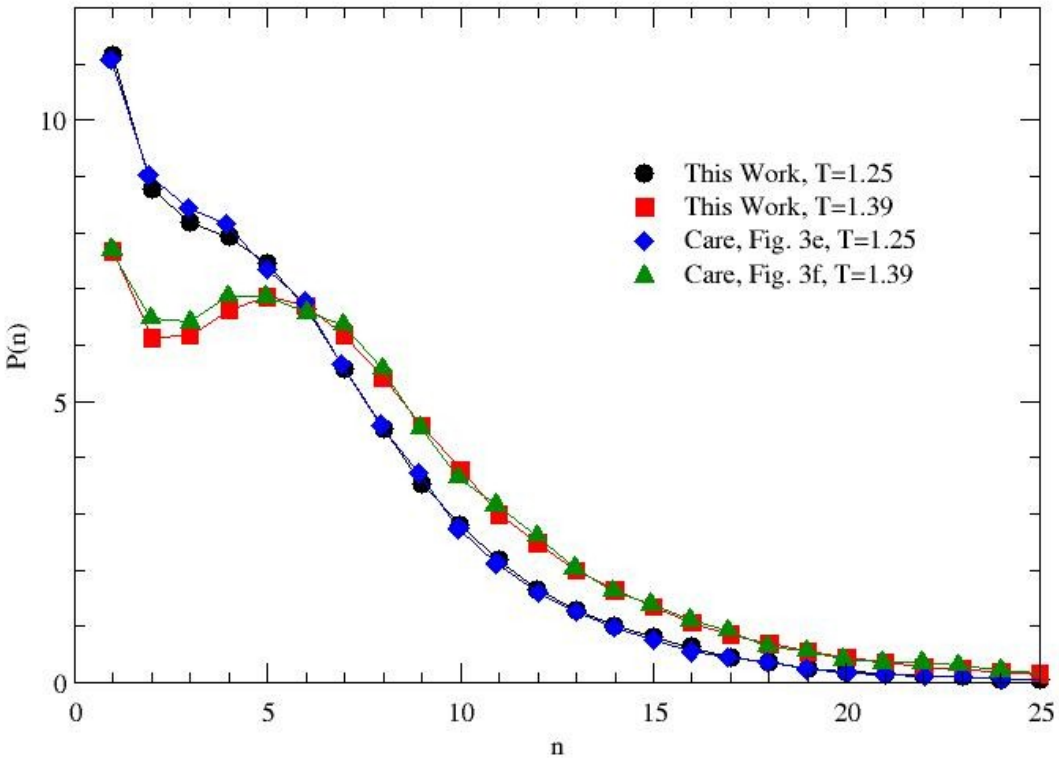

Figure 30 – A comparison of the cluster-size distribution *P(n)* calculated by Care[83] and our code. For a 128 × 128 square lattice with 512, length=3 conventional single-tailed surfactants**.**

3.7 – Testing the Code Against Known Surfactant Trends

We further verify the functioning of the code with trials designed to test the main trends with gemini surfactants. Gemini surfactants have been shown to have a lower CMC value than conventional single-tailed surfactants of the same tail length.[56] We run several comparisons of gemini and conventional single-tailed surfactants of the same tail

length. In all trials, we find that the CMC for the gemini surfactant is considerably lower than the conventional single-tailed surfactant. This trend can be observed in Figure 31 for a gemini surfactant with a tail length of 6 and a spacer length of 2 (T6-H-S2-H-T6) and the corresponding single-tailed surfactant with a tail length of 6 (H-T6) on a two dimensional 200 × 200 lattice.

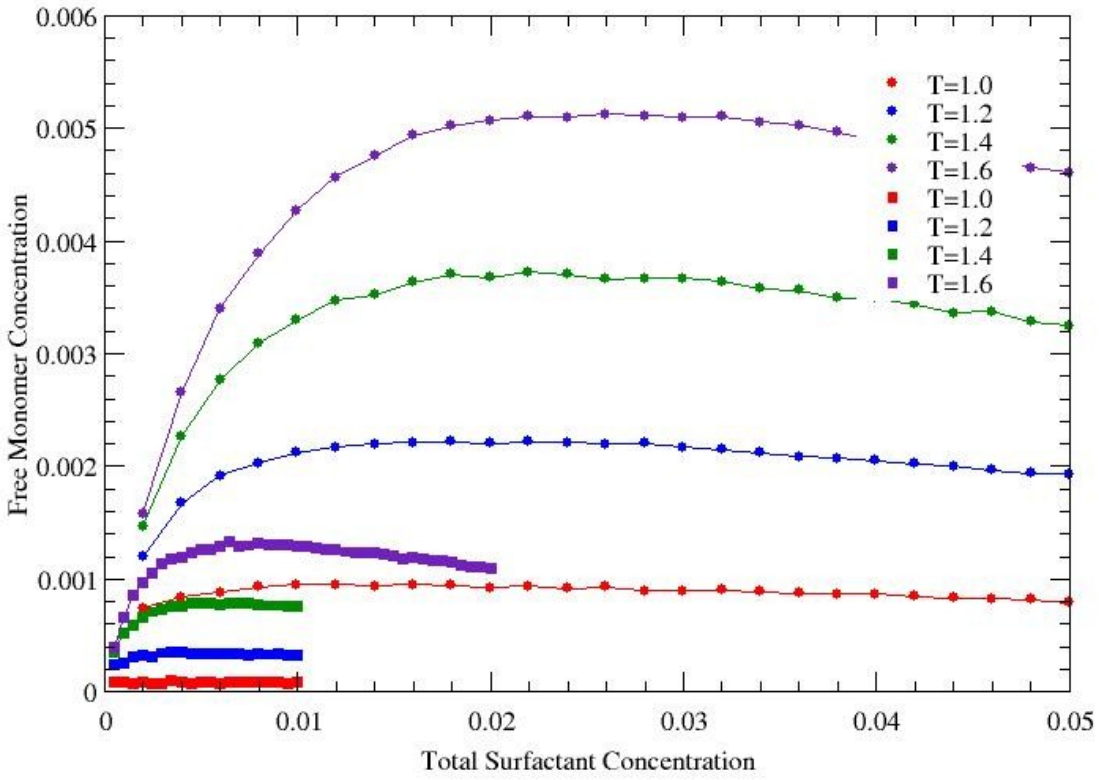

Figure 31 – A plot of the free monomer concentration versus the total surfactant concentration for a gemini surfactant with a tail length of 6 and a spacer length of 2 (squares), as well as a corresponding single-tailed surfactant with a tail length of 6 (circles) at various temperatures on a 200 × 200 two-dimensional lattice.

From Figure 31, we also see the dependence of the CMC on the temperature for both the conventional single-headed and gemini surfactants. In both cases, as the temperature of the system is increased, the value of the CMC increases. This trend has been clearly established through experimental results.[31]

Finally, for gemini surfactants one would expect to see a decrease in the CMC as the length of the tail groups increases with a constant spacer length.[9] This behaviour is confirmed in Figure 32, which shows a plot of the free monomer concentration versus the total surfactant concentration for the symmetric gemini surfactants T6-H-S6-H-T6 and T12-H-S6-H-T12 on a two dimensional 100 × 100 lattice.

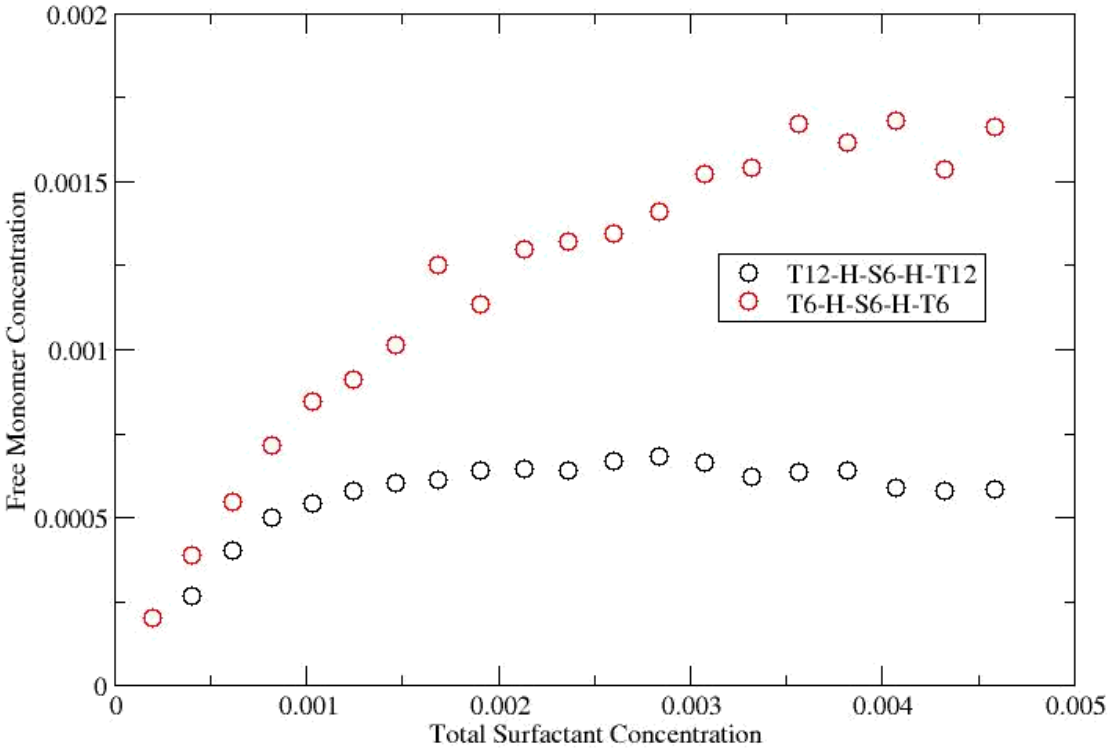

Figure 32 – A plot of the free monomer concentration versus the total surfactant concentration for a gemini surfactant with a tail length of 6 and a spacer length of 6, as well as a gemini surfactant with a tail length of 12 and a spacer length of 6 at a temperature = 2.0 on a 100 × 100 two-dimensional lattice.

Finally, optimization of the overall lattice size is important for minimizing computational time. However, unphysical effects introduced by the finite system size are always a concern. We run several symmetric and asymmetric gemini surfactants on lattices of different sizes to determine the smallest allowable system size. We observe the same trend for both the two-dimensional 100 × 100 lattice and the two-dimensional 200 × 200 lattice (Figure 33). That is, there is no observable difference in the CMC values obtained for T12-H-S6-H-T12 and T18-H-S6-H-T6 on both the 100 × 100 and the 200 × 200 two-dimensional lattice.

We do observe a decrease in the plateau for the free monomer concentration in the 200 × 200 system (26% for T12-H-S6-H-T12 and 23% for T18-H-S6-H-T6), however, the overall trends we present in the next chapter of the thesis remain the same for both system sizes. Ideally, we would continue to explore larger and larger system sizes until there was no longer a change in the plateau value of the free monomer concentration. This however would become computationally restrictive. A simple shift from the two-dimensional 100 × 100 lattice to the two-dimensional 200 × 200 lattice quadruples the effective computational time (from 1 day to 4 days per data point). Since both lattice sizes exhibit the same trend, we choose to work with the two-dimensional 100 × 100 system for all remaining trials, understanding the direction of the shift in free monomer concentration if we were to simulate a larger system.

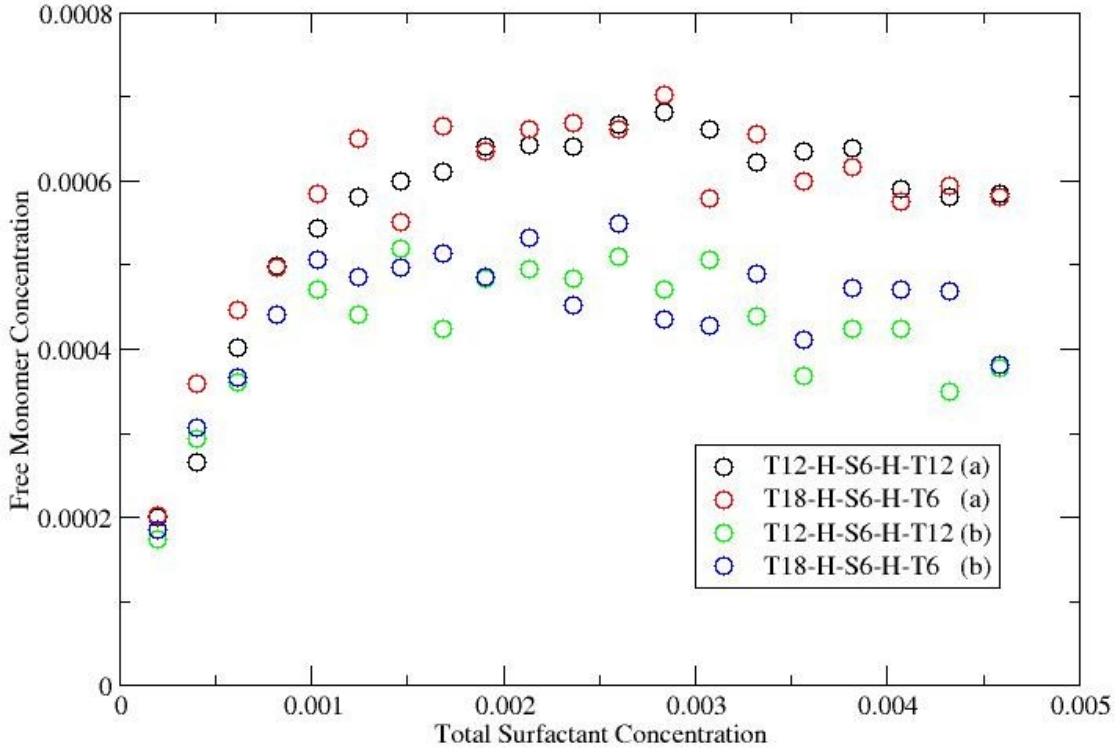

Figure 33 – A plot of the free monomer concentration versus the total surfactant concentration for a symmetric gemini surfactant with a tail of length 12 and a spacer length of 6, as well as an asymmetric gemini surfactant with a tail length of 18, a tail length of 6, and a spacer length of 6 at a temperature = 2.0 on a (a) 100 × 100 and (b) 200 × 200 two-dimensional lattice.

CHAPTER 4 – DISCUSSION

4.1 – Double-Headed Surfactant Trials

Double-headed surfactants have been readily synthesized since the mid-1980s, however, they have not received much attention in current surfactant computer simulations. Comeau et al.[12] found that the CMC values for a double-headed surfactant were significantly higher (approximately 5 times) than the corresponding single-headed surfactant of equal chain length. A series of disodium 1,2-alkanedisulfates were synthesized by the addition of chlorosulfonic acid to the corresponding 1,2-alkanediol. The CMC values, obtained from conductance and counter-ion emf measurements for this double-headed series, were compared to the values for the corresponding single-tailed sodium alkanesulfates.[12]

We model two double-headed surfactant systems and compare them to the conventional single-tailed surfactant of the same length. All surfactants are of length 32. The first double-headed surfactant has head groups located at site 1 and 2 on the chain (H2-T30) while the other has the head groups located at site 1 and 7 (H-S6-H-T24) (Figure 34).

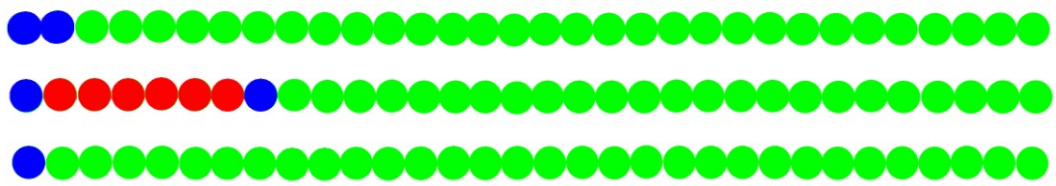

Figure 34 – The structure of the double-headed surfactants H2-T30 (top) and H-S6-H-T24 (middle) and the conventional single-tailed surfactant H-T31 (bottom). Head(●) – Tail(●) – Spacer(●)

We obtain free monomer concentrations for each system from a 100 × 100 two-dimensional lattice at a temperature of 2.0 (Figure 35). Although we model surfactants of longer length than the systems examined by either Comeau et al.[12] or Roszak et al.,[47] the CMC values we obtain change in the same direction as they observed (Table 9). Comeau et al.[12] found that the addition of the second head group increased the CMC values by approximately a factor of 5, while Roszak et al.[47] found an increase of a factor of 20. We find that the CMC values of the double-headed surfactants are approximately 1.3 higher than their conventional single-headed analog. While the size of the increase that we observe is smaller than that observed experimentally, the effect is outside of our measurement error (Table 9). It is obvious that the nature of the second head-group added has a significant impact on the CMC value and the factor of the increase. This is something we plan to examine in the future.

Upon examination of the snapshots of the systems one can visually see the difference in the average aggregate size (Figure 36). We examine the average aggregate size distribution with a plot of P(n) versus n (Figure 37). Figure 37 shows the cluster-size distribution from an average of three trials of a 100 × 100 two-dimensional lattice at temperature of 2.0 containing thirty H-T31, H2-T30 or H-S6-H-T24 surfactants. Two things are evident from this plot. First, the initial point (n=1) shows the difference in free monomer concentration for the three surfactants and confirms that CMC values increase with the addition of a second head group. Second, it is clear that the single-headed (H-T31) surfactant more readily forms larger aggregates, while the double-headed surfactants (H2-T30 and H-S6-H-T24) form smaller aggregates. This confirms the

experimental explanation that the second head group makes it more difficult for the surfactants to aggregate.[12,47]

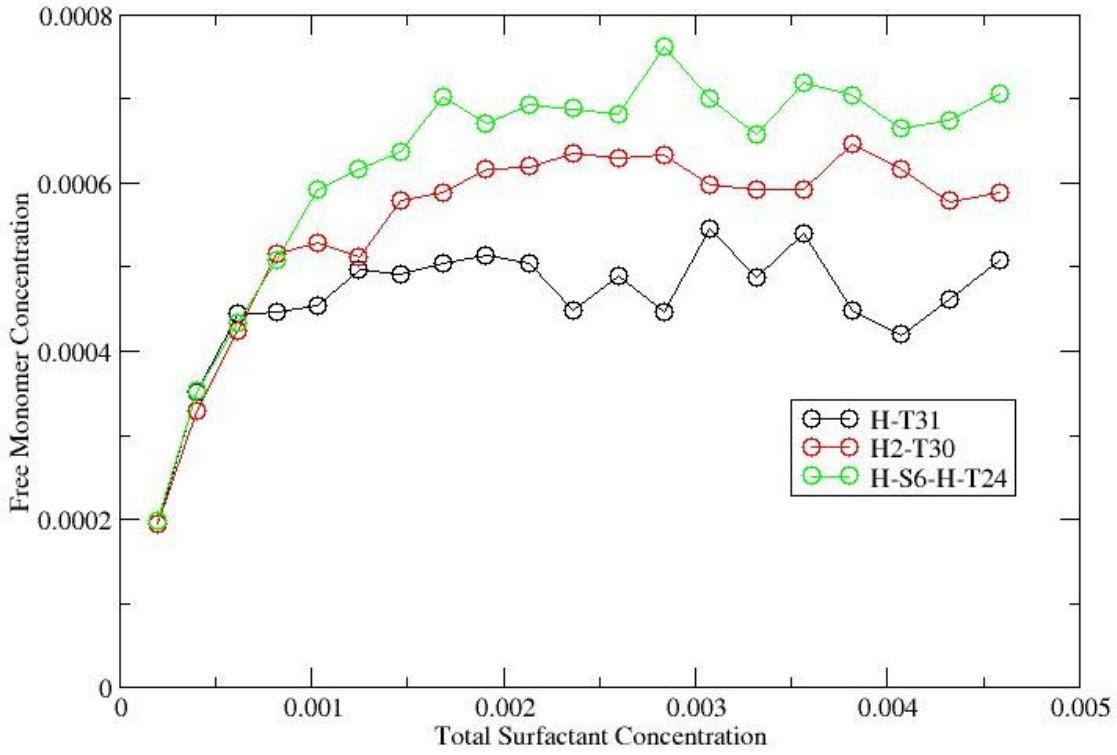

Figure 35 – A plot of the free monomer concentration versus the total surfactant concentration for two double-headed surfactants H2-T30 and H-S6-H-T24, as well as a corresponding single-headed surfactant with a tail length of 31 at a temperature = 2.0 on a 100 × 100 two-dimensional lattice.

Table 10 – The CMC values for two double-headed surfactants H2-T30 and H-S6-H-T24, as well as a corresponding single-headed surfactant with a tail length of 31 at a temperature = 2.0 on a 100 × 100 two-dimensional lattice.

Surfactant	CMC
H-T31	$4.8 \times 10^{-4} \pm 4.0 \times 10^{-5}$
H2-T30	$6.1 \times 10^{-4} \pm 2.1 \times 10^{-5}$
H-S6-H-T24	$6.9 \times 10^{-4} \pm 3.8 \times 10^{-5}$

It is also interesting to note that there is a difference in the CMC values obtained from the H2-T30 and the H-S6-H-T24 system. This suggests that the placement of the second head group has an impact on the final CMC values. This is not surprising given what has been previously reported in the literature about bolaform surfactants where the two head groups are at the extremes of the surfactant chain.[48,49,50,51]

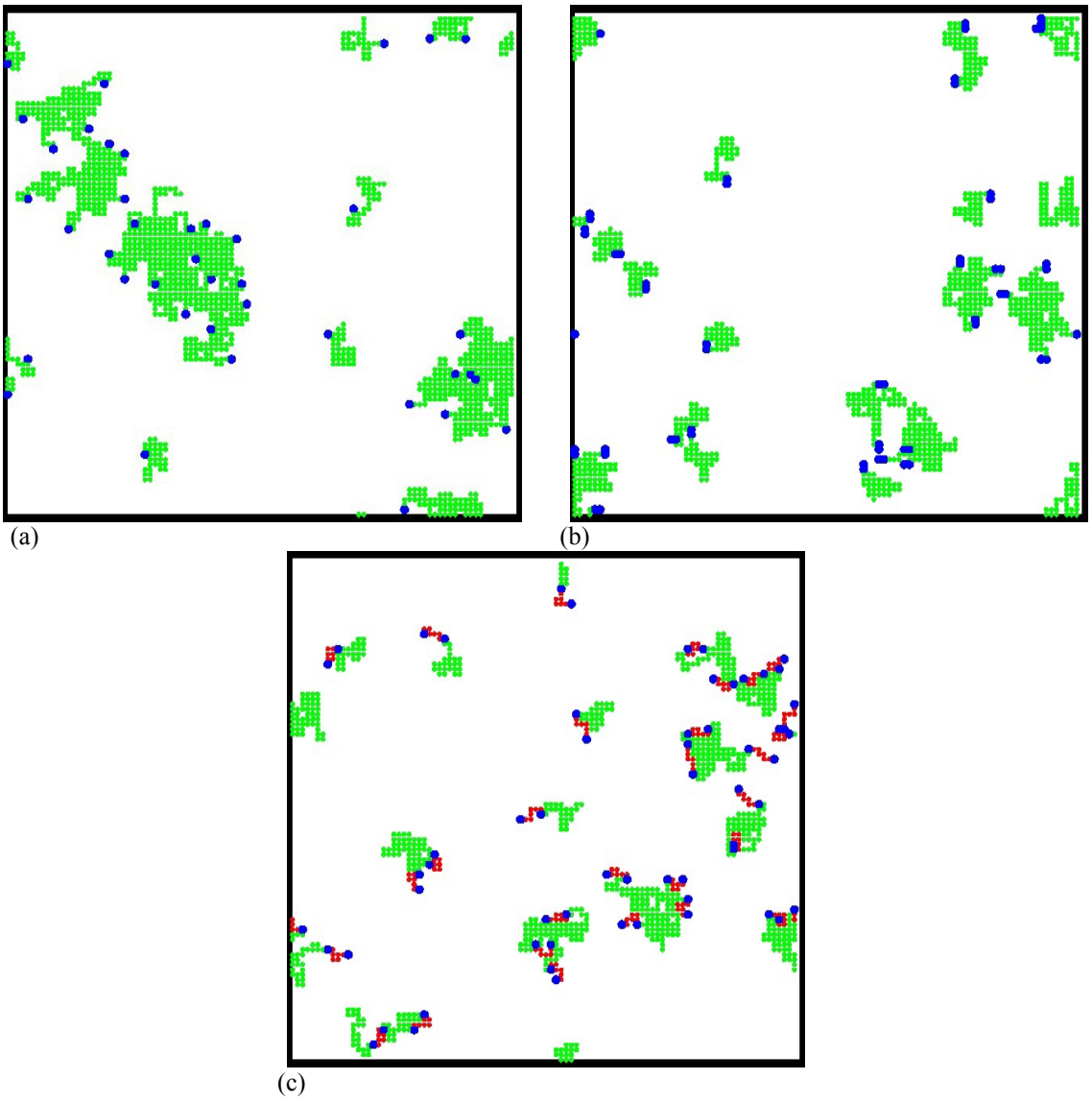

Figure 36 – Snapshots of a 100 × 100 two-dimensional lattice at temperature = 2.0 containing 30 surfactants of length 32 (a) H-T31 (b) H2-T30 (c) H-S6HT24. Head(●) – Tail(●) – Spacer(●)

Given our qualitative success in modelling double-headed surfactants, future research could start with a comprehensive series of double-headed surfactants where we vary the location of the second head group from directly adjacent to the first head to bolaform surfactants. We could also examine the effect of the size of the head group.

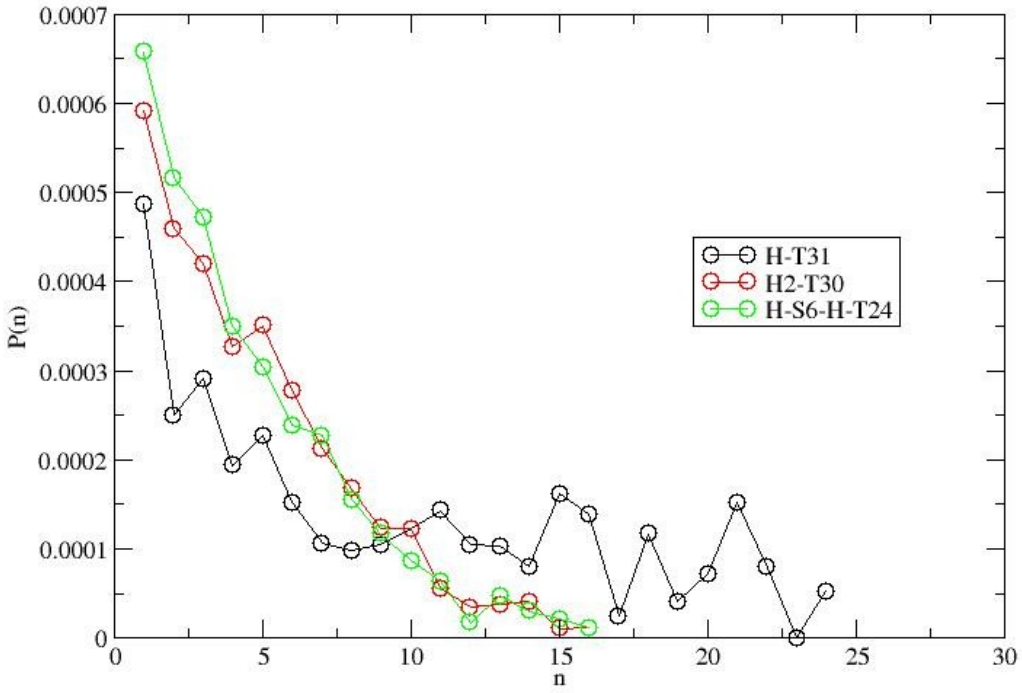

Figure 37 – A plot of P(n) versus n for the average of three trials from 100 × 100 two-dimensional lattices at temperature = 2.0 containing thirty H-T31, H2-T30 or H-S6HT24 surfactants of length 32.

4.2 – Initial Trials with Asymmetric Gemini Surfactants in Two-Dimensions

We study a series of gemini surfactants with a total path length of sixteen components at temperature = 2.0 on a 100 × 100 two-dimensional lattice. We start with completely symmetric gemini surfactants with a hydrophobic spacer length of 2, two

hydrophilic head groups and two non-rigid hydrophobic tails of length 6. The non-rigid tail groups allow many tail configurations and have the same interaction energies as the hydrophobic spacer.

The asymmetric series of surfactants consists of all the possible surfactants of length 16 between the symmetric surfactant and the most asymmetric possibility with a hydrophobic spacer length of 2, two hydrophilic head groups, a hydrophobic tail length of 1 and a hydrophobic tail length of 11 (Figure 38).

According to Wang et al.,[65] the CMC of asymmetric gemini surfactants decreases as the ratio of the difference between the two tails increases. In other words, as the gemini surfactant becomes more asymmetric, the CMC would be expected to decrease. They explain that this trend should be expected considering longer tailed conventional single-tailed surfactants and gemini surfactants have lower CMC values when compared to similar surfactants with shorter tails.

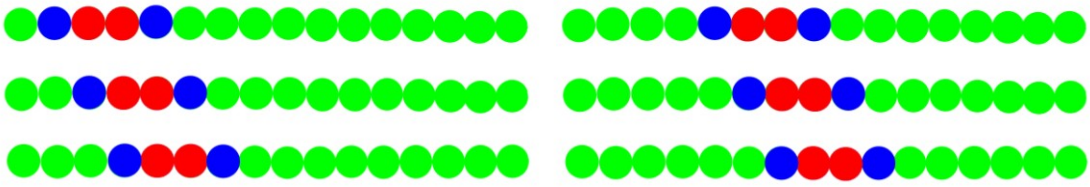

Figure 38 – A schematic diagram of the series asymmetric gemini surfactant of length 16 used for the initial trials: T11-H-S2-H-T1 (top-left), T8-H-S2-H-T4 (top-right), T10-H-S2-H-T2 (middle-left), T7-H-S2-H-T5 (middle-right), T9-H-S2-H-T3 (bottom-left) and T6-H-S6-H-T6 (bottom-right).
Head(●) – Tail(●) – Spacer(●)

In all tested systems, we do not observe a decrease in the value of the CMC, within the error of our observations. A change in symmetry has no visible effect on the CMC (Figure 39). To further understand this observed trend, we run several trials

directly related to the surfactants studied by Wang et al.[65] These results are presented in the following sections of this thesis.

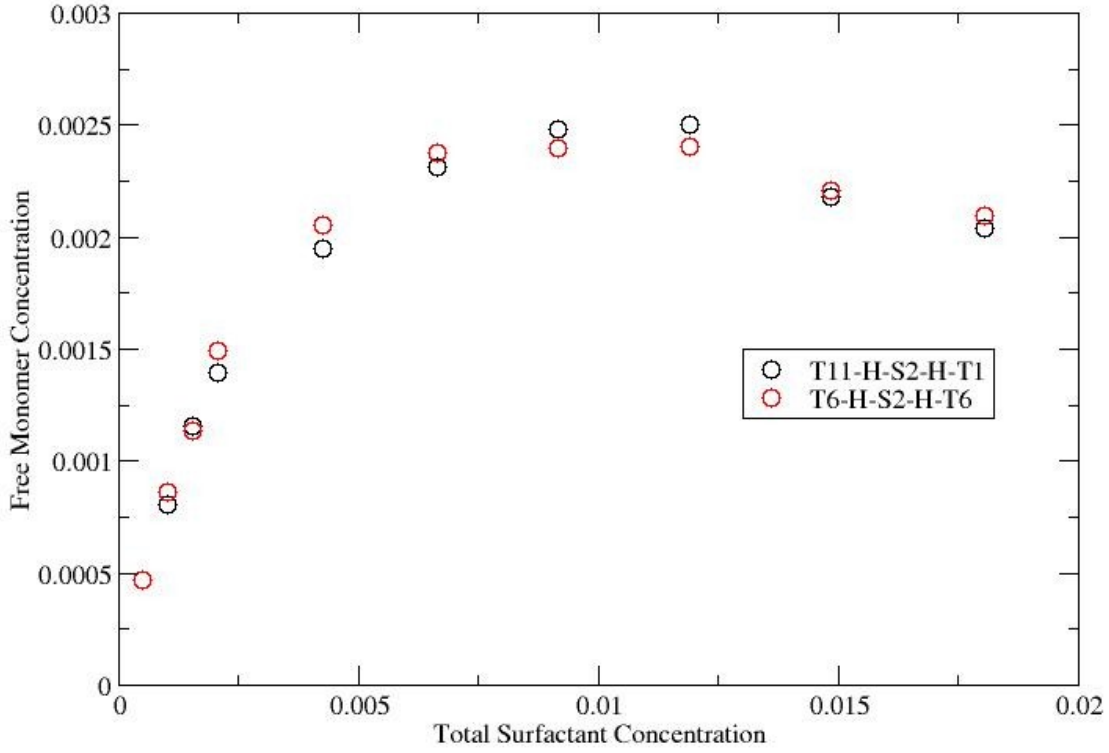

Figure 39 – A plot of the free monomer concentration versus the total surfactant concentration for the extremes of the asymmetric gemini surfactant series with a total surfactant length of 16, the symmetric gemini surfactant with a tail length of 6 and a spacer length of 2, as well as the most asymmetric gemini surfactant with a tail length of 1 and 11 and a spacer length of 2 at a temperature = 2.0 on a 100 × 100 two-dimensional lattice.

4.3 – Asymmetric Gemini Surfactants Trials in Two-Dimensions

Wang et al.[65] used microcalorimetric measurement, electrical conductivity measurement, steady-state fluorescence measurement, and time-resolved fluorescence quenching to measure the CMC and enthalpies of micellizaton of a series of asymmetric

gemini surfactants, $\left[{}_{m}H_{2m+1}(CH_3)_2N(CH_2)_6N(CH_3)_2C_nH_{2n+1} \right]Br_2$, with a constant n + m = 24 and m = 12, 13, 14, 16, 18. The study of this series of asymmetric gemini surfactants showed that the degree of asymmetry (m/n) had a measurable effect on micellization. As the m/n ratio increased, the CMC decreased linearly by about 35%, the average micelle size distribution at the CMC increased slightly and the Gibbs free energy of micellization became more negative.[65]

We model the Wang et al.[65] series of asymmetric gemini surfactants with surfactants with a total path length of 32 components at temperature = 2.0 on a 100 × 100 two-dimensional lattice. Like Wang et al.,[65] we start with a completely symmetric gemini surfactant with a hydrophobic spacer length of 6, two hydrophilic head groups and two non-rigid hydrophobic tails of length 12. We also examine the same series of asymmetric gemini surfactants, T_m-H-S6-H-T_n, where the tails n + m = 24 and m = 12, 13, 14, 16, 18 (Figure 40).

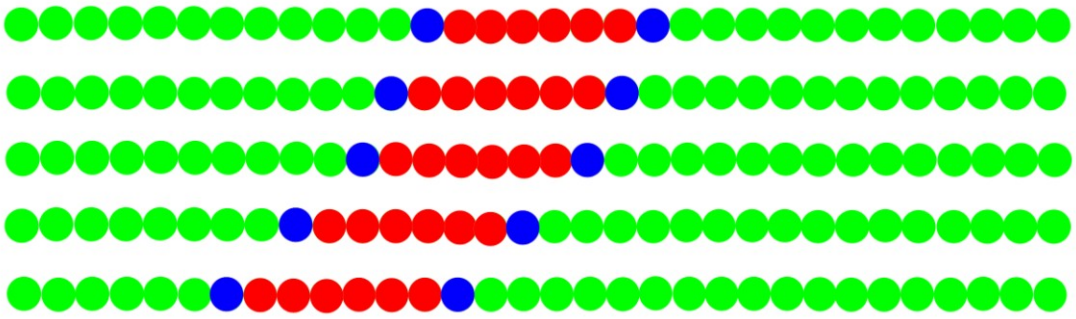

Figure 40 – The five asymmetric gemini surfactants modeled in both two- and three-dimensions. In order starting at the top: T12-H-S6-H-T12, T13-H-S6-H-T11, T14-H-S6-H-T10, T16-H-S6-H-T8, and T18-H-S6-H-T6. Head(●) – Tail(●) – Spacer(●)

Again, as in the initial trials modeling shorter chains, we observe no visible decrease in the value of the CMC as a result of increased asymmetry (Figure 41). We

extend the series to the extremes and include the surfactants T1-H-S6-H-T23 and H-S6-H-T24 (Figure 42). These surfactants also do not produce a noticeable change in the CMC values (Figure 43).

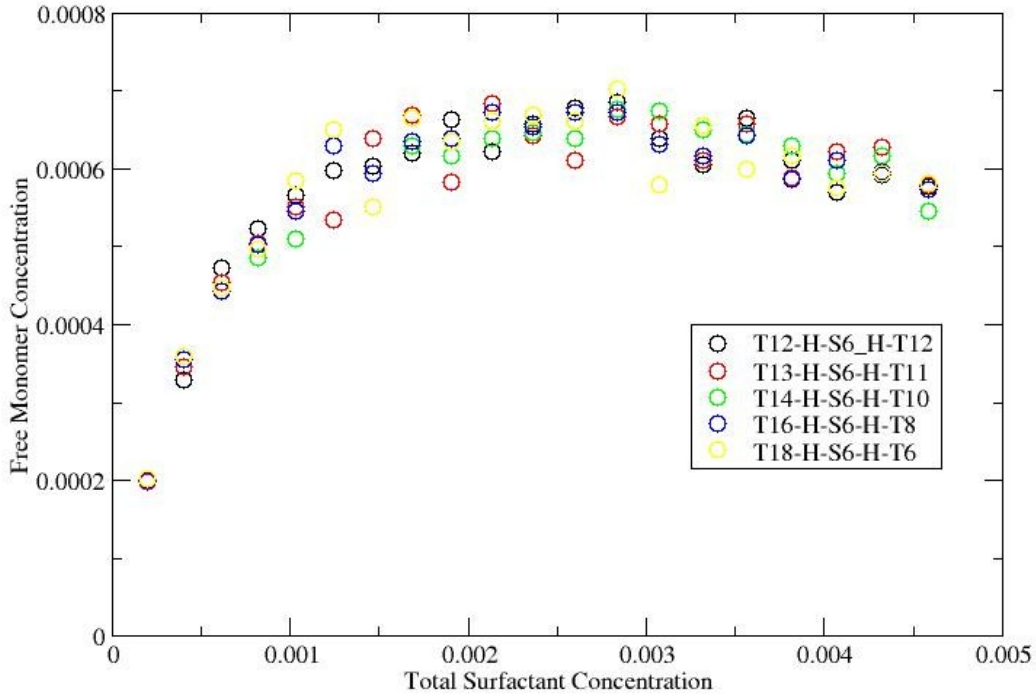

Figure 41 – A plot of the free monomer concentration versus the total surfactant concentration for the Wang et al.[65] series of asymmetric gemini surfactants at a temperature = 2.0 on a 100 × 100 two-dimensional lattice.

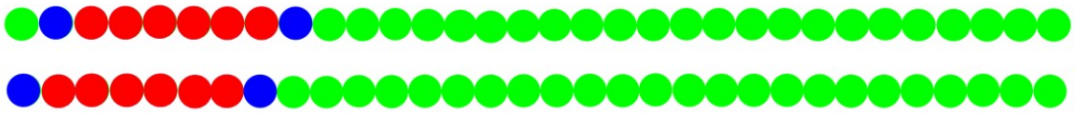

Figure 42 – The asymmetric gemini surfactants modeled to extend the Wang et al.[65] series T1-H-S6-H-T23 (top) and H-S6-H-T24 (bottom). Head(●) – Tail(●) – Spacer(●)

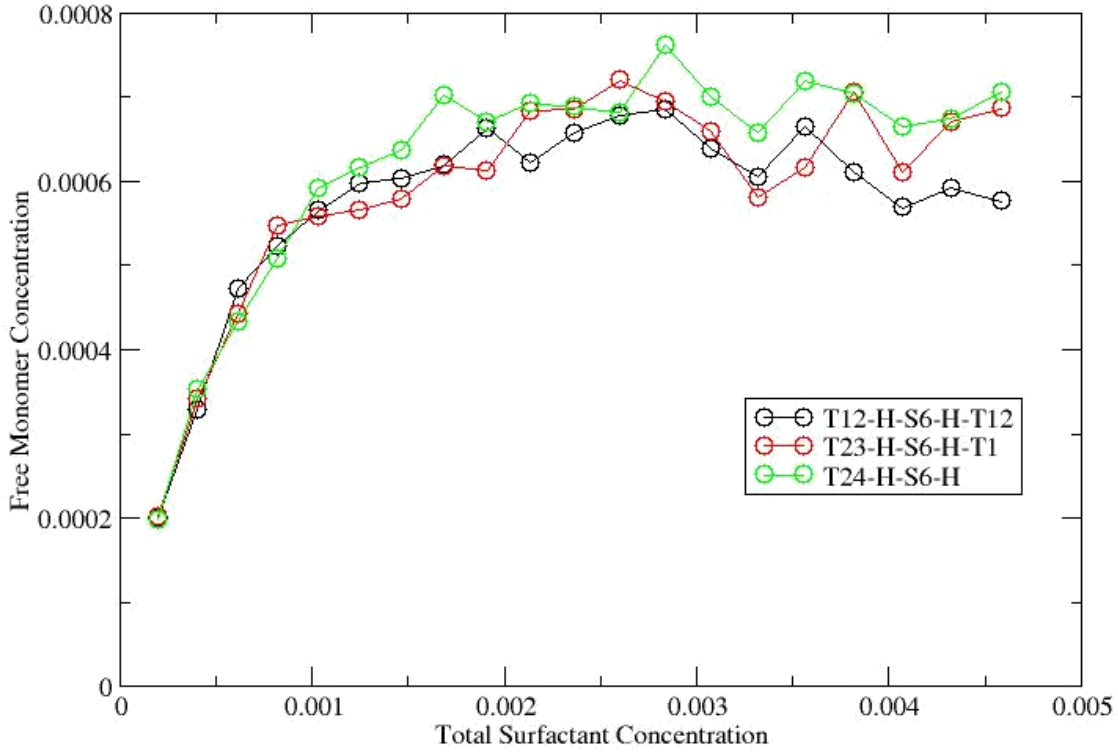

Figure 43 – A plot of the free monomer concentration versus the total surfactant concentration for the extended Wang et al.[65] series of asymmetric gemini surfactants at a temperature = 2.0 on a 100 × 100 two-dimensional lattice.

Our model of double-headed and asymmetric gemini surfactants leads to results that show surfactants made of the same components and spacer length will have the same CMC values regardless of how these components are ordered along the chain. If we double the number of head groups in the asymmetric gemini surfactants we again observe the trends previously mentioned in Section 4.1 of this thesis. We model the double-headed gemini surfactants T11-H2-S6-H2-T11 and T5-H2-S6-H2-T17 (Figure 44) at a temperature of 2.0 on a 100 × 100 two-dimensional lattice.

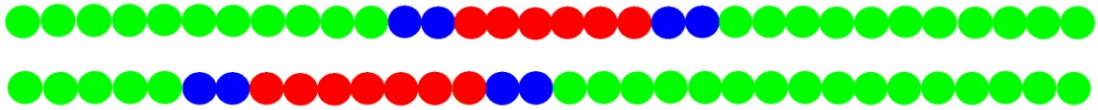

Figure 44 – The double-headed asymmetric gemini surfactants modeled to extend the Wang et al.[65] series T11-H2-S6-H2-T11 (top) and T5-H2-S6-H2-T17 (bottom). Head(●) – Tail(●) – Spacer(●)

Comparing the CMC values of the T12-H-S6-H-T12 to T11-H2-S6-H2-T11, we again find that doubling the number of head groups results in an increase in the obtained CMC (Figure 45). Again we observe no visible decrease in the value of the CMC as a result of increased asymmetry when we compare T11-H2-S6-H2-T11 and T5-H2-S6-H2-T17 (Figure 46).

We therefore do not observe the decrease in the CMC with increasing asymmetry reported by Wang et al.[65] In the first instance, the inability of our model to reproduce this effect must be attributed to a deficiency in the assumptions upon which the model is based, and/or the idealized nature of the model. At the same time, it is important to keep in mind that while the experimental observations indicate that the CMC decreases with increasing asymmetry, the size of the decrease (35% when one tail is three times longer than the other) is much smaller compared to the change in the CMC that would be observed if other architectural properties of the surfactant were changed on a similar scale. For example, if the lengths of both tails were increased by a factor of three, an increase of the CMC of several orders of magnitude could be expected.[3] From this perspective, the effect of surfactant asymmetry, though observable in experiments, is a weak one in a relative sense. As shown in Chapter 3, our model is capable of qualitatively reproducing the known dependence of the CMC on total chain length, for example. So in this broader context, our simulation results do reinforce the findings of

experiments: that relative to other architectural influences, the effect of asymmetry on the CMC is weak. If the effect of asymmetry is a weak one, it is possible that its appearance, both in experiments and simulations, may be highly sensitive to the details of the particular system.

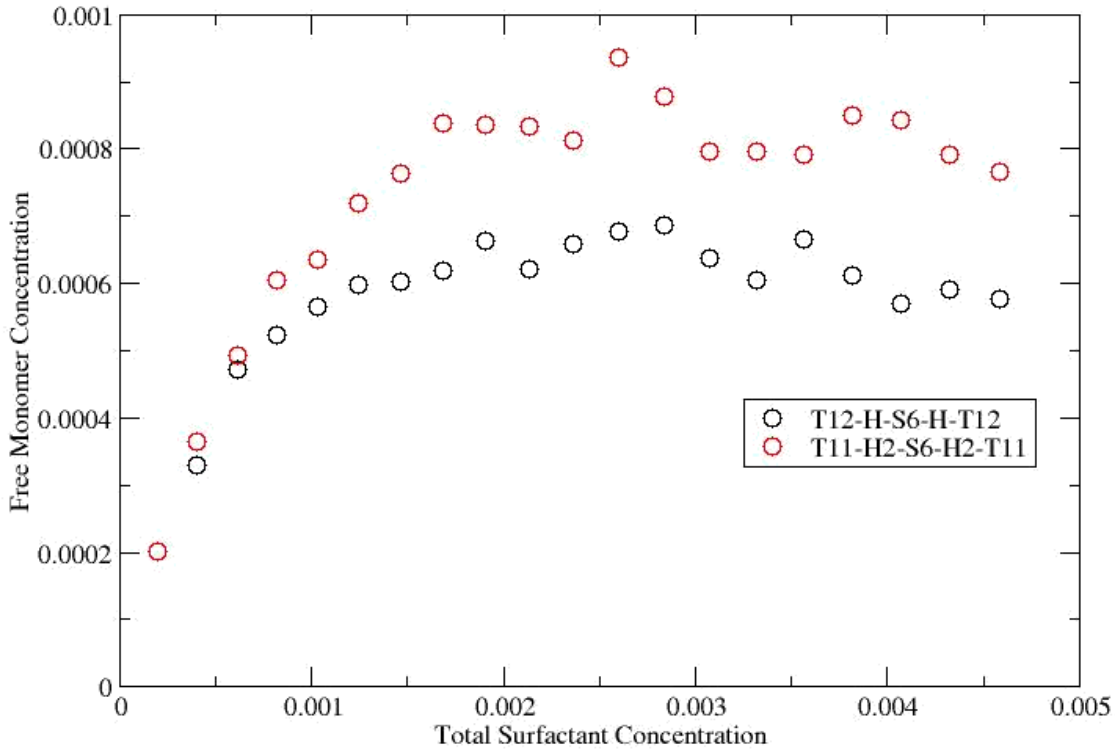

Figure 45 – A plot of the free monomer concentration versus the total surfactant concentration for double-headed and single-headed gemini surfactants at a temperature = 2.0 on a 100 × 100 two-dimensional lattice.

Given that there are presently only two studies (from the same group) of the effect of asymmetry, further investigation is required to determine if this behavior is a universal one, or perhaps varies widely from one system to another. Based on our simulation

results, and given the generic and highly idealized nature of our model system, we would conclude that there is unlikely to be a strong effect in any particular system.

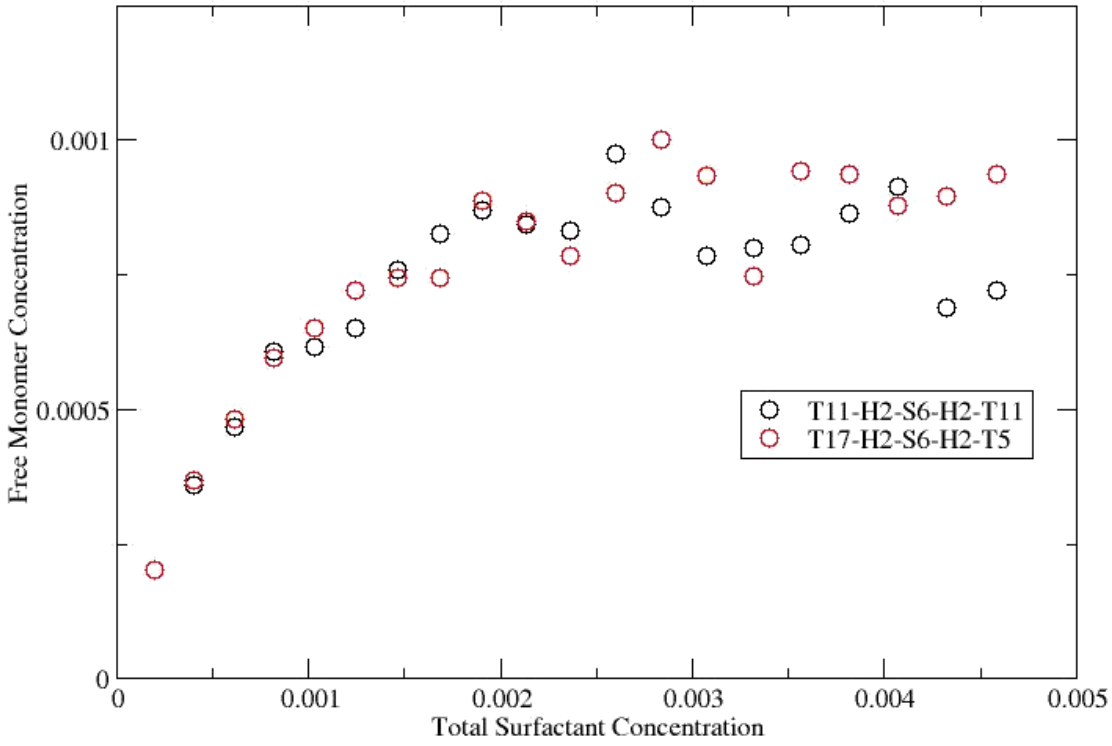

Figure 46 – A plot of the free monomer concentration versus the total surfactant concentration for the double-headed Wang et al.[65] series of asymmetric gemini surfactants at a temperature = 2.0 on a 100 × 100 two-dimensional lattice.

Finally, we examine snapshots for the different asymmetric gemini surfactants. These do indicate a difference in the cluster-size distribution and the structure of the aggregates as the surfactant symmetry varies (Figure 47). It is very interesting to see that although the CMC does not change (for example, Figure 41), the morphology of the aggregates does (Figure 48). However, T18-H-S6-H-T6 tends to form slightly larger aggregates than T12-H-S6-H-T12; they both form larger aggregates than T24-H-S6-H.

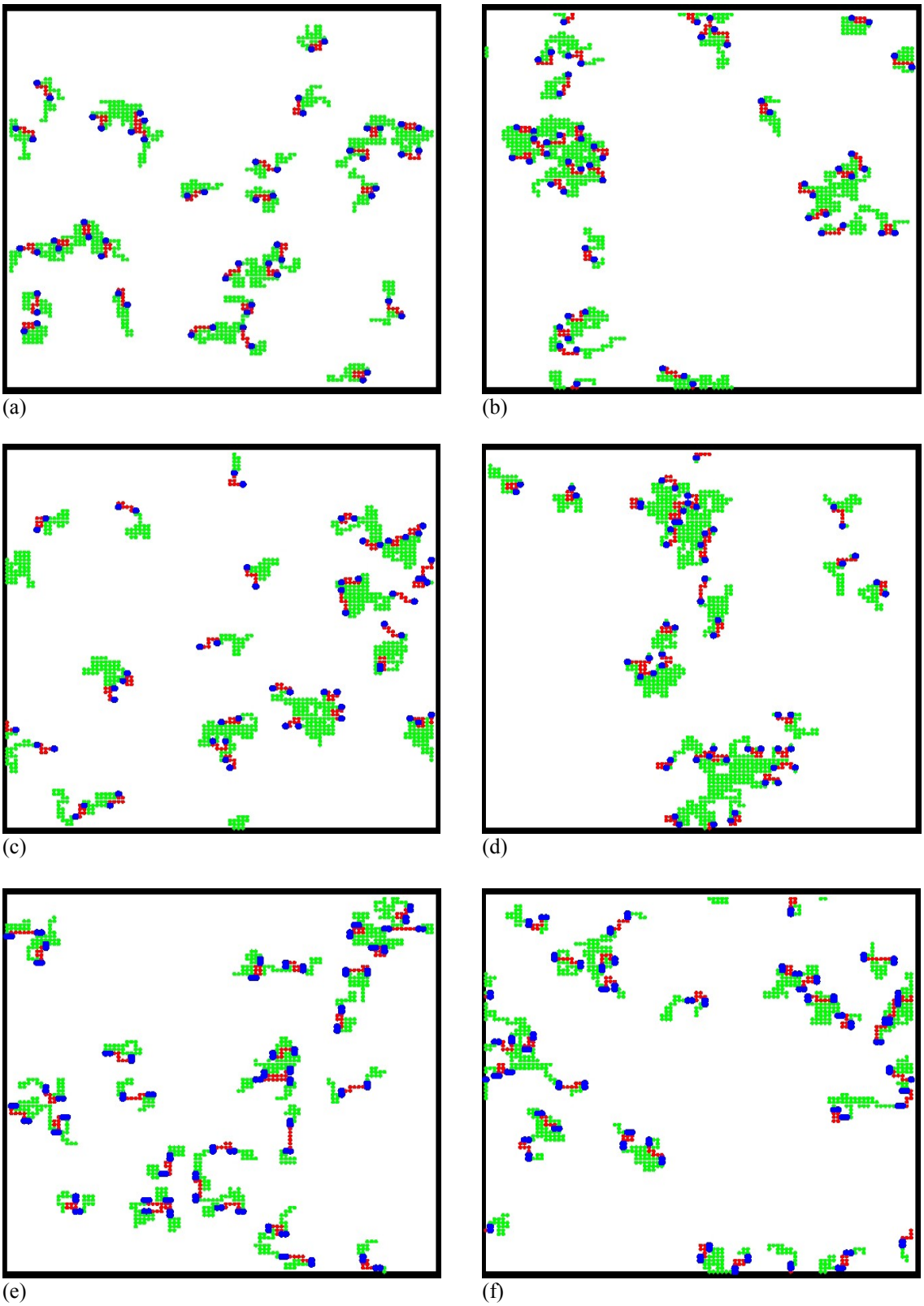

Figure 47 – Snapshots from a two-dimensional 100 ×100 lattice at temperature = 2.0 for 30 of the following asymmetric gemini surfactants: (a) T12-H-S6-H-T12 (b) T18-H-S6-H-T6 (c) T24-H-S6-H (d) T23-H-S6-H-T1 (e) T11-H2-S6-H2-T11 (f) T17-H2-S6-H2-T5. Head(●) – Tail(●) – Spacer(●)

The terminal head group clearly makes it more difficult for the surfactants to aggregate and the snapshots of the lattice show a more open structure to the aggregates of T24-H-S6-H. This phenomenon merits further study. The ability to vary the aggregate size and morphology, while maintaining a fixed CMC, may have useful applications.

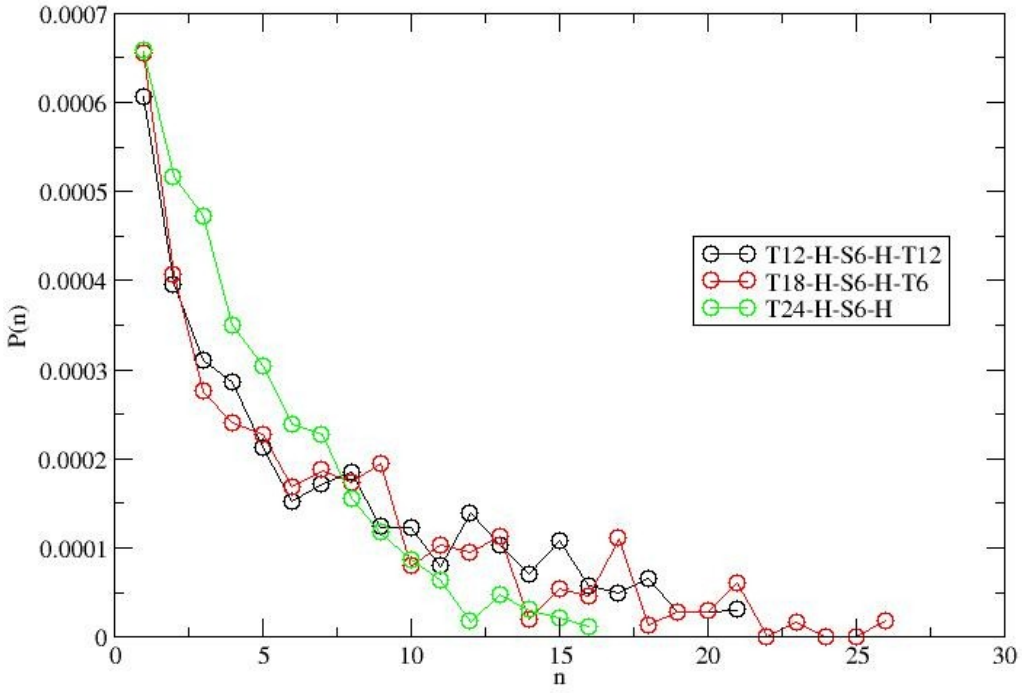

Figure 48 – A plot of P(n) versus n for the average of three trials from 100 × 100 two-dimensional lattices at temperature = 2.0 containing 30 T12-H-S6-H-T12, T18-H-S6-H-T6 or H-S6-H-T24 surfactants.

4.4 – Asymmetric Gemini Surfactants Trials in Three-Dimensions

We model the Wang et al.[65] asymmetric gemini series in three-dimensions using a 100 × 100 × 100 cubic lattice at a temperature of 2.0 (Figure 49) and obtain plots of the free monomer concentration versus total surfactant concentration (Figure 50). We again

observe no change in the CMC values with an increasing degree of asymmetry. Modeling in three-dimensions is much more computationally taxing. On average it took a month to obtain each data point on the curve. As a synthetic chemist this may not be practical if you wish to use such simulations as a precursor to synthesis. However, since the trends observed in two- and three-dimensions are consistent with one another, the two-dimensional results seem to provide qualitative trends useful for synthesis.

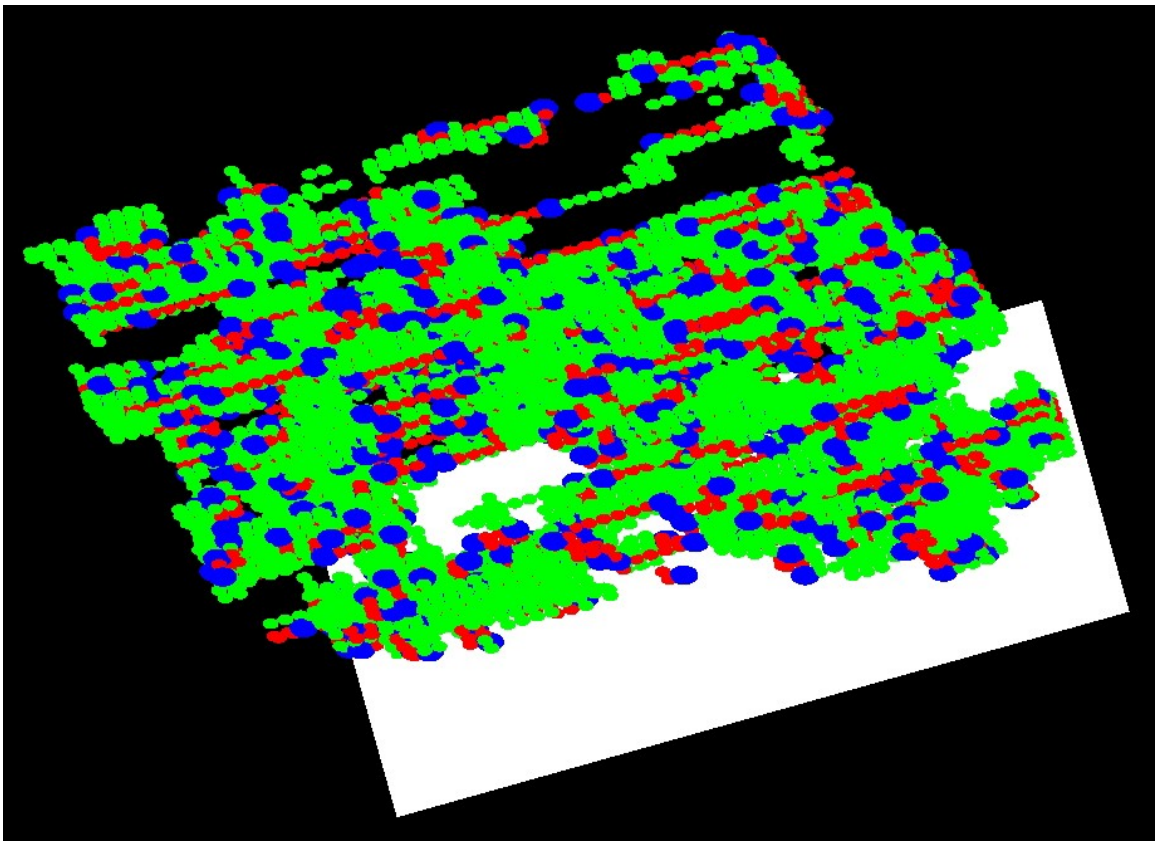

Figure 49 – A snapshot from a 100 × 100 × 100 cubic lattice with 3300 T12-H-S6-H-T12 gemini surfactants at a temperature = 2.0.

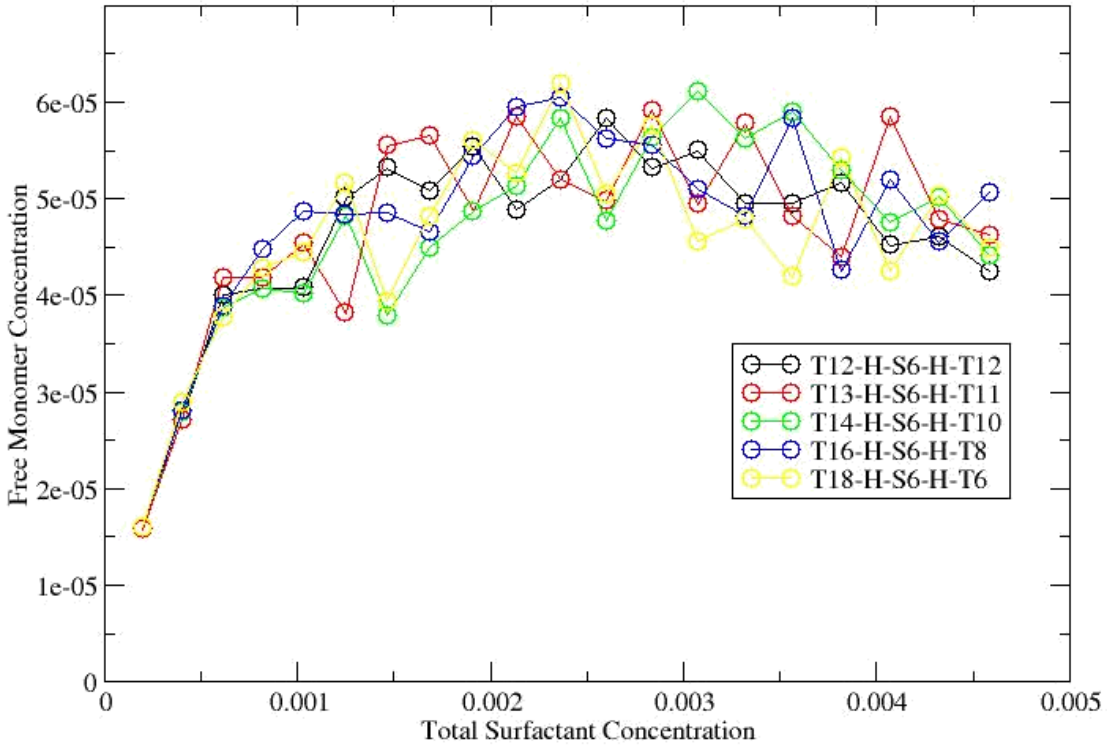

Figure 50 – A plot of the free monomer concentration versus the total surfactant concentration for the Wang et al.[65] series of asymmetric gemini surfactants at a temperature = 2.0 on a 100 × 100 × 100 three-dimensional lattice.

4.5 – Conclusions and Future Work

This work is the first to model the novel double-headed and asymmetric gemini surfactants. We find that the addition of a second head group to a linear surfactant increases the value of the CMC by a factor of 1.3 over that of their conventional single-headed analog. While the size of the increase that we observe is smaller than that observed experimentally, the effect is outside of our measurement error. The model predicts that the single-headed (H-T31) surfactant more readily forms larger aggregates,

while the double-headed surfactants (H2-T30 and H-S6-H-T24) form smaller aggregates. This confirms the experimental explanation that the second head group makes it more difficult for the surfactants to aggregate.[12,47] There is a difference in the CMC values obtained from the H2-T30 and the H-S6-H-T24 system. This suggests that the placement of the second head group has an impact on the final CMC values. This is not surprising given what has been previously reported in the literature about bolaform surfactants where the two head groups are at the extremes of the surfactant chain.[48,49,50,51]

Given our qualitative success in modeling double-headed surfactants, future research could start with a comprehensive series of double-headed surfactants where we vary the location of the second head group from directly adjacent to the first head to bolaform surfactants. In addition, we should investigate the affect of the size of the head groups.

The asymmetric gemini surfactant results obtained here do not confirm the experimental results of Wang et al.[65] We do not observe a decrease in the value of the CMC with increasing asymmetry of the tails on gemini surfactants. While the experimental observations indicate that the CMC decreases with increasing asymmetry, the size of the decrease (35% when one tail is three times longer than the other) is much smaller compared to the change in the CMC that would be observed if other architectural properties of the surfactant were changed on a similar scale. For example, if the lengths of both tails were increased by a factor of three, an increase of the CMC of several orders of magnitude could be expected.[3] From this perspective, the effect of surfactant asymmetry, though observable in experiments, is a weak one in a relative sense. Our model is capable of qualitatively reproducing the known dependence of the CMC on total

chain length, for example. So in this broader context, our simulation results do reinforce the findings of experiments: that relative to other architectural influences, the effect of asymmetry on the CMC is weak. If the effect of asymmetry is a weak one, it is possible that its appearance, both in experiments and simulations, may be highly sensitive to the details of the particular system. We should continue to examine series of asymmetric gemini surfactants to gain further insight into what has been observed.

The code created is very versatile and can model a variety of surfactant systems. It is capable of modeling systems on both two- and three-dimensional lattices, producing the same trends. As a synthetic precursor, it will likely be best used to investigate trends in two-dimensions.

BIBLIOGRAPHY

[1] L.L. Schramm, E.N. Stasiuk, and D.G. Marangoni, *Annu. Rep. Prog. Chem., Sect. C: Phys. Chem.*, **99**, 3 (2003).
[2] L.L. Schramm, Surfactants: Fundamentals and Applications in the Petroleum Industry, Cambridge University Press, New York, 2000.
[3] R. Zana, *Adv. Colloid Interfac.*, **97**, 205 (2002).
[4] P.K. Maiti and D. Chowdhury, *J. Chem. Phys.*, **109**, 5126 (1998).
[5] R.G. Larson, *J. Chem. Phys.*, **89**, 1642 (1988).
[6] V. Kapila, J.M. Harris, P.A. Deymier, and S. Raghavan, *Langmuir*, **18**, 3728 (2002).
[7] S.K. Talsania, Y. Wang, R. Rajagopalan, and K.K. Mohanty, *J. Colloid Interface Sci.*, **190**, 92 (1997).
[8] M.J Lawrence, *Chem. Soc. Rev.*, **23**, 417 (1994).
[9] D.J. Shaw, Colloid and Surface Chemistry – Fourth Edition, Butterworth-Heinemann Ltd., Toronto, 1992, Chapter 4.
[10] B.J. Ravoo, J.B.F.N. Engberts, *Langmuir*, **10**, 1735 (1994).
[11] M. Sagisaka, M. Hino, Y. Nakanishi, Y. Inui, T. Kawaguchi, K. Tsuchiya, H. Sakai, M. Abe and A. Yoshizawa, *Langmuir*, **25**, 10230 (2009).
[12] E.K. Comeau, E.J. Beck, J.F. Caplan, C.V. Howley, and D.G. Marangoni, *Can. J. Chem.*, **73**, 1741 (1995).
[13] F.M. Menger and C.A. Littau, *J. Am. Chem. Soc.*, **113**, 1451 (1991).
[14] D. Langevin, *Annu. Rev. Phys. Chem.*, **43**, 341 (1992).
[15] G. Arya and A.Z. Panagiotopoulos, *Comput. Phys. Commun.*, **169**, 262 (2005).
[16] D.J. Jaeger and E.L.G. Brown, *Langmuir*, **12**, 1976 (1996).
[17] P. Goon, C. Manohar, and V.V. Kumar, *J. Colloid Interf. Sci.*, **189**, 177 (1997).
[18] A. Dominguez, A. Fernandez, N. Gonzalez, E. Iglesias, and L. Montenegro, *J. Chem. Educ.*, **74**, 1227 (1997).
[19] E. Ruckenstein and R. Nagarajan, *J. Phys. Chem.*, **79**, 2622 (1975).
[20] A. Ben-Naim and F.H. Stillinger, *J. Phys. Chem.*, **84**, 2872 (1980).
[21] D. Wu, Y. Feng, G. Xu, Y. Chen, X. Cao, and Y. Li, *Colloid Surface A*, **299**, 117 (2007).
[22] J.N. Israelachvili, D.J. Mitchell, and B.W. Ninham, *J. Chem. Soc. Faraday Trans. 2*, **72**, 1525 (1976).
[23] C. Tanford, The Hydrophobic Effect: Formation of Micelles and Biological Membranes, John Wiley & Sons Inc., New York, 1973.
[24] M.A. Floriano, E. Caponetti, and A. Z. Panagiotopoulos, *Langmuir* **15**, 3143 (1999).
[25] S.K. Talsania, Y. Wang, R. Rajagopalan, and K.K. Mohanty, *J. Colloid Interface Sci.*, **190**, 92 (1997).
[26] H. Gharibi, R. Behjatmanesh-Ardakani, S.M. Hashemianzadeh, S.M. Mousavi-Khoshdel, S. Javadian, and B. Sohrabi, *Theor. Chem. Acc.*, **115**, 1 (2006).
[27] M. Zaldivar and R.G. Larson, *Langmuir*, **19**, 10434 (2003).
[28] E. Johnson, G. Olofsson, and B. Jonsson, *J. Chem. Soc., Faraday Trans.*, **83**, 3331 (1987).
[29] J.C. Desplat and C.M. Care, *Mol. Phys.*, **87**, 441 (1996).

[30] E.D. Goddard and G.C. Benson, *Can. J. Chem.*, **35**, 986 (1957).
[31] M.S. Akhter and S.M. Alawi, *Colloid Surface A*, **175**, 311 (2000).
[32] M. McCoy, *CENEAR*, **81**, 15 (2003).
[33] S.T. Hyde, *Pure Appl. Chem.*, **64**, 1617 (1992).
[34] S.A. Safran, P.A. Pincus, D. Andelman, and F.C. MacKintosh, *Phys. Rev. A*, **43**, 1071 (1991).
[35] P.K Maiti, Y. Lansac, M.A. Glaser, and N.A. Clark, *Langmuir*, **18**, 1908 (2002).
[36] D.J. Jobe and V.C. Reinsborough, *Aust. J. Chem.*, **34**, 320 (1984).
[37] J.A. MacInnis, G.D. Boucher, R. Palepu, and D.G. Marangoni, *Can. J. Chem.*, **77**, 340 (1999).
[38] N.A.J.M. Sommerdijk, T.L. Heoks, K.J. Booy, M.C. Feiters, R.J.M. Nolte, and B. Zwanenburg, *Chem. Commun.*, 743 (1998).
[39] D.F. Ewing, J.W. Goodby, S. Guenais, P. Letellier, G. Mackenzie, I. Piastrelli, and D. Plusquellec, *J. Chem. Soc., Perkin Trans. 1*, 3459 (1997).
[40] B.L. Bales, A.M. Howe, A.R. Pitt, J.A. Roe, and P.C. Griffiths, *J. Phys. Chem. B*, **104**, 264 (2000).
[41] J. Haldar, V.K. Aswal, P.S. Goyal, and S. Bhattacharya, *Pramana – J. Phys.*, **63**, 303 (2004).
[42] E.W. Anacker and A.E. Westwall, *J. Proc. Montana Acad. Sci.*, **9**, 4 (1960).
[43] J.B. Peri, *J. Am. Oil Chem. Soc.*, **35**, 110 (1958).
[44] B. Lindman, *J. Phys. Chem.*, **87**, 1377 (1983).
[45] D.J. Cebula and R.H. Ottewill, *J. Coll. Polym. Sci.*, **260**, 1118 (1982).
[46] T.M. Herrington and S.S. Sahi, *Colloids Surf.*, **17**, 103 (1986).
[47] K.Z. Roszak, S.L. Torcivia, K.M. Hamill, A.R. Hill, K.R. Radloff, D.M. Crizer, A.M. Middleton, and K.L. Caran, *J. Colloid Interf. Sci.*, **331**, 560 (2009).
[48] J.H. Fuhrhop and T. Wang, *Chem. Rev.*, **104**, 2901 (2004).
[49] T.W. Davey, W.A. Ducker, and A.R. Hayman, *Langmuir*, **16**, 2430 (2000).
[50] Y. Moroi, Y. Murata, Y. Fukuda, Y. Kido, W. Seto, and M. Tanaka, *J. Phys. Chem.*, **96**, 8610 (1992).
[51] S. Franceschi, V. Andreu, N. de Viguerie, M. Riviere, A. Lattes, and A. Moisand, *New J. Chem.*, **22**, 225 (1998).
[52] K. Ikeda, T. Nakasima, K. Esumi, and K. Meguro, *Bull. Chem. Soc. Jpn.*, **62**, 578 (1989).
[53] K. Tamaki, Y. Ohara, Y. Akimoto, and K. Koshishi, *Bull. Chem. Soc. Jpn.*, **67**, 856 (1994).
[54] K. Meguro, K. Ikeda, A. Otsuji, M. Taya, M. Yasuda, and K. Esumi, *J. Colloid Interface Sci.*, **118**, 372 (1987).
[55] M. Frindi, B. Michels, H. Levy, and R. Zana, *Langmuir*, **10**, 1140 (1994).
[56] F.M. Menger and J.S. Keiper, *Angew. Chem., Int. Ed. Engl.*, **39**, 1906 (2000).
[57] G. Bai, J. Wang, H. Yan, Z. Li, and R.K. Tomas, *J. Phys. Chem. B.*, **105**, 3105 (2001).
[58] J.B.R.N. Engberts, T. Bam, J. Karhauser, S. Karaborni, and N.M. van Os, *Colloids Surf. A*, **118**, 41 (1996).
[59] S.K. Hait and S.P. Moulik, *Curr. Sci. India*, **82**, 1101 (2002).
[60] Y. Sun, Y. Feng, H. Dong, Z. Chen, and L. Han, *Cent. Eur. J. Chem.*, **5**, 620 (2007).

[61] R. Oda, L. Bourdieu, and M. Schmutz, *J. Phys. Chem. B*, **101**, 5913 (1997).
[62] R. Oda, I. Huc, and S.J. Candau, *Chem. Commun.*, 2105 (1997).
[63] F.M. Menger and W.V. Peresypkin, *J. Am. Chem. Soc.*, **125**, 5340 (2003).
[64] C. Wang, S.D. Wettig, M. Foldvari, and R.E. Verrall, *Langmuir*, **23**, 8995 (2007).
[65] X. Wang, J. Wang, Y. Wang, J. Ye, H. Yan and R.K. Thomas, *J. Phys. Chem. B*, **107**, 11428 (2003).
[66] G. Bai, J. Wang, Y. Wang, H. Yan, and R.K. Thomas, *J. Phys. Chem. B*, **106**, 6614 (2002).
[67] M.P. Allen and D.J. Tildesley, Computer Simulation of Liquids, Oxford Science Publications, Oxford, 1987.
[68] D. Frenkel and B. Smit, Understanding Molecular Simulations: From Algorithms to Applications, 2nd edition, Academic Press, New York, 2002.
[69] O.G. Mouritsen, Computer Simulations of Phase Transitions and Critical Phenomena, Springer-Verlag, New York, 1984.
[70] K. Binder and D.W. Heermann, Monte Carlo Simulation in Statistical Physics, Springer-Verlag, New York, 1992.
[71] K.J. Laidler and J.H. Meiser, Physical Chemistry, 2nd edition, Houghton Mifflin Company, Toronto, 1995.
[72] N. Metropolis and S. Ulam, *J. Amer. Stat. Assoc.*, **44**, 335 (1949).
[73] N. Metropolis, A. Rosenbluth, M. Rosenbluth, A. Teller, and E. Teller, *J. Chem. Phys.*, **21**, 1087 (1953).
[74] D.M. Ceperley, *AIP Con. Proc.*, **690**, 85 (2003).
[75] M. Girardi and W. Figueiredo, *J. Chem. Phys.*, **112**, 4833 (2000).
[76] C.S. Shida and V.B. Henriques, *J. Chem. Phys.*, **115**, 8655 (2001).
[77] J.N.B. de Moraes, W. Figueiredo, and V.B. Henriques, *J. Chem. Phys.*, **113**, 6404 (2000).
[78] R.G. Larson, L.E. Scriven, and H.T. Davis, *J. Chem. Phys.*, **83**, 2411 (1985).
[79] R.G. Larson, *J. Chem. Phys.*, **96**, 7904 (1992).
[80] P.K. Maiti, K. Kremer, O, Flimm, D. Chowdhury, and D. Stauffer, *Langmuir*, **16**, 3784 (2000).
[81] K.M. Layn, P.G. Debenedetti, and R.K. Prud'homme, *J. Chem. Phys.*, **109**, 5651 (1998).
[82] A. Bhattacharya and S.D. Mahanti, *J. Phys.: Condens. Matter*, **12**, 6141 (2000).
[83] C.M. Care, *J. Chem. Soc. Farad. T. 1*, **83**, 2905 (1987).
[84] S.Y. Kim, A.Z. Panagiotopoulos, and M.A. Floriano, *Mol. Phys.*, **100**, 2213 (2002).
[85] P.H. Nelson, G.C. Rutledge, and T.A. Hatton, *J. Chem. Phys.*, **107**, 10777 (1997).
[86] J.N.B. de Moraes and W. Figueiredo, *J. Chem. Phys.*, **110**, 2264 (1999).
[87] F.T. Wall and F. Mandel, *J. Chem. Phys.*, **63**, 4592 (1975).
[88] K. Kremer and G.S. Grest, Monte Carlo and Molecular Dynamics Simulations in Polymer Science, Oxford University Press, New York, 1995.
[89] D.W. Heermann and K.Binder, Monte Carlo Simulation in Statistical Physics, 2nd ed., Springer-Verlag, Berlin, 1992.
[90] Y. Xu, J. Feng, H. Liu, Y. Hu, and J. Jiang, *Mol. Simulat.*, **33**, 261 (2007).
[91] Y. Xu, J. Feng, Y. Shang, and L. Honglai, *Chin. J. Chem. Eng.*, **15**, 560 (2007).

[92] H.D. Burrows, M.J. Tapia, C.L. Silva, A.A.C.C. Pais, S.M. Forseca, J. Pina, J.S. Melo, Y. Wang, E.F. Marques, M. Knaapila, A.P. Monkman, V.M. Garamus, S. Pradham, and U. Scherf, *J. Phys. Chem. B*, **111**, 4401 (2007).
[93] Y.J. Chen, G.Y. Xu, S.L. Yuan, and H.Y. Sun, *Chinese Chem. Lett.*, **16**, 688 (2005).
[94] E. Khurana, S.O. Nielsen, and M.L. Klein, *J. Phys. Chem. B*, **110**, 22136 (2006).
[95] S. Karaborni, K. Esselink, P.A.J. Hilbers, B. Smit, J. Karthäuser, N.M. van Os, and R. Zane, *Science*, **266**, 254 (1994).
[96] M.C.P. van Eijk, M. Bergsma, and S.-J. Marrink, *Eur. Phys. J. E*, **7**, 317 (2002).
[97] R. Oda, M. Laguerre, I. Huc, and B. Desbat, *Langmuir*, **18**, 9659 (2002).
[98] P.K. Maiti and D. Chowdhury, *Europhys. Lett.*, **41**, 183 (1998).
[99] A.T. Bernardes, T.B. Liverpool and D. Stauffer, *Phys. Rev. E*, **54**, R2220l (1996).